The Synthesis, Characterization and Performance Evaluation of Polyphenylenediamine- and Polypyrrole-Clay Composites for Removal of Oxo-Anionic Wastewater Contaminants

Lindani Mbalenhle Mdlalose

A thesis submitted to the Faculty of Science, University of the Witwatersrand in fulfilment of the requirements for the degree of Doctor of Philosophy

2018

DEDICATION

This work is dedicated to my forever loving mom, Zehlile Zwane and my dad, Warrant Officer Mbuso Mdlalose for being the home base where I always draw motivation. I also dedicate it to my late grandmother who taught me who I am and believed in me. Her wisdom words will always echo in my mind. Thank you Ngwane.

DECLARATION

I declare that this thesis is my own work, unaided work. It is being submitted for the Degree of Doctor of Philosophy to the University of the Witwatersrand, Johannesburg, South Africa. It has not been submitted before for any degree or examination to any other university.

.....

Ms. Lindani Mbalenhle Mdlalose

School of Chemistry, University of the Witwatersrand, Johannesburg. 2018

This thesis is submitted after examination and approval by the following supervisor

.....

Prof. Luke Chimuka

School of Chemistry, University of the Witwatersrand, Johannesburg, 2018

ABSTRACT

Contamination of water bodies by numerous pollutants is a worldwide problem that endangers the environment and health of human beings, animals and aquatic life. Hexavalent chromium (Cr(VI)) for example is used in different metal products and processes which makes it a common environmental contaminant. Because of its high mobility in aqueous phase, and improper storage or unsafe disposal practices, leakage of Cr(VI) into water streams and ground water is a common occurrence. While Cr(III) is an essential micronutrient, Cr(VI), however is highly toxic posing serious health risks. Additionally, phosphorus is a limiting nutrient for the growth of organisms in most ecosystems, but, excessive discharge of phosphate ions in water systems leads to profuse algal growth, and is detrimental to both the environment and the ecosystem.

This research focused on the development of suitable functional adsorbents for the removal of Cr(VI) complexes and phosphate ions from wastewater. Poly(para-phenylene)- (P*p*PD) and polypyrrole-based composites were synthesized through chemical oxidation polymerization, and investigated for Cr(VI) remediation. Poly(phenylenediamine) isomers were synthesized through different chemical oxidation methods for the uptake of phosphate ions in wastewater. Transition metals modified bentonite clay adsorbents were developed to remove phosphate ions in aqueous solution.The adsorbents were characterized using Fourier-transform infrared spectroscopy (FT-IR), X-ray diffractometer (XRD), Brunauer-Emmett-Teller (BET), Scanning electron microscopy (SEM), Energy-dispersive X-ray spectroscopy (EDX), Thermogravimetric analyzer (TGA) and X-ray photoelectron spectroscopy (XPS) instruments. Adsorption kinetics and isotherm models were investigated.

In the first study of this work (paper I), P*p*PD and P*p*PD-clay composite were successfully prepared and applied for Cr(VI) removal and reduction in aqueous solution. Characterization by XRD demonstrated that P*p*PD molecules intercalated into clay galleries. Additionally, P*p*PD functional groups dominated in the composite even though the signal bands were smaller than the pristine polymer bands indicating that there was a

formation of polymeric structure inside the organoclay interlayer spaces. Batch adsorption studies showed that pH, adsorbent dosage, contact time and Cr(VI) concentration affected the degree of adsorption. The Langmuir maximum adsorption capacity for Cr(VI) was 217.4 mg/g and 185.2 mg/g whereas for total Cr it was 193.3 mg/g and 148.8 mg/g for P*p*PD and P*p*PD-organoclay, respectively at an optimum pH of 2.

Paper II focused on the chemistry of Cr(VI) adsorption by P*p*PD and adsorbent regeneration. The adsorption mechanism on the material surface was revealed by XPS and FT-IR. Cr(VI) was reduced to Cr(III) which complexed onto the adsorbent surface at the studied pH of 2 and 8. Desorption of the adsorbed Cr was conducted using NaOH (0.05 M) and HCl (0.1 M). The P*p*PD adsorbent performed optimally for eight cycles and still retained about 80% adsorption efficiency at the 10^{th} cycle using an initial Cr(VI) concentration of 100 mg/L. Treatment with the regenerants showed irreversible oxidation reaction for the adsorbents while still removing Cr(VI) for several cycles. To investigate the toxicological impact on seed germination due to contact with used adsorbents, phytotoxicity test was investigated. Seed germination severely diminished to 35% and 14% (respective to control) in the presence of P-*p*-PD-MMT and P-*p*-PD.

In paper III polypyrrole-clay composite was synthesized and also proved to be an effective adsorbent for Cr(VI) removal. A percentage Cr(VI) removal of 99% was obtained at pH 2 using adsorbent dosage of 0.15g for 100 mg/L Cr(VI) concentration for 3h in a batch mode. Due to its excellent adsorption properties, the composite was regenerated using different varied concentrations of eluents (NaOH, NH_4OH, HCl, NH_4Cl and HNO_3). Desorption and regeneration using 0.01 M NaOH and 0.5 M HCl gave more regeneration cycles where the first 5 regeneration efficiencies were still greater than 80%.
EDX determined the elemental components of the polypyrrole-clay composite before and after Cr(VI) adsorption. It demonstrated a significant decrease of Cl^- ions after adsorption which is attributed to ion exchange mechanism between Cl^- ions and Cr(VI) during the adsorption process. Investigation of the adsorption behaviour revealed a decrease in thermal stability of the composite after several adsorption cycles while treating the adsorbent with the regenerants as a result of material oxidation and deterioration due to Cr(VI) exposure in acidic medium and the impact of the regenerants. According to FT-IR analysis, polypyrrole-clay bands shifted to a higher wavenumber after Cr(VI) adsorption

due to the change in skeletal vibrations as a result of Cr(VI) species adsorbed onto its surface.

Paper (IV) described synthesized adsorbents for phosphate removal. The study presented the development and performance of two sets of poly(phenyelenediamine) (PPD) isomers synthesized from ammonium persulphate ($(NH_4)_2S_2O_8$) and potassium dichromate ($K_2Cr_2O_7$) as oxidants. The chemical structure of the adsorbents were determined using FT-IR, TGA and XRD. Amorphous morphology dominated in all the polymers with poly(*m*-phenylenediamine) P*m*PD being more amorphous and P*p*PD was the least.

Batch adsorption studies showed improved adsorption capacity for $K_2Cr_2O_7$ synthesized polymers. $K_2Cr_2O_7$ oxidant played a major role in providing trivalent chromium metal which improved the phosphate uptake. This is attributed to the Lewis acid-base interaction where trivalent chromium acts as an acid and phosphate ions serve as a base. Batch adsorption results showed that solution pH, contact time and initial concentration influenced phosphate adsorption with the maximum adsorption capacities of 143 mg/g, 217 mg/g and 69.0 mg/l for P*o*PD, P*m*PD and and P*p*PD adsorbents, respectively. Adsorption reached equilibrium at about 300 min at an optimum pH of 2.0. The adsorption isotherms were described by Langmuir isotherm and the kinetic data were described better by pseudo-second order kinetic rate model implying adsorption onto homogeneous surfaces and the mechanism of adsorption was attributed to chemisorption. Desorption was conducted on the meta substituted PPD using NaOH (0.05 M) which displayed effective desorption capacity and exhibited commendable adsorption for re-use. The adsorbent also proved to be selective to phosphate ions at the background of much higher concentrations of sulphate and nitrate anions due to the presence of Coulombic and Lewis-acid-base interactions.

In paper (V), remediation of phosphate ions was examined using modified bentonite clay as an adsorbent. Modification was achieved by incorporating Fe, Ni and Co metal salts using precipitation method. Adsorbents were characterized by FT-IR and XRD. The results showed significant amorphosity for metal modified bentonite compared to the parent bentonite. The adsorption capacity for all studied bentonite-based materials increased with increasing initial phosphate concentration and adsorption mechanisms were influenced by the solution pH. The maximum adsorption capacity of 6.57 mg/g, 20.88 mg/g, 29.07 mg/g

and 46.95 mg/g were obtained for Bent, Fe-Bent, Ni-Bent and Co-Bent, respectively. The adsorption rate fitted pseudo-second order for all adsorbents. Langmuir isotherm model described the phosphates removal for all adsorbents at an optimum pH of 3.

ACKNOWLEDGEMENTS

"A man's dignity isn't measured by the people he has around him when he's at the peak of his success, but by his ability not to forget those who helped him when his need was greatest." Paulo Coelho.

Firstly, I would like to give thanks to the Lord almighty who sustained and carried me throughout the duration of this work. I would like to express my sincere appreciation to my lead supervisor, Prof Luke Chimuka for his encouragements, friendly supervision and for being patient with me. The confidence you have instilled in me will forever live. With that I feel prepared for any life path I'd like to choose.

I am extremely grateful for the opportunity of having to carry my research at the Council for Scientific and Industrial Research (CSIR). I am thankful to my CSIR supervisors, Dr Avashnee Chetty for always giving directions and proper planning of my PhD study. Your critics were never easy to swallow but invaluable for producing high quality of science. To Dr Mohammed Balogun for giving different approaches to mould this research work. Thank you for the sincere coaching and timely encouragement in making this task successful. Special thanks to my Competency Area Manager, Dr Mamoeletsi Mosia for giving me the opportunity to freely do my research even though her presence made me a bundle of nerves. Thank you for pushing me to complete the thesis; one side-look from you was enough for me to do my best.

I owe my appreciation to Dr Katlego Setshedi and Nomvuyo Nomadolo who supported and contributed to my work from the day of arrival. I also acknowledge Dr Vongani Chauke for proofreading and showing interest in this work. Dr Matshawandile Tukulula is acknowledged for enlightening me with the first glance of this research. Thanks also go to Polymers and Composites group for providing a warm working environment and for all the fruitful discussions in the meetings.

My sincere gratitude to Prof Maris Klavins at the University of Latvia (Riga) for hosting me in his laboratory and for providing all the chemicals. My six months stay in your lab was cheerful and productive. I thank your group in Environmental Science Department for technical assistance, particularly Mr Konstantins Viligurs, Ms Anna Trubača-Boginska, Dr Agris Bērziņš, Mr Andy Kraukli and Dr Linda Ansone for assisting with different characterization techniques. I thank Christopher Deeks and Dr Jon Treacy from Thermo Fisher, UK for assisting with XPS analysis.

Thanks to my colleagues at the School of Chemistry more especially the Environmental Analytical Chemistry Research group for a great time we shared together. To my friends at UNISA (NanoWS Research Unit), Prof Edward Nxumalo, Nozipho Gumbi (BFF), Kholiswa Yokwana and Dr Machawe Motsa thank you for microscopic analysis and for holding my hand all the way.

I am deeply thankful to my best buddy Hlakaniphani Mkhonza for all the support and understanding (lol). To my supporting family, Donsi, Thando and my best aunts, many thanks for all the love and prayers. To my friends Sindisiwe Chauke, Nozipho Gumbi, Abongile Ndamase, Heena Ranchod, Khuthadzo Mudzanani, Funeka Nkosi, Nqobile Xaba, Nomasonto Rapulenyane and Bonani Seteni thank you for insightful conversations and all the business lunches.

Finally, my special appreciation goes to the funding sources that made my PhD work possible. My PhD research was funded by the CSIR and NRF-PDP scholarship. Funding from NRF-DAAD and Erasmus Mundus (Aesop project) are also acknowledged.

PRESENTATIONS AND MANUSCTRIPS

Conference attended

Lindani Mdlalose, Mohammed Balogun, Katlego Setshedi, Luke Chimuka, Avashnee Chetty. Cr(VI) removal from water by poly(*p*-phenylenediamine)-organoclay-based composite: Adsorption behavior and mechanism. Poster presentation. SACI Gauteng North Section Young Chemist Symposium. 19 October, 2016, University of Limpopo, South Africa.

Manuscripts

I Lindani Mdlalose, Mohammed Balogun, Katlego Setshedi, Matshawe Tukulula, Luke Chimuka, Avashnee Chetty. Synthesis, characteriazation and optimization of poly(*p*-phenylenediamine)-based organoclay composite for Cr(VI) remediation. **Published** in Applied Clay Science Journal, 139 (2017) 72-80.

II Lindani Mdlalose, Mohammed Balogun, Maris Klavins, Christopher Deeks, Jon Treacy, Luke Chimuka, Avashnee Chetty. The chemistry of Cr(VI) adsorption on to poly(*p*-phenylenediamine) adsorbent. **Manuscript submitted.**

III Lindani Mdlalose, Mohammed Balogun, Katlego Setshedi, Luke Chimuka, Avashnee Chetty. Chemical regeneration of polypyrrole montmorillonite clay for Cr(VI) removal in wastewater. **Manuscript in preparation**.

IV Lindani Mdlalose, Mohammed Balogun, Maris Klavins, Luke Chimuka, Avashnee Chetty. Adsorption of phosphates from aqueous solutions by poly(phenylenediamine) isomers. **Manuscript in preparation**.

V Lindani Mdlalose, Mohammed Balogun, Katlego Setshedi, Luke Chimuka, Avashnee Chetty. Phosphates adsorption using inorganically modified bentonite clay. **Manuscript under review**.

For all the listed manuscripts, the principal author was involved in planning, performing the experiments, from adsorbents synthesis, characterization and application for pollutants remediation in water. The interpretation of data, writing and revision of manuscripts were done by the principal author. Co-authors revised the manuscripts and suggested improvements.

TABLE OF CONTENTS

Section ***Page***

LIST OF FIGURES

Figure ***Description*** ***Page***

LIST OF TABLES

LIST OF ABBREVIATIONS

ADPA	Aminodiphenylamine
BET	Brunauer-Emmett-Teller
Cr(VI)	Hexavalent chromium
Cr(III)	Trivalent chromium
1,5 DPC	1,5 diphenlycarbazide
DPA	Diphenylamine
DAN	Diaminonaphthalene
EDTA	Ethylenediaminetetraacetic acid
ETAAS	Electrothermal atomic absorption spectroscopy
FI	Flow injection
FT-IR	Fourier-transform infrared spectroscopy
GPC	Gel permeation chromatography
HPLC	High performance liquid chromatography
IC	Ion chromatography
ICP-MS	Inductively coupled plasma mass spectrometry
LC	Liquid chromatography
LOD	Limit of detection
PANI	Polyaniline
PD	Phenylenediamine
Ppy	Polypyrrole
PPD	Polyphenylenediamine
P*m*PD	Poly-meta-phenylenediamine
P*o*PD	Poly-ortho-phenylenediamine
P*p*PD	Poly-para-phenylenediamine
SEM	Scanning electron microscopy
TEM	Transmission electron microscopy
TGA	Thermogravimetric analyzer
XPS	X-ray photoelectron spectroscopy
XRD	X-ray diffractometer
XRF	X-ray fluorescence

CHAPTER 1

INTRODUCTION

1.1. Background

Water is indispensable to life. It sustains life and good health but it is also essential for many industries and agriculture. Over the years the amount of potable water has been diminishing and is now a scarce commodity. This can be attributed mainly to rapid industrial growth, increased and intensive agricultural activities, growth of megacities and the attendant rural-to-urban migrations and unreliable rainfall and rain distribution (WWF, 2013).

South Africa is one of the driest countries in the world (WWF, 2013). According to available data the country experiences only half of the global rainfall average annually (DWAF, 2008). This classifies it as a semi-arid region. While much of the available water is used for agricultural and domestic purposes the major mining and mass production industries also depend on this scarce resource. These sectors of the economy, especially the mining industry, generate significant volumes of wastewater which pose serious contamination risks to the rest of the fresh water resource. Most notably, there has been an outcry about the environmental dangers of acid mine drainages (Council for Geoscience, 2010). The alarming headlines have ignited frantic searches for new and more efficient methods to treat and handle the toxic effluents.

Industrial wastewater is often a toxic milieu of numerous pollutants. It contaminates ground water as a result of the discharge leaching into the soil. According to the postulated principle of Integrated Water Resources Management (IWRM), water is considered as a system which is ground water at some point which eventually becomes surface water. Therefore, contamination of ground water can severely endanger the entire water system. Hence, release of wastewater to the environment requires maximum prudence (van der Zaag, 2006).

1.2. Problem statement and motivation

The quality of water is defined as poor when certain characteristics such as colour, suspended matter, turbidity, pathogens, hardness, taste, odour and harmful chemicals are in excess (van der Zaag, 2006). The presence of significant amounts of dissolved harmful

chemicals (both organic and inorganic) in water has been of interest to environmentalists due to the adverse effects they have on human and animal health. In particular, heavy metals present a serious challenge even in low concentrations since they tend to bio-accumulate in organisms such as fish and are readily shuttled along the food chain. When effluents containing complex mixtures of pollutants are discharged into ground water, they get incorporated rendering toxic water. Thus, the presence of toxic heavy metals and anions are of concern.

Cr is the seventh most abundant component on earth. Like most heavy metals, Cr get introduced into natural water bodies from a variety of production industries and from corrosion inhibitor used in water pipes. The toxicity of chromium (Cr) mainly depends on its chemical speciation with common oxidation states being Cr(0), Cr(III) and Cr(VI). In the terrestrial environments, trivalent and hexavalent Cr are the most stable oxidation states while Cr(0) is the solid metallic form produced mainly from steel manufacturing(Oliveira, 2012). At low concentrations, Cr(III) is essential for mammal metabolism whereas Cr(VI) state is highly toxic and may cause death to humans and animals if consumed in large doses (Zayed, et al., 1998). Cr(VI) ions exist in different chromate forms depending on the pH present and redox potential. Cr(VI) is extremely soluble with great mobility through membranes and in the environment (Oliveira, 2012). Cr(III) form on the other hand tends to precipitate at usual ground water pH conditions. Since Cr(VI) is defined 500 times more toxic than Cr(III), the Cr(VI) effluents to surface water regulated by USEPA is below 0.05 mg/L while less than 2 mg/L is regulated for total Cr (Gupta et al., 2010). All Cr(VI) principal species are a threat to living organisms and may cause lung cancer, skin irritation, kidney and liver damage (Gupta et al., 2010; Miretzky et al., 2010).

Phosphorus element has always been recognized as an essential nutrient for living organisms. However, excessive concentrations of phosphorus adversely affect aquatic ecosystems such as rivers and lakes. Enrichment of water bodies by phosphorus result in dense growth of plants including algae and it impacts on the ecological balance of the affected water. This excessive plant growth brings about subsequent harmful effects of eutrophication. With progressive eutrophication stages, dissolved oxygen depletes to perilously low levels causing fish death, filter congestion, unpleasant odour of water and deterioration of recreational and aesthetic values. These circumstances are consequently

risky to human health as a result of exposure to waterborne toxins. In light of more stringent environmental standards and regulations concerning phosphorus in water, the U.S. Environmental Protection Agency has recommended that the total phosphorus should be below 0.05 mg P/L in a watercourse where it goes into a lake and should not go beyond 0.1 mg/L in rivers that do not release directly into either lakes or reservoirs (Loganathan et al., 2014).

Various techniques have been applied for the uptake of oxo-anions in aqueous solutions. These include coagulation, solvent extraction, chemical precipitation, ion exchange, adsorption and membrane technologies (Subramani & Jacangelo, 2015). They suffer from one or more shortcomings which include high capital costs, incomplete metal removal, consumption of many reagents, generation of secondary pollution and high volume of toxic sludge generation (Lata, et al., 2015). There is a need to develop better technologies for the removal of toxic oxo-anions in wastewater. New materials with high binding capacities, even in low pollutant concentrations are required.

Adsorption technology is gaining in popularity due to its simplicity and versatility of making adsorbents. Among a vast of developed adsorbents, polymeric adsorbents have been widely studied due to their varied functional groups and tuneable structures. The polymers of the polyaniline family, to which polyphenylenediamine belongs, have been well researched in water treatment processes (Stejskal, 2015). They are able to recover heavy metals like the most investigated conducting polymers (polyaniline and polypyrrole) (Li et al., 2009; Skodova et al., 2013). Studies have been carried out to assess the adsorption ability of these polymers and it derivatives for various pollutants ranging from anionic to heavy metals (Yu et al., 2013; Zhao et al., 2010; Zhang et al., 2012).

In view of developing low cost, easily available and effective adsorbents, matrix such as clay, have been implemented as support materials to make polymer composite adsorbents. For well dispersed filler within the matrix, small amounts of filler are utilised to achieve high performance efficiencies. Clay is readily available and cheap. It is made of phyllosilicate minerals containing silicon, hydroxides and aluminium oxides. Layers of clay are negatively charged and frequently stabilized by interlayer cations like sodium and potassium (Mabrouk et al., 2010). Molecules of water intercalate between the layers

expanding clay structure, as a result the dissolved ions diffuse into the interlayer space (Lin et al., 2010).

Composites offer a number of advantages in adsorption technology in terms of its properties and performance as adsorbents (Setshedi et al., 2013). In clay-based polymer composites, polymers with functional groups containing donor atoms like nitrogen enhances the adsorption performance of clays towards different pollutants, while keeping the adsorbent cost low.

In this work, we developed clay based polymer composites and functionalized polymer adsorbents to remediate Cr(VI) and phosphate ions from wastewater. Aromatic amine polymers ie. PPD and Ppy were chosen for this study since they readily prepared by oxidation polymerization and they possess ion exchange and redox properties. Determination of chromium species present in water and on the adsorbent surface after Cr(VI) removal was one of the key areas of the study to be investigated. Another focus was to enhance phosphate ions remediation through modification of polymeric matrix and clay particles with metallic groups which are capable of complexing phosphate ions. Among the various adsorbents, imine/ amine based polymers and inorganic metal oxide were often reported for phosphate removal. However these conventional adsorbents regularly exhibit low selectivity in the presence of other competing ions and also low sensitivity at low phosphate concentration. In this research, facile synthesis methods were developed to improve the removal of phosphate ion in aqueous solution. The primary constituents of the prepared adsorbents included polymeric backbone with nitrogen donor groups and Lewis-acid type metal-cation to strongly coordinate with the phosphate ions through ligand exchange mechanism.

1.3.Thesis outline

The thesis is divided into the chapters below:

Chapter 1

General introduction, problem statement and project justification are briefly discussed.

Chapter 2

This chapter gives the literature review of polymers of aromatic diamines and derivatives, synthesis, environmental applications and analytical methods used to determine chromium and phosphate ions

Chapter 3

The research objectives and approach are presented in this section.

Chapter 4

This chapter contains a collection of five manuscripts which have been produced from this work, and indicated below.

Paper I

In this paper the synthesis, characterization and optimization of poly(*p*-phenylediamine)-based organoclay composite for Cr(VI) remediation is reported

Paper II

In this paper, the chemical interaction of poly(*p*-phenylediamine)-based adsorbents after Cr(VI) removal and the regeneration of the adsorbents are investigated.

Paper III

In this paper, effect of different eluents for chemical regeneration of polypyrrole-montmorillonite clay composite for Cr(VI) removal is reported

Paper IV

In this paper, different synthesis methods of poly(phenylenediamine) isomers and application on the adsorption of phosphates from water are described.

Paper V

In this paper simple modification of bentonite clay by metal salts and its ability for phosphates adsorption in water is reported.

Chapter 5

The overall conclusion from all five technical manuscripts is given and recommendations are presented in this chapter.

References

Council for Geoscience (2010) Mine water management in the Witwatersrand Gold Fields with special emphasis on acid mine drainage. Report to the inter-ministerial committee and acid mine drainage December 2010.

DWAF (2008) Report of the department of water affairs and forestry April 2007 to March 2008.

Gupta, V.K., Rastogi, A., Nayak, A., 2010. Journal of Colloid and Interface Science Adsorption studies on the removal of hexavalent chromium from aqueous solution using a low cost fertilizer industry waste material. *Journal of Colloid And Interface Science*, 342(1), pp.135–141.

Lata, S., Singh, P.K. & Samadder, S.R., 2015. Regeneration of adsorbents and recovery of heavy metals: a review. *International Journal of Environmental Science and Technology*, 12(4), pp.1461–1478.

Li X, Ma X, Sun J, Huang M., 2009. Powerful Reactive Sorption of Silver (I) and Mercury (II) onto Poly (o -phenylenediamine) Microparticles. *Langmuir*. 25, pp.1675–1684.

Loganathan, P., Vigneswaran, S. & Kandasamy, J., 2014. Removal and Recovery of Phosphate From Water Using Sorption. *Environmental Science & technology*, 44, pp 847-907.

Miretzky, P. & Cirelli, A.F., 2010. Cr (VI) and Cr (III) removal from aqueous solution by raw and modified lignocellulosic materials : A review. *Journal of Hazardous Materials*, 180(1–3), pp.1–19.

Oliveira, H., 2012. Chromium as an Environmental Pollutant : Insights on Induced Plant Toxicity. *Journal of Botany*., 2012, pp 1-8..

Škodová J, Kopecký D, Vrňata M, 2013. Polypyrrole–silver composites prepared by the reduction of silver ions with polypyrrole nanotubes. *Polymer Chemistry*, 4(12), p.3610.

Stejskal, J., 2015. Polymers of phenylenediamines. *Progress in Polymer Science*, 41(C), pp.1–31.

Subramani, A. & Jacangelo, J.G., 2015. Emerging desalination technologies for water treatment: A critical review. *Water Research*, 75, pp.164–187.

Van der Zaag P, Savenije H. Water as an economic good: The value of pricing and the failure of markets. Value of water research report series No. 19, July 2006.

Yu W, Zhang L, Wang H, Chai L., 2013. Adsorption of Cr(VI) using synthetic poly(m-phenylenediamine). *Journal of hazardous materials*, 260, pp.789–95.

WWF and CSIR, 2013. An introduction to South Africa's Water Sources Areas: Report , pp. 1-29.

Zayed, Adel, C Mel Lytle, Jin-hong Qian, and Norman Terry. 1998. Chromium Accumulation , Translocation and Chemical Speciation in Vegetable Crops . *Planta* 206 pp. 293-299 .

Zhang L, Wang H, Yu W, Su, Z., Chai, L., Lia, J., Shia, Y., 2012. Facile and large-scale synthesis of functional poly(m-phenylenediamine) nanoparticles by Cu2+-assisted method with superior ability for dye adsorption. *Journal of Materials Chemistry*, 22(35), p.18244.

Zhao P, Jiang J, Zhang F, Zhao W, Liu J, Li R., 2010. Adsorption separation of Ni(II) ions by dialdehyde o-phenylenediamine starch from aqueous solution. *Carbohydrate Polymers*, 81(4), pp.751–757.

CHAPTER 2

LITERATURE REVIEW

Polymers of aromatic amine and derivatives: The synthesis, environmental applications and analytical methods to determine chromium and phosphate ions

---

2.1 Polymers of aromatic amines and derivatives: Their synthesis and environmental applications

Phenylamine polymers such as polyaniline (PANI) (with its derivative copolymers) are one of the most studied class of conductive polymers (Stejskal, 2015). For years, PANI has been considered a material with good properties such as environmental stability, high electrical conductivity and gas separation efficiencies (Stejskal, 2015). Extensive research provided that these polymers exhibit potential applications in light emitting diodes, batteries, electrocatalyst, electronic devices, corrosion inhibitors, sensor, and as detectors (Li et al., 2002). Thus far, phenylamine polymers have been prepared by several techniques namely: chemical oxidative polymerization, electrochemical, photo-induced electron-transfer, photo-oxidative polymerization, and plasma polymerization (Li et al., 2002).

However, challenges such as insolubility in common organic solvents and poor mechanical properties restrict its practical use. More investigations on aromatic diamine polymers have been studied lately as they have shown various advanced functions in comparison to PANI and other mono phenylamine polymers. Multifunctionality in aromatic diamines is due to additional free amino group per polymer repetitive unit (Li et al., 2010).

The most studied aromatic diamine monomers which are susceptible to oxidation polymerization include phenylenediamines (PDs) (*o*-PD, *m*-PD, *p*-PD), diaminonaphthalene (DAN) (1,8 DAN, 2.3 DAN, 1.5 DAN) and aminodiphenylamine (ADPA) (4-ADPA, 2-ADPA) (Fig 2.1). Polymerization for respective monomers occurs via oxidation of one or both amino functional group to give linear polyaminoaniline, linear polyaminonaphthylamine, ladder polyphenazine and phenazine segment containing polymers. While many studies have focused on aromatic diamines with a primary amine on the aromatic structure, numerous other studies particularly for industrial applications focus on diphenyl amine (DPA) polymers which have secondary amine on the aromatic structure (Li et al., 2008). DPA and its derivatives are predominantly used as a stabilizing compound for mono or multi-base missiles propellants and explosives containing nitrocellulose (Li et al., 2008). They are also subjectable to polymerization by several techniques such as chemical oxidation, electrochemical and mechanochemical polymerization. DPA also display improved solubility properties compared to PANI (Li et al., 2008). The different properties are associated with different changes in the backbone arrangements during polymerization. In

short, the polymerization of aniline and substituted anilines proceed through the formation of N-C coupling while for DPA it is said to occur through 4,4-phenyl phenyl coupling mechanism (Stejskal, 2015a).

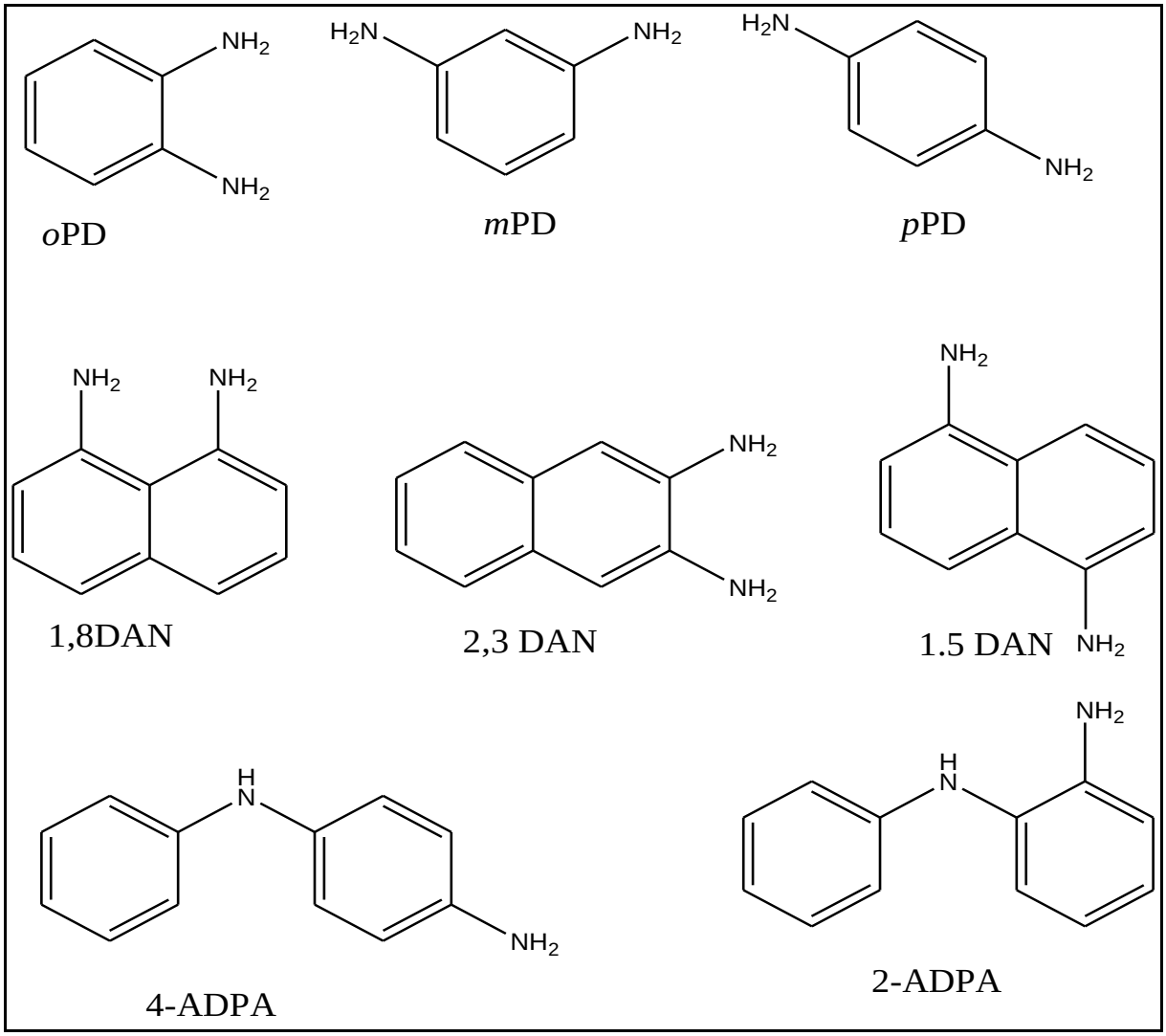

Fig 2.1: Examples of aromatic diamine monomers cited to make polymers in this review

Maximum attention has been devoted to conducting polyaromatics such as polypyrrole (Ppy) and PANI (Gok & Sari, 2002; Guimard et al., 2007). The conductivity and other properties of polyaromatics can also be altered significantly by doping for the interest of showing their potential application in high energy density batteries, solar cells and other electronic devices. Of late, there is a plenty of scope on using PANI derivatives (Wang et al., 2016). Anilines with various substituents like alkyl and alkoxy on the aromatic ring also make PANI derivatives through oxidative polymerization (Gok & Sari, 2002). These were also found to exhibit enhanced solubility in most organic solvents but give low molecular weight compared to PANI. The unique properties of polyaromatic amines which include their charge

conjugation asymmetry and high redox activity encourage more evaluations from the chemistry point of view (Wang et al., 2016). The present work is devoted to principles of polyaromatic diamine synthesis using different approaches. Their use in detection of pollutants in complex environmental matrices is discussed with emphasis on their potential as solid adsorbents.

2.1.1 Polymerization techniques

Different methods of polymerization can be used to obtain polyaromatic diamines. This section describes three polymerization techniques for synthesis of polyaromatic diamines used for environmental pollution monitoring and remediation. Some possible structures are shown in Fig. 2.2.

2.1.1.1 Chemical polymerization

Chemical oxidation polymerization method is the most widely used protocol for the production of poly aromatic diamines and poly diphenylamines owing to its simplicity. The polymerization mechanism is assumed to occur according to cation-radical interaction followed by poly recombination of cation-radical intermediates during oxidation (Orlov et al., 2006). In accordance with the cation-radical mechanism, primary amine undergoes polymerization via N-C dimerization (head-to-tail addition) in contrast to diphenylamine which undergoes C-C dimerization (tail-to-tail addition) of the monomer due to nitrogen atom causing steric hindrance.

Although fundamental investigations have been carried out to genuinely understand the polymerization mechanisms which include chain propagation and how the poly conjugated chain grow to preserve the activity centre until the termination step, the definite answer is not well-known. Possible structures have been reported in literature for different polyphenylene diamine and polydiphenylamines (Huang et al., 2006). The chemical oxidation method is scalable for a wide variety of poly aromatic amines. It occurs by introducing an oxidant into a reaction mixture of a monomer solution. For a typical reaction, a measured amount of monomer such as p-phenylenediamine is dissolved in a minimal amount of diluted hydrochloric acid solution. The solution is further mixed with an oxidant such as ammonium peroxydisulphate. Upon oxidant addition, there is a rapid change of solution colour related to

poly aromatic diamine formation which is left for 24 hours. The crude product residue is collected by filtration and washed using deionized water.

In the case of phenylenediamine isomers, it was discovered that polymerization strongly depends on the monomer structure as well as the solution polymerization medium (Huang et al., 2006). As listed in Table 2.1, a higher yield for P*m*PD was obtained in water than in HCl while for P*o*PD and P*p*PD HCl and glacial acid gave higher yields when ammonium peroxydisulphate. The lower polymerization product was speculated to be due to lower molecular weight resulting from weaker capability to polymerize in a chosen medium hence the polymers show different macromolecular structures (Huang et al., 2006). The polymerization reaction of aromatic diamines like phenylenediamines are prepared in acidic medium (HCl and glacial acetic acid) using effective oxidants including persulphate, iodine, hydrogen peroxide, iron (III) chloride, ceric ammonium nitrate and copper nitrate (Stejskal, 2015). Persulphates are frequently used and added dropwise during the reaction to obtain high molecular weight since the process is highly exothermic (Stejskal, 2015). The resulting product is usually dried at 60 °C or lower to avoid possibilities of polymer crosslinking (Xin et al., 2002).

The chemical oxidative polymerization of pyrrole (Ppy) is generally initiated by using oxidizing agents such as ferric (III) chloride, peroxydisulfate, diazonium salts, ozone, nitrous acid and lead dioxide (De Jesus et al., 1997). Ferric (III) chloride is the most commonly used oxidant in solutions containing dopants such as chloride, perchlorate and nitrate ions (Muhammad et al., 2016). These anions exhibit anion exchanging behaviour due to its high mobility in the polymer matrix. The Ppy coupling mechanism involves pyrrole oxidation to form radical cation which then links with another radical/monomer to form a dimer and lastly the double charged dimer mislay two protons to re-aromatize to form an easily oxidizable stable dimer which leads to oligomers and eventually a polymer (Blinova et al., 2007).

Polymerization of DAN is traditionally made by electrochemical oxidation polymerization (see Section 2.1.1.2). During the process, this polymer adhere tight and become dense to the electrode which generally makes it hard for further polymerization of residual monomer. Additionally electrochemical oxidation polymerization produces lower yields. As an alternative way of improving polymerisation efficiency and specific surface area of the polymer, chemical oxidation polymerization was implemented using ferric chloride and

ammonium persulphates as oxidants (Li et al., 2004). Seemingly, ammonium peroxydisulphate gave a lower polymerization yield than ferric chloride due to residual of iron in the polymer which was confirmed by ICP and XRF analysis. Furthermore, the iron chloride oxidant produced a ladder chain with minimal $–NH_2$ groups whereas ammonium persulphate presented a linear chain with more free $–NH_2$ groups. This was further confirmed by a low adsorption capacity for silver for iron oxide synthesized polymer than ammonium persulfate polymer, with additional $–NH_2$ groups in the latter to bind with the silver ions under same experimental conditions (Li et al. 2004).

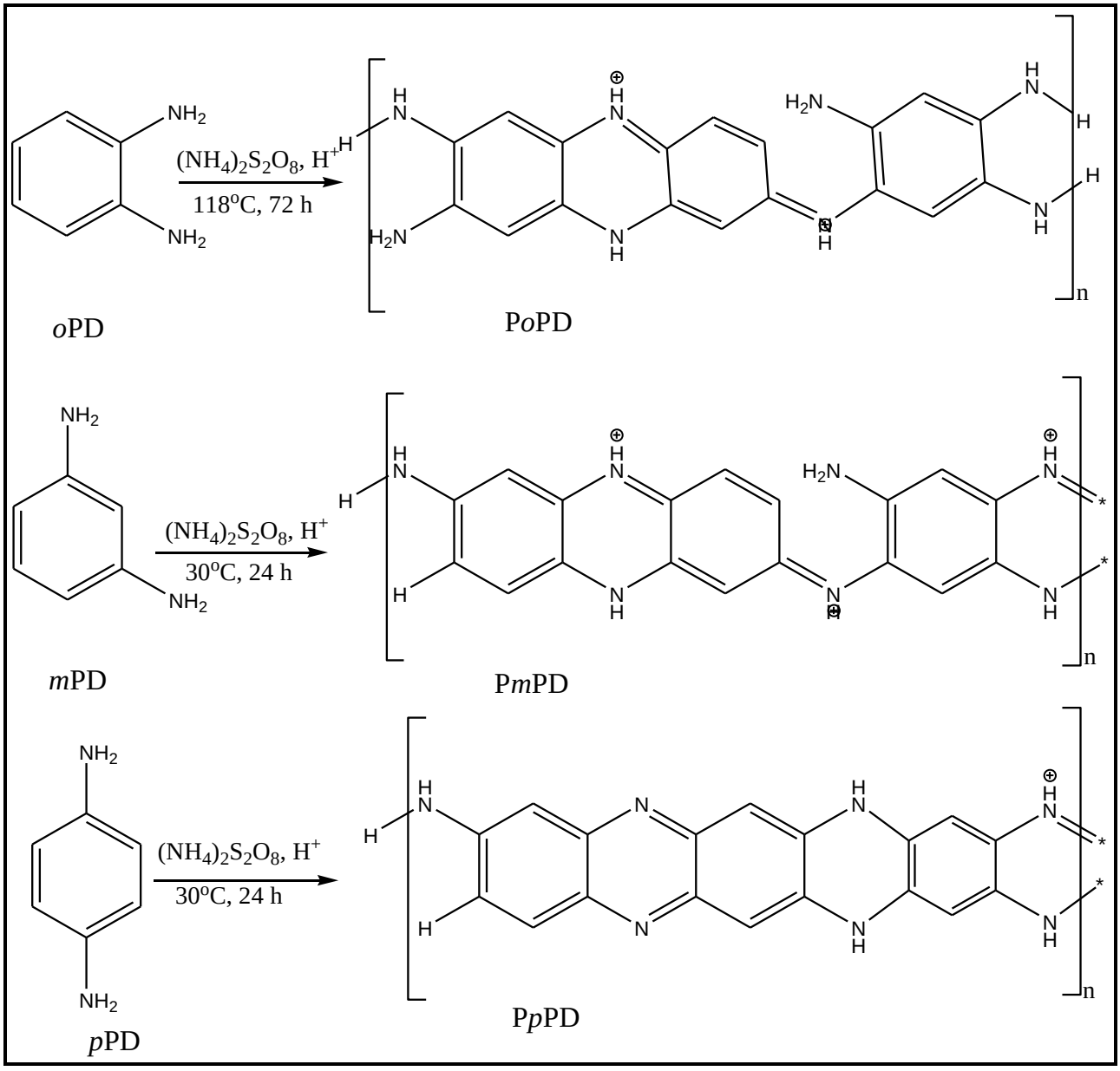

Fig. 2.2 Possible structures of Poly *p*-, *m*-, and *o*-phenylenediamines

Table 2.1:Physical properties of PPD isomers obtained by chemical oxidation polymerization reaction using ammonium peroxydisulphate (Huang et al., 2006).

Polymers micro-particles	Medium	Temperature °C	Solubility in H_2O, HCl, NaOH	Yield (%)
P*p*PD	HCl (1 M)	30	Insoluble	90
P*p*PD	H_2O	30	Partly soluble	80
P*m*PD	HCl (1 M)	30	Insoluble	45
P*m*PD	H_2O	30	Insoluble	83
P*o*PD	CH_3COOH	118	Insoluble	96
P*o*PD	H_2O	100	Partly soluble	80

2.1.1.2 Electrochemical polymerization

Aromatic amines can also be polymerized using electrochemical oxidization technique by cyclic voltammetry (potentiodynamic), constant potential (potentiostatic) and constant current (galvanostatic) (Li et al., 2002). Polymerization is basically attained by the existence of electrical current through a solution of the monomer, solvent and electrolyte mixture. As compared to the previously mentioned chemical oxidation polymerization method which yields a bulk and powdery polymer, this system produces thin films which are deposited at the electrode surface. The most suitable power supply in the cell is cyclic voltammetry because it reveals the reversibility of electron transfer during the polymerization and also scans the electroactivity of the polymer film. However, all the mentioned power suppliers are regularly used to quantitatively assess the macroscopic growth of polymer films. The cyclic voltammetry constantly verified throughout polymerization is dependent on the species and concentration of the monomer, electrolyte and electrode used.

Electropolymerization process has been found convenient for immobilizing conductive polymers on various substrates by controlling the electrochemical parameters at the electrode surface. This polymer modified electrode have shown improved sensitivity, selectivity and

reduced fouling effects in many applications. Hathoot et al. (2012) prepared poly 1,5 DAN by means of repeated potential cyclic method on a glassy carbon electrode surface. The polymer growth was simply observed by suppression of the intensity of the monomer oxidation peak current in successive potential cycles. The modified electrode was later rinsed with distilled water to remove impurities.

The same electropolymerization procedure for poly 1,5 DAN synthesis was carried out on a Pt electrode by cyclic voltammetry in 1.0 M $HClO_4$ solution (GuedesdaSilva et al., 2011). The voltammograms were carried out between -0.1 V and +0.9 V for several scans and the obtained film was thoroughly rinsed with deionized water. Scanning electron microscope characterization showed a relatively homogeneous polymer with a porous structure.

Phenylenediamine isomers were also electropolymerized on palladium glassy carbon electrode to give polyphenylenediamine. Potentiostatic technique and cyclic voltammetry were compared upon electropolymerization. The voltammetric behaviour for *o*PD and *m*PD displayed a continuous decrease in oxidation current with the minimal current observed after about 60 cycles (Dai et al., 2006). This indicated that the formation of P*o*PD and P*m*PD films hindered further contact of monomers to the electrode surface. As a result of poor conductivity no peak reduction was observed during the formation of these polymers. On the other hand, during *m*PD electropolymerization, there was rapid decrease in the current signal with a broad oxidation peak at +0.64 V in the first volumetric scan. Potentiostatic polymerization agreed with the cyclic voltammetry. The *m*PD oxidation potential was the utmost positive among the PD isomers. These findings were consistent with phenylenediamine isomers electropolymerization using platinum glassy carbon electrode (Zhou et al., 2010).

Ppy is usually synthesized by electrochemical approaches, where pyrrole is dissolved in a solvent in the presence of an electrolyte (Maksymiuk, 2006). The conductive form of Ppy is directly produced at the anode of an electrochemical cell and combines the electrolyte as a counterion. The film properties are controlled by varying the electrolyte, concentration, temperature or the current used for the polymerization process (Maksymiuk, 2006).

2.1.1.3 Enzyme-catalyzed oxidative polymerization

Polyaromatic amines can also be produced by means of an enzyme catalysed oxidation process. This method has aroused research interest because it is an environmentally benign procedure. A typical procedure for enzyme-catalyzed oxidative polymerization in a homogeneous system involves horseradish peroxidative as a catalyst in a mixture of 1,4-dioxane and phosphate buffer to give out polymeric materials (Li et al., 2002). The method is dependent on the reaction time, solvent composition, monomer properties and the amount of oxidant. It has been noted that a high concentration of the solvent (1,4-dioxane) results in sharp decrease of polymerization yield. This was assumed to be due to the catalyst (horseradish peroxidative) denaturation by 1,4-dioxane. Polymer yields with high molecular weight of black powder are obtained with the increased monomer and oxidant amount. There is limited advanced work done on enzyme-catalzed polymerization for aromatic amines in comparison to chemical and electro-oxidation polymerization. With that, not enough characterization on macromolecular structure, properties and functionality of the polymers have not been well investigated.

Comparing chemically, electrochemically and enzyme-catalyzed oxidization polymerization of aromatic amines with respect to polymerization conditions and the resulting polymers reveals that each technique has its unique feature for the synthesis. When a fine polymer product is required for application, electrochemical polymerization is preferable while from the view point of mass production, chemical polymerization is more appropriate since it fast and does not require unique experimental design. For this research we devised a simple chemical polymerization method where we could even incorporate clay solid support to tailor aggregation performances of the polymers.

2.1.2 Adsorption of trace elements and phosphates from water

There is a growing demand for remediation of polluted water from industrial activities as contaminated water poses a serious threat to humans and the environment. Heavy metals for example are directly or indirectly discharged into aqueous streams and are cumulative poison which does not break down in the environment. They are described as elements with atomic weight between 63.5 g/mol and 200.6 g/mol and atomic density greater than 5 g/cm^3 (Fu & Wang, 2011). The toxic metals of concern in industrial wastewater treatment plants include zinc, copper, nickel, mercury, cadmium, lead and chromium (Uddin, 2017). Chromium compounds are extensively used in industry for various purposes. The effluents of these

industries may get released into aquatic environment. This metal is listed as one of the top 26 toxic metals according to USEPA. The discharge limit is regulated to be only 0.05 mg/L (Yu et al., 2013).

Water purification methods such as chemical precipitation, membrane filtration, biological treatment and adsorption has been explored in industry for removal of contaminants (Ihsanullah et al., 2016). Some of the constraints with some of these technologies include high equipment and energy costs, incomplete contaminant removal, generation of sludge, need for specialized skills, and complexity for implementation.

Adsorption however, has proved to be a capable and widely used approach because it is easy to implement and produces fewer toxic by-products (Ihsanullah et al., 2016). In order for an adsorbent to be considered a good adsorbent; it should achieve high adsorption rates, be robust, and have a number of binding sites for pollutants. Most importantly it must be cheap, be easy to make and recyclable (Zanella et al., 2014). Taking into consideration the number of functional groups such as amines and aromatic moieties in polyaromatic amines (diphenylamines and phenylenediamines), they are expected to offer numerous binding sites for metals and organics. Interactions which are possible to enable binding of pollutants onto polyaromatic amines include electrostatic attraction, coordination or complex formation, hydrogen bonding and π-π stacking interaction, which has inspired broad research on these polymers as adsorbents.

The polymers of aniline family are known to be effective adsorbents for heavy metals, noble metals and aromatic pollutants (Olad et al., 2007; Stejskal, 2014). Polymer composites and controlled morphology structures of these polymers are well predetermined for water purification application as shown in Table 2.2.

A typical example is the use of different oxidation states of P*m*PD as an adsorbent for Cr(VI) ions in water as reported by Yu et al. (2013). P*m*PD can bind Cr(VI) ion in water through electrostatic interactions with Cr(VI) and reduction of Cr(VI) to Cr(III), enables chelation of Cr(III) onto the polymer surface as indicated in. The study highlighted the strong oxidizing character of Cr(VI) in acidic medium which enabled formation of Cr(III) on the adsorbent following the equation below:

$HCrO_4^- + 7\ H^+ + 3e^- \rightarrow Cr^{3+} + 4\ H_2O$

The adsorption ability of Cr(VI) ions was observed to be highly dependent on solution pH where pH 2 was the optimum. Furthermore, different oxidation states of the polymer obtained when changing the polymerization medium (i.e. H_2O, 1 M NaOH and 2 M NaOH) played a major role, with 2 M NaOH (lowest oxidation state) giving the highest adsorption capacity of 500 mg/g at a shorter time for Cr(VI) uptake.

Li et al. (2011) described poly(aniline-1,8-diaminonaphthalene) synthesis and its application for selective removal of Cr(VI) ions from water. Adsorption mechanism agreed with the above study when using P*m*PD as an adsorbent. It was proven that Cr(VI) ions removal was due to electrostatic adherence on the protonated amino groups in acidic medium which then accelerates the redox reaction and formation of Cr(III) ions which are held by adjacent amine groups through metal coordination. The presence of competing ions such as K^+, Ca^{2+}, Mg^{2+} had no significant effect on Cr(VI) removal, while SO_4^{2-} and CO_3^{2-} substantially competed with Cr(VI) on the adsorbent binding sites.

Polyaromatic diamines are also found to be effective in removing cationic heavy metals. A controlled morphology structure of P*p*PD was synthesised for Pb ion remediation in water (Wang et al., 2008). Upon synthesis, poly(-N-vinylpyrrolidone) (PVP) was used as a surfactant to control the morphology of the polymer particles. The optimal adsorption capacity was 1300 mg/g which was again estimated to increase to 2890 mg/g when decreasing the adsorbent dosage for batch studies. UV-Vis measurements showed by the formation of new absorption bands that there is a formation of a complex between polymer ligands and Pb ions.

According to Huang et al. (2007), the adsorption mechanism for the removal of Pb ions using P*m*PD was mainly due to amine/imine (=N-/-NH2) groups from adsorbent binding sites that is capable of binding a Pb metal ion through sharing an electron pair to form a metal complex. The main objective of the study was to investigate adsorption and desorption of lead ions. The chosen eluents for regeneration were HCl, HNO_3 and EDTA. It was discovered that for practical reusability, EDTA was the most effective eluent compared to HCl and HNO_3. EDTA gave the highest Pb ions desorption of 94.2% in 30 min. Regeneration using HCl and HNO_3 was basically an ion exchange mechanism where the H^+ ions exchange with Pb^{2+} adsorbed on the material. On the other hand EDTA forms a stable Pb complex due

to the presence of nitrogen and oxygen atom in the carboxyl group with lone pairs that could easily bind the metal ion through electron sharing (Huang et al., 2007).

Bhaumik et al. (2011) carried out an investigation on chemical regeneration of polypyrrole/Fe_3O_4 magnetic nanocomposite used for Cr(VI) adsorption. Optimum Cr(VI) desorption was obtained using 0.5 M NaOH where 14% of Cr(VI) could be extracted and 2 M HCl was used to leach out the reduced form of Cr(VI) to Cr(III). The degree of reduction was confirmed by determining the total Cr remaining in the solution using ICP-OES and XPS analysis for adsorbent surface (Bhaumik et al., 2011). The composite was successfully re-used for two adsorption cycles without loss of its initial adsorption capacity. Polyacrylonitrile/Ppy nanofiber loaded with Cr(VI) presented better re–use performance of five cycles when 0.01 M NaOH was used for Cr(VI) desorption compared to 0.05 M NaOH and 5% ammonia (J. Wang, Pan, He, & Cao, 2013c). For 0.05 M NaOH only three cyles were achieved and the reason was based on the instability of Ppy at high alkaline conditions (J. Wang et al., 2013).

The discharge of nutrients such as phosphates into water channels has been identified a risk to natural environments due to severe effects of eutrophication. Thus the improvement on the removal of phosphate in water is vital. Among various adsorbents reported for phosphates removal, aromatic amine polymers were seldom investigated.

Wang et al. (2017) described PANI fabricated with titanium dioxide (TiO_2) for the removal of phosphates from contaminated water. The superior performance was due to PANI adsorption sites (amine/imine) and hydrated titanium oxide species at a pH range of 1-6. The maximum adsorption capacity fitted by Langmuir isotherm was 12.11 mg/g. According to XPS analysis, the main adsorption site for phosphates arose from the TiO_2 component shown by a binding energy at 133.14 eV indicating strong Ti-P interaction. The exhausted adsorbent was treated with NaOH (0.1 M) to desorb phosphates and HCl (0.1 M) was used as a regenerant. PANI contribution on adsorption was puny, however, its reversible redox properties played a major role for adsorbent regeneration. Doping PANI with HCl introduced chloride ions which supported phosphate removal through ion exchange as was confirmed by EDS analysis. The regenerated adsorbent presented 98% of phosphate removal after 5 cycles. According to this study, the overall adsorption mechanism was attributed to electrostatic attraction, hydrogen bonding and ion exchange (Wang et al., 2017).

PANI nanofibers modified with natural silica and HCl treated silica were also prepared for phosphate removal (Najim at al., 2017). The fibers are presumed to have more superior properties compared to the conventional bulk PANI. Phosphate adsorption kinetics were found to be higher for HCl treated natural fiber than natural silica fiber. Phosphate initial concentration was 20 mg/L and 39.85% and 20.75% removal was obtained for acid treated and non-treated silica fibers respectively at pH 1. This was associated with anion exchange process between chloride ions from the acid treated fiber and phosphates. Chloride ions act as a mobile dopant on the PANI surface and readily exchange with phosphate anions. Higher removal percent for acid treated silica fiber was also due to its high surface area which allowed access to phosphate ions (Najim et al., 2017).

Ppy coated sawdust was also used as a cost effective adsorbent for phosphate uptake (Bajpai et al., 2009). The maximum adsorption capacity of 30.39 mg/g was obtained at 50 °C. Removal process was mainly associated with ion exchange between chloride ions (from iron chloride oxidant) and phosphate in acidic pH. The positively charged pyrrole rings contributed on phosphate removal through electrostatic interaction (Bajpai et al., 2009).

This section showed that polymers of aromatic amine are more effective in trace elements removal particularly Cr(VI) than phosphate ions. These polymers perhaps require modification with strong Lewis acids to immobilization phosphate ions which has strong ligand strength.

Table 2.2: Adsorption of trace elements by poly aromatic diamine based materials

Adsorbent	Characterization techniques	Pollutant	Adsorption Capacity (mg/g)	Kinetics	Reference
Poly(*m*-phenylenediamine)	BET, FT-IR, XPS, XRD and TGA	Cr(VI)	500	Pseudo-2nd order	(Yu et al., 2013)
Poly(*m*-phenylenediamine)/ palygorskite	SEM, FT-IR, and BET	Cr(VI)	153	Pseudo-2nd order	(Xie et al., 2014)
Poly(*m*-phenylenediamine)/Fe3O4/o-MWCNTs	TEM, FT-IR, and XRD	Cr(VI)	346	Pseudo-2nd order	(Tian et al., 2015)
Poly(aniline-1,8-diaminonaphthalene)	FT-IR and XPS	Cr(VI)	150	Pseudo-2nd order	(Li et al., 2011)
Poly(*o*-phenylenediamine)	SEM, TEM, FT-IR, UV-Vis, XPS and GPC	Pb(II)	500	Pseudo-2nd order	(Han et al., 2011)
Poly(*m*-phenylenediamine) Poly(*p*-phenylenediamine)	-	Pb(II) Pb(II)	242 253	Pseudo-2nd order Pseudo-2nd order	(Huang et al., 2006)
Poly(*p*-phenylenediamine) microparticles	SEM, TEM, FT-IR and UV-Vis	Pb(II)	3000	-	(Wang et al., 2008)
Poly(*m*-phenylenediamine)	FT-IR, XPS, XRD and GPC	Ag(I)	1693	-	(Zhang et al., 2011)

Poly(*o*-phenylenediamine)	FT-IR, XRD, TEM, XPS and laser particle size analyzer	Ag(I)	533	Pseudo-2nd order	(Li et al., 2009)
Poly(1,8-diaminonaphthalene)	FT-IR, SEM, BET and CHNS elemental analyzer	Cu(II)	23	-	(Kilian et al. 2008)
Poly(1,8-diaminonaphthalene)/multiwalled carbon nanotubes	FT-IR, SEM, TGA, BET and TEM	Cd(II) Pb(II)	101 175	- -	(Nabid et al., 2014)
Polypyrrole/attapulgite	FT-IR, SEM, TEM and XPS	Cr(VI)	48	Pseudo-2nd order	(Chen et al., 2014)
Graphene/Fe_3O_4 polypyrrole	FT-IR, XRD, TEM, TGA and XPS	Cr(VI)	348	Pseudo-2nd order	(Yao et al., 2014)
Polypyrrole/graphene oxide–Fe3O4	SEM, TEM, XRD, XPS, TGA, Zeta potential and BET	Cr(VI)	293	-	(Wang et al., 2015)
Polydiphenylamine	-	Ni(II) Cu(II) Zn(II) Pb(II) Cd(II)	57 23 36 19 24	- - - - -	(Jourjon et al., 2005)

2.1.3 Description of adsorption mechanism: kinetics and isotherms

Determination of adsorption kinetic is essential as it provides the insight onto the mechanism and rate controlling steps of adsorption. The commonly used models for solute adsorption from an aqueous phase are pseudo-first order and pseudo second order (Demiral et al., 2008). The three diffusion steps for adsorption processes are: (a) solute movement from the bulk solution to the film surrounding the adsorbent, (b) solute transport from the film to the adsorbent surface and (c) from the surface to the pores and binding to the active sites of the adsorbent (Hu et al., 2011). The Lagergren pseudo first order is mainly suitable for the initial few minutes in the interaction time and mostly affected by the initial concentration. Pseudo second-order cover the whole range of contact time and it's mostly affected by different adsorption parameters (Aly et al., 2014). When a system obeys a pseudo-second order model, it is assumed that the rate limiting step is chemical adsorption which may involve valancy forces through ion exchange or sharing of electrons between the adsorbent and the analyte (Hu et al., 2011).

The equilibrium relationship on the interaction between the adsorbate and the adsorbent is described by adsorption isotherms. The Freundlich model assumes the heterogeneity on the adsorbent surface suggesting that the adsorbent has more than one adsorption sites. The Langmuir isotherm assumes a uniform surface signifying that a single layer of active sites is involve for adsorption and once occupied, no further adsorption can occur (Hu et al., 2011; Huang et al., 2013)

2.1.4 Other environmental advances of polyaromatic amines

For environmental application, polyaromatic amines have been well investigated for the detection of heavy metals in water. The principle of making a sensor is for qualitative detection of pollutants for early warnings when pollution event happens in water supply system or exceeding the environmental regulated concentrations in wastewater.

(Li et al., 2014) fabricated an electroactive composite membrane made up of poly(1,5-DAN) nanoparticles for heavy metals detection. For electrochemical experiment measurements, the membrane homogeneity and thickness was examined. Initially, the

composite membrane electrode was exposed to oxidation/reduction cycle of 0.5 V and -0.3 V while assessing the open circuit potential. Thereafter the open circuit signal responses to metal ions (silver, mercury and copper) were recorded after the addition of metal ions at the reduction of -0.3 V. The composite membrane gave different potential time responses for open circuit with the change in metal ions in $HClO_4$. For Hg^{2+} and Ag^{+} there is an impulsive oxidation to the polymer composite membrane while a coordination response primarily arises between Cu^{2+} and amino/imino groups of the polymer chain since Cu^{2+} is the weakest oxidant among the other metals. The composite membrane revealed promising properties such as stable activity, long cycling lifetimes, dense membrane arrangement and most importantly solid adhesion into the electrode. These features are not observed for the pure electrosynthesized poly(1,5-DAN) membrane electrode.

Among a group of well-studied electroconductive aromatic amine polymers such as PANI and PPy, poly(1,8-DAN) is a newly developed multifunctional electroactive polymer. This polymer can extend its utility in other electrocatalytic devices because it possesses chelating properties owing to its electron donating amines on the polymer chain (Nguyen et al., 2011). Studies have shown that poly(1,8-DAN) can be implemented as an optical sensing system for the detection of Hg in dilute solution. Pristine poly(1,8-DAN) however suffers from poor selectivity in the presence of other soft Lewis acids which can interfere. Secondly, its films has relatively low specific surface area which results limited sites to contact with metal ions. Nguyen et al. (2011) fabricated polyDAN carbon nanotubes based interdigitated arrays electrodes to improve the sensor sensitivity and stability towards Hg^{2+} detection. According to the obtained results, poly(1,8-DAN) carbon nanotubes composite by square wave voltammetry could possibly be a promising design for Hg^{2+} detection with a very sensitive signal. In addition, using interdigitated arrays showed capability to detect various metal ions simultaneously.

Electrochemical deposition of diaminonaphthalene (1,8-DAN) and phenylenediamine polymers on carbon substrates have been well studied as electrodes for metal sensing. The sensitivity of poly(1.8 DAN) is well investigated electrochemically towards detecting Cu^{2+} ions in water and orange juice on a rotating disk electrode (Mariame et al., 2009). Another study done by Kudelski et al. (1999) showed the complex formation of Cu^{2+} and VO^{2+} ions with poly(1.8-DAN). This shows the strong affinity of poly(1.8DAN) in metal ion and

selectivity as a result of favourable binding sites. It was discovered that the presence of amino groups that does not partake in the polymerization reaction are responsible of accumulation metal ions via a complexation reaction.

A comparative study of Cu^{2+} accumulation was investigated on three different electrodes. A bare carbon paste substrate, carbon paste electrode modified with 1,8 DAN monomer before polymerization and carbon paste electrode with poly(1,8 DAN) (Mariame et al., 2009). From the obtained measurements, no response of Cu^{2+} was found after preconcentrating for 5 min for a bare carbon electrode and a monomer modified electrode. However, the modified carbon paste electrode after electropolymerization presented Cu^{2+} accumulation with a well distinct anodic stripping peak at –0.6 V. The 1,8(DAN) polymer and its electrochemical properties showed selectivity of metal ions due to its favourable binding sites geometry. The presence of other metal ions (Pb^{2+}, Cd^{2+}, Zn^{2+}, Ni^{2+}, Fe^{2+} and Co^{2+}) were analysed for interference studies on Cu^{2+}. At lower concentrations of the chosen metal ions, the peak current intensity of Cu^{2+} was not affected, but at 100 times concentrations as large as that of Cu^{2+}, the interfering ion more especially Pb^{2+} began to decrease the electrode response of Cu^{2+} due to its tendency to form stable complex with poly(1,8 DAN). It was also noted that Hg^{2+} seemingly escalates the peak current of Cu^{2+} as it can be reducing at the surface creating a mercury film hence a suitable masking agent was required (Mariame et al., 2009). From this work poly(1,8 DAN) has been shown to detect copper and the method was positively applied for copper determination in tap water and orange juice samples.

The same approach has been done by using phenylenediamine isomers with graphite for the detection of Pb^{2+} by stripping voltammetry (Adraoui et al., 2005). To develop an effective sensor, polymerized phenylenediamine was handled in two ways. In one case polymerization simply occurred at the surface of the electrode with the monomer in the solution whereas for the second sensor, electropolymerization was performed with monomers already combined with carbon paste to form a modified carbon paste electrode. The ability of these fabricated electrodes to accumulate Pb^{2+} was measured by anodic stripping voltammetry. Out of the three phenylenediamine polymers (*o. m,* and *p*), the best response was attained with the P*p*PD modified carbon plate electrode based on the obtained sensitivity and the limit of detection but all polymers were able to preconcentrate

Pb^{2+}. The difference in the experimental results observed was attributed to the electropolymerization mechanism of monomers with respect to the amino group positions. Poly(*o*-phenylenediamine) and poly(*p*-phenylenediamine) oxidation involve only a single amino group, whereas in poly(*m*-phenylenediamine) both amino groups are oxidized leading to lower degree of protonation.

2.2 Analytical methods used for chromium and phosphate quantification

The growing awareness on the increase in environmental pollution levels has resulted a concern for people's well-being and global ecosystems. The ability to determine pollutants in different chemical forms is beyond question since the impact or harmfulness of an element and its comportment depend largely on its chemical form and concentration. Traditionally, quantitative methods focused on the total content of a particular element in a measured sample. However nowadays, different analytical techniques are available which are capable of investigating the chemical multiforms by quantitative speciation analysis particularly for elements in contact with living organisms. Sensitive and reliable analytical methods are desirable for determination and detection of pollutants in aquatic environments even at a trace level. This section describes the commonly used methods for chromium and phosphate ions determination in environmental samples.

2.2.1 Determination of chromium

The main forms of chromium found in water samples are trivalent chromium (Cr(III)) and hexavalent chromium (Cr(VI)). Cr(VI) is a water soluble species and highly toxic and irritant to human tissues even at low concentrations (Quality, 1996). Cr(III) on the other hand is an essential micro element for cellular metabolism (Quality, 1996). It is therefore vital to have simple analysis methods to be able to distinguish Cr metal species. Different spectroscopic and chromatographic techniques have been implemented separately or in combination for Cr quantitative analysis. In Table 2.3 a summary of analytical procedures developed and reported for total Cr, and Cr(III) and Cr(VI) speciation in water samples.

The pE-pH diagram for chromium (Fig 2.3) provides a representation of the stability of species at different redox conditions. There are eight species of chromium in aqueous

solution. These include Cr^{3+}, chromium hydroxide ($Cr(OH)_3$) and tetrahydroxochromate ($Cr(OH)_4^-$) depending on the concentration and the pH but generally, Cr(III) has a low solubility at neutral and alkaline pH making it relatively immobile in aqueous phase (Cook & Olive, 2012). Cr(VI) on the other hand is soluble throughout the pH range and its oxo-species include dichromate ($Cr_2O_7^{2-}$), hydrochromate ($HCrO_4^-$) and chromate (CrO_4^{2-}) (Cook & Olive, 2012).

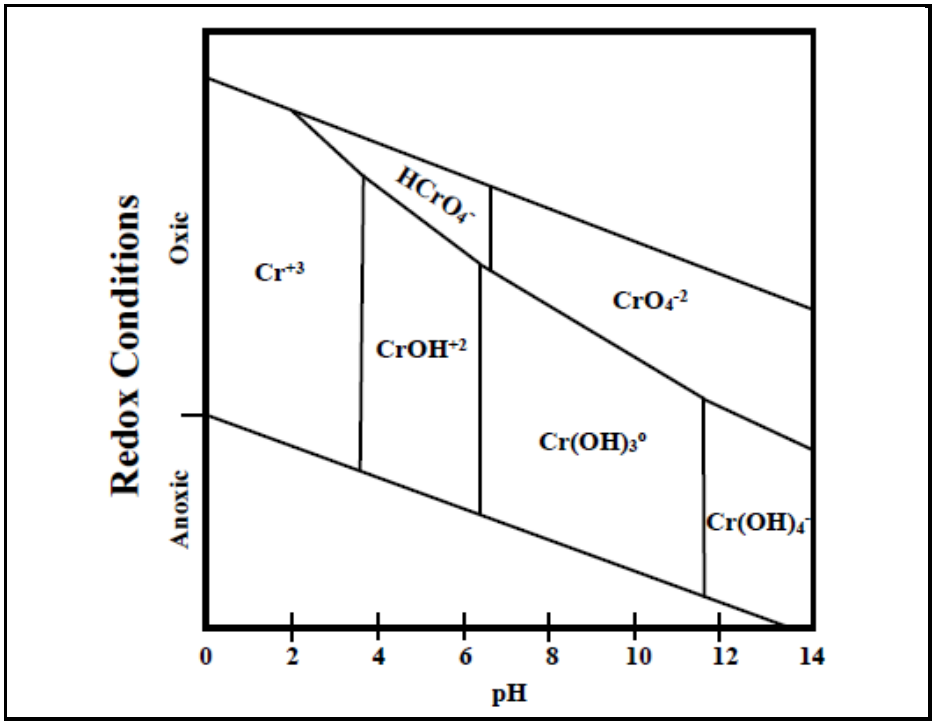

Fig 2.3 Speciation diagram of chromium in aqueous solution (McNeill & Mclean, 2012)

Cr(III) is kinetically inert and in most methods it is converted to Cr(VI) (Ruz et al., 1985; Sperling et al., 1992; Tu, 2002; Qiu et al., 2014). Cr species conversion may lead to some drawbacks such as incomplete conversion (more especially at low concentrations), sample contamination by oxidation/ reduction agents, interferences introduction from other metal ions and it is a time-consuming pre-treatment process (Sperling et al., 1992). Therefore, direct quantification or methods that separate individual species followed by direct analysis are favoured because they are relatively fast. For Cr(VI) determination, a calorimetric method is commonly used (Karthik et al., 2015; Tian et al., 2015). This method involves a pink coloured complex formed from 1.5-diphenylecarbazide (DPC) and Cr(VI) in acidic medium and its measured spectrophotometrically at 540 nm (Park et al., 2007). The UV-

based calorimetric method for Cr(VI) determination is a method of choice for a number of researchers due to its simplicity (Park et al., 2007; Qiu et al., 2014). However, it is not feasible for sample matrix with high concentrations of molybdenum, vanadium and mercury (McNeill & Mclean, 2012).

Total Cr concentration on samples obtained from different tannery effluents were determined by three analytical techniques, namely, inductively coupled plasma atomic emission spectroscopy (ICP-AES), flame atomic absorption spectroscopy (FAAS) and UV-visible spectroscopy (1.5-DPC method) (Balasubramanian, 1999). Prior to determination, the samples were oxidized with KMnO4 at high temperature to convert Cr(III) that might be present to Cr(VI). The results were critically evaluated and UV method was defined better than the ICP-AES and FAAS method. This findings were associated with matrix effect interferences for later methods due to high concentrations of mineral acids and electrolytes in the sample leading to high concentration values (Balasubramanian, 1999). It has been reviewed that numerous authors quantified Cr(VI) during their investigations using FAAS, ICP-OES and ICP-MS without taking into account that Cr(VI) could possibly be reduced to Cr(III) more especially at low pH values (Miretzky & Cirelli, 2010).

In Cr species determination, sample preparation and/ extraction techniques are vital prior to detection step using analytical instruments. FAAS is a common analysis technique for total Cr determination with a number of advantages including simple procedure, good selectivity and low cost (Pantsarkallio & Manninen, 1997). However, this technique measures the total Cr and the direct measurement of Cr(III) and Cr(VI) is impossible (Gómez & Callao, 2006). As a result, several preconcentration methods/steps based on liquid-liquid extraction, cloud point extraction, solid phase micro-extraction and liquid phase micro-extraction are required before analysis with FAAS (Gómez & Callao, 2006). For online separation, solid-phase extraction using ion exchangers or chelating resins is recommended. Flow inject (FI) on-line pre-concentration coupled with FAAS is commonly used for trace level metals determination (S. L. Zhao et al., 2015). The pre-concentration step of Cr(III) is not as simple as for Cr(VI) due to kinetic inertness of Cr(III) (Sperling, et al., 1992). As a result, efficient complexation is hindered and hence poor sensitivity and low sampling frequency. Using the FI technique separation of the single or group of

analytes from interfering with the signal is possible and thereby achieving some degree of pre-concentration with improved sensitivity (S. L. Zhao et al., 2015).

Table 2.3 Analytical methods for Cr determination in water

Sorbent	**Analyte**	**Determination technique**	**LOD (µg/L)**	**Reference**
Activated alumina	Cr(VI) Cr(III)	FI-FAAS	0.8 1.0	(Sperling, et al., 1992)
DPC	Cr(VI), Total Cr	FI-UV	-	(Ruz et al., 1985)
RP	Cr(VI), Cr(III)	HPLC-FAAS	60	(Syty, Christensen, & Rains, 1988)
Oxidation DDTC/C_{18} RP	Total Cr Cr(VI)	FI-ETAAS	0.018 0.016	(Sperling, Yint, et al., 1992)
EDTA	Cr(III), Cr(VI)	HPLC-ICP-MS	< 1.0	(Bednar, Kirgan, & Jones, 2009)
Ion exchange resin	Total Cr, Cr(III)	FI-FAAS	0.2	(Cespon-Romero et al. 1996)
DPC	Total Cr, Cr(VI)	FAAS-UV	45	(Tu, 2002)
EDTA	Cr(III), Cr(VI)	IC-ICP-MS	0.2	(Chen et al., 2007)
-	Cr(III), Cr(VI)	IC-ICP-MS	0.5	(Pantsarkallio & Manninen, 1997)
DPC	Cr(VI)	UV	-	(Karthik & Meenakshi, 2015)
DPC	Cr(VI)	UV	-	(Tian et al., 2015)
-	Cr(VI), Total Cr	IC, ICP-AES	-	(Hu et al., 2005)
DPC	Cr(VI), Total Cr	UV	-	(Qiu et al., 2014)
-	Total Cr	FAAS	-	(Zhu et al., 2016)
DPC	Total Cr, Cr(VI)	FAAS, UV	-	(Kumar eta l.,2008)
-	Cr(VI), Total Cr	ICP-OES	-	(Guo etal., 2011)
-	Cr(VI)	ICP-AES	-	(Kumar et al., 2013)
DPC	Total Cr, Cr(VI)	ICP-OES, UV	-	(Gu et al., 2012)

DPC	Cr(VI), Cr(III)	UV	-	(Park et al., 2007)
-	Cr(VI)	ICP-MS	-	(Wang et al., 2013)

LOD, limit of detection; DPC, diphenyl carbazide; DDTC, diethyl dithiocarbamate; EDTA, Ethylenediaminetetraacetic acid; RP, reversed phase; FI, flow injection.

Sperling et al., (1992), used micro-column packed with activated alumina to pre-concentrate both Cr species. Sorbent activated alumina can function as an anion and a cation exchanger depending on the solution pH. The FI coupled with FAAS detection successfully quantified Cr species through sequential species-selective sorption with pH 7 for Cr(III) and pH 2 for Cr(VI (Sperling et al., 1992).

A selective method established from combining FI sorbent extraction with electrothermal atomic absorption spectrometry (ETAAS) was developed and found to determine Cr species even at low concentrations (Sperling et al., 1992). In the study, Cr(VI) was pre-concentrated selectively on a C_{18} bonded silica column and diethyldithiocarbamate (DDTC) was as a chelating agent. Total Cr was converted to Cr(VI) using potassium peroxydisulfate oxidant at 105 °C and the product was quantitatively measured. Conditions for extraction of Cr(VI) on the sorbent and oxidation of Cr(III) to Cr(VI) were evaluated and optimized and low detection limits (LODs) were obtained (Sperling et al., 1992).

Hyphenated techniques play a major role in speciation analysis. Chromatographic separation procedures hyphenated with sensitive and selective detectors improve the analytical performance of the instruments. High performance liquid chromatography/ inductively coupled plasma mass spectrometry HPLC/ICP-MS has substantiated to be a reliable analytical tool for Cr speciation (Markiewicz et al., 2015). The diversity of HPLC in separation and the robustness of ICP-MS including multi-isotope detection support the capabilities of coupled HPLC/ICP-MS. Bednar et al. 2009 reported HPLC Cr speciation on a anion exchange column by separating Cr(III) from Cr(VI) using EDTA. The Cr(III)-EDTA complex was confirmed by intense violet colour. The solution was then analysed by direct ICP-MS and HPLC-ICP-MS with a developed reaction cell (RC) for total Cr and speciation quantification (Bednar et al., 2009). It was discovered that when RC was used, commonly polyatomic interferences were reduced while different Cr isotopes were used. The process showed reliability, robustness and versatility in quantifying the redox species

in complex environmental matrices and the LOD was less than 1.0 (µg/L) (Bednar et al., 2009).

Another preferably used hyphenated technique for Cr speciation is IC-ICP-MS. The use of ICP-MS as detector result in low detection limits and large dynamic range for most elements (Pantsarkallio & Manninen, 1997). These properties are lacking in other conventional techniques used for speciation like UV and AAS detectors. It has been shown that by combining the IC with the ICP-MS, no pre-concentration step is required (Pantsarkallio & Manninen, 1997). The challenges that have been experienced on Cr speciation in water is that Cr(III) exists as cationic aqua-hydro complexes whereas Cr(VI) is typically in a form of an anion chromate. So to preserve both of these species, the approach is to use anion exchange and cation exchange guard column in series or in mixed mode (Barnowski & Jakubowski, 1997). Another approach involves derivatization of Cr(III) using complexing agents so that if forms an anionic complex (Bednar et al., 2009).

Chen et al. (2007) reported Cr speciation by implementing anionic complexes to stabilize Cr(III) and effective anion exchange column. For sample matrix with high chloride ions (Cl), ICP-MS have some interference limitations since Cl^- has the same mass as the Cr isotope. This problem was solved by using various ammonium salt eluents before ICP-MS detection (Chen et al., 2007)

2.2.2 Determination of phosphate

There are five different oxidation states of phosphorus (P) but P (V) is the limiting nutrient distributed widely in the hydrosphere (Torres-Dorante et al., 2005). The Eh-Eh diagram in Fig 2.4 describes equilibrium distributions and the predominant P species are phosphoric acid (H_3PO_4), dihydrogen phosphate ($H_2PO_4^-$), hydrogen phosphate (HPO_4^{2-}) and phosphate ($PO4^{3-}$) (Hanrahan et al., 2005). The species charge determines the environmentally applicable reactions such as its mobility during adsorption/desorption and the level of protonation which influences its detection (Warwick etal., 2013).

Generally, for quantification of phosphate in water samples, wet chemical calorimetric analysis is used on a UV detector (Roig et al., 1999). This method is only suitable for orthophosphates and thus different forms of phosphorus are converted to orthophosphate

through oxidation using perchloric acid, nitric acid, sulphuric acid or persulfate prior to analysis (Galhardo & Masini, 2000). Fundamentally, orthophosphates react with molybdate and antimomony potassium tartrate in acidic medium to form heteropoly acids; consequently detection is based either on the molybdophosphate reduction (blue method-using ascorbic acid) or yellow vanadomolybdate complexing methods (Neves et al., 2008). The colour is proportional to the concentration of phosphorus present and complex analysis should be performed within 30 minutes on UV-Vis spectrophotometry.

The molybdenum blue method is widely used because it is less susceptible to interferences and displays high sensitivity (Neves et al., 2008; Sjosten & Blomqvist, 1997; Galhardo & Masini, 2000; Shahat et al., 2018). The presence of ascorbic acid and potassium antimony tartrate enhances selectivity by hindering silicate interference.

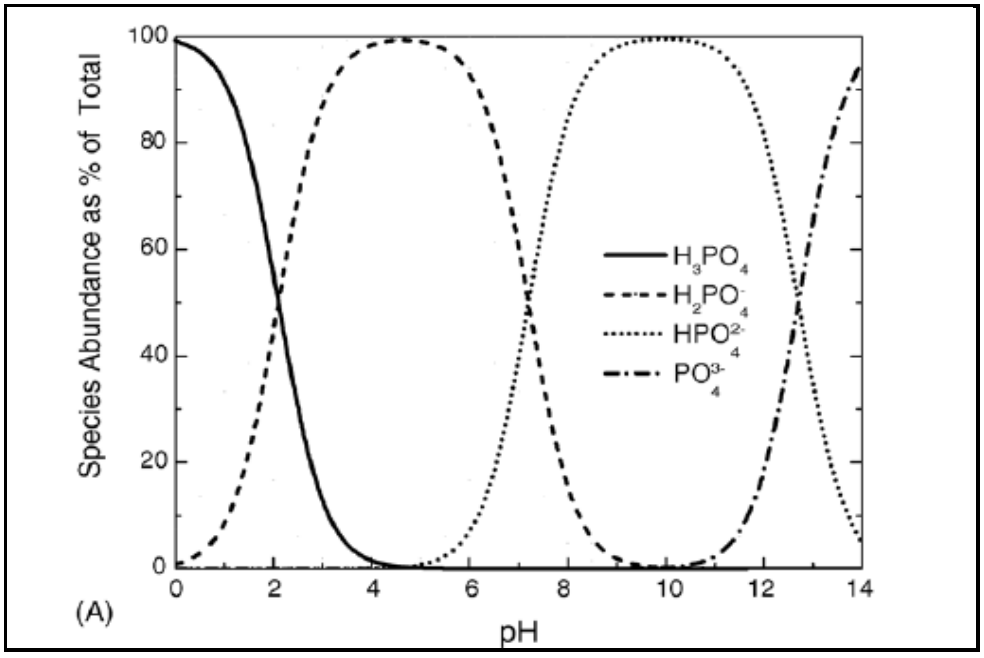

Fig 2.4 Speciation diagram of phosphorus in aqueous solution (Hanrahan et al., 2005)

ICP-MS technique which is mostly used for detection of metals and metalloid have been used for phosphorus determination since it has low background peaks (Jiang & Houk, 1988). On this study, the phosphorus was separated by reversed phase liquid chromatography (LC) using tetraalkylammonium salt as ion pairing agent and ICP-MS detected $^{31}P^{+}$ isotope. The detection limit ranged from 8-20 µg/L.

IC analysis have been reviewed for the determination of anions including phosphates in water (Michalski, 2006). Colina & Gardiner (1999) firstly developed an oxidation method to convert phosphorus to phosphate using hydrogen peroxide in a closed vessel microwave digestion method. The obtained recovery was then determined for phosphate by IC. The oxidant choice was based on that the main product after oxidation is water and is amenable to analysis by IC (Colina & Gardiner, 1999). The detection limit for phosphate was 0.251 mg/l. Simultaneous analysis of different anions including phosphates were investigated in water on a trace level using IC after pre-concentration (Kapinus et al., 2004). Here the pre-concentration step removed water and was carried out using an ion exchange concentrating column which was directly connected to the IC instead of the sample loop (Kapinus et al., 2004).

To enhance the sensitivity of phosphate analysis, IC coupled to the ICP-MS as a secondary detector was investigated (McDowell et al., 2004). Phosphate solution was injected into the IC column and the effluent was collected on an automated fraction collector. The attained fractions were analyzed by ICP-MS. The peak assignments were based on the IC retention times and verified by MS secondary detector (McDowell et al., 2004)

With different methodologies reviewed in this section, UV-Vis using 1,5 DPC method for Cr(VI) and ascorbic acid-blue method for phosphate determination were the less complicated methods. In the present investigation UV-Vis was used for both Cr and phosphate determination since high concentrations of analytes were quantified and low interferences were expected. Part of this work used FAAS for total Cr determination.

References

Adraoui, I., El Rhaz, M., Amine, A., Idrissi, L., Curulli, A., & Palleschi, G., 2005. Lead determination by anodic stripping voltammetry using a p-phenylenediamine modified carbon paste electrode. *Electroanalysis*, 17(8), pp.685–693.

Akkaya, T., Gülfen, M. & Olgun, U., 2013. Adsorption of rhodium(III) ions onto poly(1,8-diaminonaphthalene) chelating polymer: Equilibrium, kinetic and thermodynamic study. *Reactive and Functional Polymers*, 73(12), pp.1589–1596.

Aly, Z. Graulet, A., Hanley, T. 2014. Removal of aluminium from aqueous solutions using PAN-based adsorbents: Characterisation, kinetics, equilibrium and thermodynamic studies. *Environmental Science and Pollution Research*, 21(5), pp.3972–3986.

Balasubramanian, S., 1999. Determination of total chromium in tannery waste water by inductively coupled plasma-atomic emission spectrometry, flame atomic absorption spectrometry and UV-visible spectrophotometric methods. *Talanta*, 50(3), pp.457–467.

Bajpai, Rohit, S., Namdeo, M., 2009. Removal of Phosphate Anions from Aqueous Solutions Using Polypyrrole-Coated Sawdust as a Novel Sorbent. *Journal of Applied Polymer Science*, 111, pp.3081–3088.

Barnowski, C. & Jakubowski, N., 1997. Speciation of Chromium by Direct Coupling of Ion Exchange Chromatography With Inductively Coupled Plasma Mass Spectrometry. *Journal of Analytical Atomic Spectrometry*, 12, pp.1155–1161.

Bednar, A.J., Kirgan, R.A. & Jones, W.T., 2009. Comparison of standard and reaction cell inductively coupled plasma mass spectrometry in the determination of chromium and selenium species by HPLC-ICP-MS. *Analytica Chimica Acta*, 632(1), pp.27–34.

Bhaumik, M., Maity, A., Srinivasu, V. V., & Onyango, M. S., 2011. Enhanced removal of Cr(VI) from aqueous solution using polypyrrole/Fe3O4 magnetic nanocomposite. *Journal of Hazardous Materials*, 190(1–3), pp.381–390.

Blinova, N. V., Stejskal, J., Trchová, M., Prokeš, J., & Omastová, M., 2007. Polyaniline and polypyrrole: A comparative study of the preparation. *European Polymer Journal*, 43(6), pp.2331–2341.

Cespon-Romero, R.M., Yebra-Biurrun, M.C. & Bermejo-Barrera, M.P., 1996. Preconcentration and speciation of chromium by the determination of total chromium and chromium(III) in natural waters by flame atomic absorption spectrometry with a chelating ion-exchange flow injection system. *Analytica Chimica Acta*, 327(1), pp.37–45.

Chen, Z., Meghraj, M. & Naidu, R., 2007. Speciation of chromium in waste water using ion chromatography inductively coupled plasma mass spectrometry. *Talanta*, 72(2), pp.394–400.

Colina, M. & Gardiner, P.H.E., 1999. Simultaneous determination of total nitrogen, phosphorus and sulphur by means of microwave digestion and ion chromatography. *Journal of Chromatography A*, 847(1), pp.285–290.

Cook, W.G. & Olive, R.P., 2012. Pourbaix diagrams for the nickel-water system extended to high-subcritical and low-supercritical conditions. *Corrosion Science*, 58, pp.284–290.

Dai, Y.Q., Zhou, D.M. & Shiu, K.K., 2006. Permeability and permselectivity of polyphenylenediamine films synthesized at a palladium disk electrode. *Electrochimica Acta*, 52(1), pp.297–303.

De Jesus, M.C., Fu, Y. & Weiss, R.A., 1997. Conductive polymer blends prepared by in situ polymerization of pyrrole: A review. *Polymer Engineering & Science*, 37(12), pp.1936–1943.

Demiral, H., Demiral, I., Tumsek, F., Karabacakoglu, B., 2008. Adsorption of chromium(VI) from aqueous solution by activated carbon derived from olive bagasse and applicability of different adsorption models. *Chemical Engineering Journal*, 144(2), pp.188–196.

Fu, F. & Wang, Q., 2011. Removal of heavy metal ions from wastewaters: A review. *Journal of Environmental Management*, 92(3), pp.407–418.

Uddin, M.K., 2017. A review on the adsorption of heavy metals by clay minerals, with special focus on the past decade. *Chemical Engineering Journal*, 308, pp.438–462.

Gok, A. & Sari, B., 2002. Chemical synthesis and characterization of some conducting polyaniline derivatives: Investigation of the effect of protonation medium. *Journal of*

Applied Polymer Science, 84(11), pp.1993–2000.

Galhardo, C.X. & Masini, J.C., 2000. Spectrophotometric determination of phosphate and silicate by sequential injection using molybdenum blue chemistry. *Analytica Chimica Acta*, 417, pp.191–200.

Gómez, V. & Callao, M.P., 2006. Chromium determination and speciation since 2000. *TrAC - Trends in Analytical Chemistry*, 25(10), pp.1006–1015.

Gu, H., Rapole, S. B., Sharma, J., Huang, Y., Cao, D., Colorado, H. A., Guo, Z., 2012. Magnetic polyaniline nanocomposites toward toxic hexavalent chromium removal. *RSC Advances*, 2(29), p.11007.

Guedes da Silva, Q., VieiraBarbosa, N., dePieriTroiani, E., & CensiFaria, R. 2011. Electrochemical Determination of Norepinephrine on Cathodically Pretreated Poly(1,5-diaminonaphthalene) Modified Electrode. *Electroanalysis*, 23(6), pp.1359–1364.

Guimard, N.K., Gomez, N. & Schmidt, C.E., 2007. Conducting polymers in biomedical engineering. *Progress in Polymer Science*, 32(8–9), pp.876–921.

Guo, X., Fei, G. T., Su, H., & De Zhang, L., 2011. High-performance and reproducible polyaniline nanowire/tubes for removal of Cr(VI) in aqueous solution. *Journal of Physical Chemistry C*, 115(5), pp.1608–1613.

Han, J., Dai, J. & Guo, R., 2011. Highly efficient adsorbents of poly(o-phenylenediamine) solid and hollow sub-microspheres towards lead ions: a comparative study. *Journal of colloid and interface science*, 356(2), pp.749–56.

Hanrahan, G., Salmassi, T. M., Khachikian, C. S., & Foster, K. L., 2005. Reduced inorganic phosphorus in the natural environment: Significance, speciation and determination. *Talanta*, 66(2 SPEC. ISS.), pp.435–444.

Hathoot, A.A., Yousef, U. S., Shatla, A. S., & Abdel-Azzem, M., 2012. Voltammetric simultaneous determination of glucose, ascorbic acid and dopamine on glassy carbon electrode modified by NiNPs@poly 1,5-diaminonaphthalene. *Electrochimica Acta*, 85, pp.531–537.

Hu, J., Chen, G. & Lo, I.M.C., 2005. Removal and recovery of Cr(VI) from wastewater by maghemite nanoparticles. *Water Research*, 39(18), pp.4528–4536.

Hu, X.J., Wang, J., Liu, Y., Li, X., Zeng, G., Bao, Z., Zeng, X., Chen, A., Long, F., 2011. Adsorption of chromium (VI) by ethylenediamine-modified cross-linked magnetic chitosan resin: Isotherms, kinetics and thermodynamics. *Journal of Hazardous*

Materials, 185(1), pp.306–314.

Huang, M., Peng, Q., Li, X., 2006. Rapid and Effective Adsorption of Lead Ions on Fine Poly(phenylenediamine) Microparticles. *Chemistry - A European Journal*, pp.4341–4350..

Huang, M., Lu, H. & Li, X., 2007. Efficient multicyclic sorption and desorption of lead ions on facilely prepared poly (m -phenylenediamine) particles with extremely strong chemoresistance. *Journal of Colloid and Interface Science*, 313, pp.72–79.

Huang, W., Zhu, R., He, F., Dan Li, D., Zhu, Y., Zhang, Y., 2013. Enhanced phosphate removal from aqueous solution by ferric-modified laterites : Equilibrium , kinetics and thermodynamic studies. *Chemical Engineering Journal*, 228, pp.679–687.

Ihsanullah, Abbas, A., Al-Amer, A. M., Laoui, T., Al-Marri, M. J., Nasser, M. S., Atieh, M. A. 2016. Heavy metal removal from aqueous solution by advanced carbon nanotubes: Critical review of adsorption applications. *Separation and Purification Technology*, 157, pp.141–161.

Jiang, S.-J. & Houk, R.S., 1988. Inductively coupled plasma mass spectrometric detection for phosphorus and sulfur compounds separated by liquid chromatography. *Spectrochimica Acta Part B: Atomic Spectroscopy*, 43(4–5), pp.405–411.

Jouad, E.M., Jourjon, F., Le Guillanton, G., & Elothmani, D., 2005. Removal of metal ions in aqueous solutions by organic polymers: Use of a polydiphenylamine resin. *Desalination*, 180(1–3), pp.271–276.

Kapinus, E.N., Revelsky, I. A., Ulogov, V. O., & Lyalikov, Y. A., 2004. Simultaneous determination of fluoride, chloride, nitrite, bromide, nitrate, phosphate and sulfate in aqueous solutions at 10-9 to 10-8% level by ion chromatography. *Journal of Chromatography B: Analytical Technologies in the Biomedical and Life Sciences*, 800(1–2), pp.321–323.

Karthik, R. & Meenakshi, S., 2015. Removal of Cr(VI) ions by adsorption onto sodium alginate-polyaniline nanofibers. *International journal of biological macromolecules*, 72, pp.711–7.

Kilian, K. & Pyrzynska, K., 2008. Affinity of some metal ions towards 1,8-diaminonaphthalene conductive polymer. *Reactive and Functional Polymers*, 68(5), pp.974–980.

Kudelski, A., Bukowska, J. & Jackowska, K., 1999. Trapping of Cu 2𝑐 and VO 2𝑐 ions in conducting polymer matrices – EPR studies. *Journal of Molecular Structure*, 482–

483, pp.291–294.

Kumar, P.A., Chakraborty, S. & Ray, M., 2008. Removal and recovery of chromium from wastewater using short chain polyaniline synthesized on jute fiber. *Chemical Engineering Journal*, 141(1–3), pp.130–140.

Kumar, R., Ansari, M.O. & Barakat, M. a., 2013. DBSA doped polyaniline/multi-walled carbon nanotubes composite for high efficiency removal of Cr(VI) from aqueous solution. *Chemical Engineering Journal*, 228, pp.748–755.

Li, C.-Y., Wen, T.-C., Guo, T.-F., & Hou, S.-S., 2008. A facile synthesis of sulfonated poly(diphenylamine) and the application as a novel hole injection layer in polymer light emitting diodes. *Polymer*, 49(4), pp.957–964.

Li, Q., Qian, Y., Cui, H., Zhang, Q., Tang, R., & Zhai, J., 2011. Preparation of poly(aniline-1,8-diaminonaphthalene) and its application as adsorbent for selective removal of Cr(VI) ions. *Chemical Engineering Journal*, 173(3), pp.715–721.

Li, X., Ma, X., Sun, J., & Huang, M., 2009. Powerful Reactive Sorption of Silver (I) and Mercury (II) onto Poly (o -phenylenediamine) Microparticles. *Langmuir*, (25), pp.1675–1684.

Li, X.-G., Huang, M.-R. & Li, S.-X., 2004. Facile synthesis of poly(1,8-diaminonaphthalene) microparticles with a very high silver-ion adsorbability by a chemical oxidative polymerization. *Acta Materialia*, 52(18), pp.5363–5374.

Li, X.G., Huang, M. R., Duan, W., & Yang, Y. L., 2002. Novel multifunctional polymers from aromatic diamines by oxidative polymerizations. *Chemical Reviews*, 102(9), pp.2925–3030.

Maksymiuk, K., 2006. Chemical reactivity of polypyrrole and its relevance to polypyrrole based electrochemical sensors. *Electroanalysis*, 18(16), pp.1537–1551.

Mariame, C., Rhazi, M. & Adraoui, I., 2009. Determination of traces of copper by anodic stripping voltammetry at a rotating carbon paste disk electrode modified with poly(1,8-diaminonaphtalene). *Journal of Analytical Chemistry*, 64(6), pp.632–636.

Markiewicz, B., Komorowicz, I., Sajnóg, A., Belter, M., & Barałkiewicz, D., 2015. Chromium and its speciation in water samples by HPLC/ICP-MS - Technique establishing metrological traceability: A review since 2000. *Talanta*, 132, pp.814–828.

McDowell, M.M., Ivey, M. M., Lee, M. E., Firpo, V. V. , Salmassi, T. M., Khachikian, C. S., & Foster, K. L. 2004. Detection of hypophosphite, phosphite, and orthophosphate

in natural geothermal water by ion chromatography. *Journal of Chromatography A*, 1039(1–2), pp.105–111.

McNeill, L. & Mclean, J., 2012. State of the Science of Hexavalent Chromium in Drinking Water. *Water Research Foundation*.

Michalski, R., 2006. Ion chromatography as a reference method for determination of inorganic ions in water and wastewater. *Critical Reviews in Analytical Chemistry*, 36(2), pp.107–127.

Miretzky, P. & Cirelli, A.F., 2010. Cr (VI) and Cr (III) removal from aqueous solution by raw and modified lignocellulosic materials : A review. *Journal of Hazardous Materials*, 180(1–3), pp.1–19.

Muhammad Ekramul Mahmud, H.N., Huq, A.K.O. & Yahya, R. binti, 2016. The removal of heavy metal ions from wastewater/aqueous solution using polypyrrole-based adsorbents: a review. *RSC Advances*, 6(18), pp.14778–14791.

Nabid, M.R., Sedghi, R., Behbahani, M., Arvan, B., Heravi, M. M., & Oskooie, H. A., 2014. Application of poly 1,8-diaminonaphthalene/multiwalled carbon nanotubes-COOH hybrid material as an efficient sorbent for trace determination of cadmium and lead ions in water samples. *Journal of Molecular Recognition*, 27(7), pp.421–428.

Najim, T.S. & Salim, A.J., 2017. Polyaniline nanofibers and nanocomposites: Preparation, characterization, and application for Cr(VI) and phosphate ions removal from aqueous solution. *Arabian Journal of Chemistry*, 10, pp.S3459–S3467.

Neves, M.S.A.C., Souto, M. R. S., Victal, M. A., & Rangel, O. S. S., 2008. Spectrophotometric flow system using vanadomolybdophosphate detection chemistry and a liquid waveguide capillary cell for the determination of phosphate with improved sensitivity in surface and ground water samples. *Talanta*, 77, pp.527–532.

Nguyen, D.T., Tran, L. D., Le Nguyen, H., Nguyen, B. H., & Van Hieu, N., 2011. Modified interdigitated arrays by novel poly(1,8-diaminonaphthalene)/carbon nanotubes composite for selective detection of mercury(II). *Talanta*, 85(5), pp.2445–2450.

Olad, A. & Nabavi, R., 2007. Application of polyaniline for the reduction of toxic Cr(VI) in water. *Journal of Hazardous Materials*, 147(3), pp.845–851.

Orlov, A. V., Ozkan, S. Z., Bondarenko, G. N., & Karpacheva, G. P., 2006. Oxidative polymerization of diphenylamine: Synthesis and structure of polymers. *Polymer Science Series B*, 48(1), pp.5–10.

Pantsarkallio, M. & Manninen, P.K.G., 1997. Simultaneous determination of toxic arsenic and chromium species in water samples by ion chromatography inductively coupled plasma mass spectrometry. *Journal of Chromatography A*, 779(1–2), pp.139–146.

Park, D., Lim, S. R., Yun, Y. S., & Park, J. M., 2007. Reliable evidences that the removal mechanism of hexavalent chromium by natural biomaterials is adsorption-coupled reduction. *Chemosphere*, 70(2), pp.298–305.

Qiu, B., Xu, C., Sun, D., Yi, H., Guo, J., Zhang, X., Wei, S., 2014. Polyaniline Coated Ethyl Cellulose with Improved Hexavalent Chromium Removal. *ACS Sustainable Chemistry & Engineering*, (2) pp.2070-2080.

Quality, D., 1996. Chromium in Drinking-water Background document for development of WHO Guidelines for Drinking-water Quality. , 2.

Roig, B., Gonzalez, C. & Thomas, O., 1999. Simple UV / UV-visible method for nitrogen and phosphorus measurement in wastewater. *Talanta*, 50, pp.751–758.

Ruz, J., Rios, A., Castro, M. D. L. De, & Valcfircel, M., 1985. Simultaneous and Sequential Determination of Chromium (VI) and Chromium (III) by Unsegmented Flow Methods. A*nalytical Chemistry*,(322), pp.499–502.

Shahat, A., Hassan, H. M. A., Azzazy, H. M. E., Hosni, M., & Awual, M. R., 2018. Novel nano-conjugate materials for effective arsenic(V) and phosphate capturing in aqueous media. *Chemical Engineering Journal*, 331(August 2017), pp.54–63.

Sjosten, A. & Blomqvist, S., 1997. Influence of Phosphate Concentration and Reaction Temperature when Using the Molybdenum Blue Method for Determnation of Phosphate in Water. *Water Research* , 31(7), pp.1818–1823.

Sperling, M., Xu, S. & Welz, B., 1992. Determination of Chromium(III) and Chromium(VI) in Water Using Flow Injection On-Line Preconcentration with Selective Adsorption on Activated Alumina and Flame Atomic Absorption Spectrometric Detection. *Analytical Chemistry*, (64), pp.3101–3108.

Sperling, M., Yint, X. & Welzs, B., 1992. Differential Determination of Chromium (v1) and Total Chromium in Natural Waters Using Flow Injection On-line Separation and Preconcentration Electrothermal Atomic Absorption Spectrometry. *Analyst* , 117(117) pp.629-635.

Stejskal, J., 2015. Polymers of phenylenediamines. *Progress in Polymer Science*, 41(C), pp.1–31.

Syty, A., Christensen, R.G. & Rains, T.C., 1988. Determination of Added Chromium (III)

and Chromium (VI) in Natural Water by Ion-pairing High-performance Liquid Chromatography With Detection by Atomic Absorption Spectrometry. *Journal of Analytical atomic Spectrometry*, (3), pp.193–197.

Tian, Z., Yang, B., Cui, G., Zhang, L., Guo, Y., & Yan, S., 2015. Synthesis of poly(m-phenylenediamine)/iron oxide/acid oxidized multi-wall carbon nanotubes for removal of hexavalent chromium. *RSC Advances*, 5(3), pp.2266–2275.

Torres-Dorante, L.O., Claassen, N., Steingrobe, B., & Olfs, H. W., 2005. Hydrolysis rates of inorganic polyphosphates in aqueous solution as well as in soils and effects on P availability. *Journal of Plant Nutrition and Soil Science*, 168(3), pp.352–358.

Tu, R., 2002. Speciation of Cr (III) and Cr (VI) in water after preconcentration of its 1,5-diphenylcarbazone complex on amberlite XAD-16 resin and determination by FAAS *Talanta*, (57), pp.1199–1204.

Uddin, M.K., 2017. A review on the adsorption of heavy metals by clay minerals, with special focus on the past decade. *Chemical Engineering Journal*, 308, pp.438–462.

Wang, B.J., Jiang, J., Hu, B., & Yu, S., 2008. Uniformly Shaped Poly (p - phenylenediamine) Microparticles : Shape-controlled Synthesis and Their Potential Application for the Removal of Lead Ions from Water. *Advanced. Functional Materials*, (18)pp.1105–1111.

Wang, H., Yuan, X., Wu, Y., Chen, X., Leng, L., Wang, H., Zeng, G., 2015. Facile synthesis of polypyrrole decorated reduced graphene oxide-Fe3O4 magnetic composites and its application for the Cr(VI) removal. *Chemical Engineering Journal*, 262, pp.597–606.

Wang, J., Pan, K., He, Q., & Cao, B., 2013. Polyacrylonitrile/polypyrrole core/shell nanofiber mat for the removal of hexavalent chromium from aqueous solution. *Journal of Hazardous Materials*, 244–245, pp.121–129.

Wang, L., Shan, J., Feng, F., & Ma, Z., 2016. Novel redox species polyaniline derivative-Au/Pt as sensing platform for label-free electrochemical immunoassay of carbohydrate antigen 199. *Analytica Chimica Acta*, 911, pp.108–113.

Wang, N., Feng, J., Chen, J., Wang, J., & Yan, W., 2017. Adsorption mechanism of phosphate by polyaniline/TiO2 composite from wastewater. *Chemical Engineering Journal*, 316, pp.33–40.

Warwick, C., Guerreiro, A. & Soares, A., 2013. Sensing and analysis of soluble phosphates in environmental samples: A review. *Biosensors and Bioelectronics*, 41(1), pp.1–11.

Xie, A., Ji, L., Luo, S., Wang, Z., Xu, Y., & Kong, Y., 2014. Synthesis, characterization of poly(m-phenylenediamine)/palygorskite and its unusual and reactive adsorbability to chromium(vi). *New Journal of Chemistry*, 38(2), p.777.

Yao, W., Ni, T., Chen, S., Li, H., & Lu, Y., 2014. Graphene/Fe3O4 at polypyrrole nanocomposites as a synergistic adsorbent for Cr(VI) ion removal. *Composites Science and Technology*, 99, pp.15–22.

Yu, W., Zhang, L., Wang, H., & Chai, L., 2013. Adsorption of Cr(VI) using synthetic poly(m-phenylenediamine). *Journal of hazardous materials*, 260, pp.789–95.

Zanella, O., Tessaro, I.C. & Féris, L.A., 2014. Desorption- and decomposition-based techniques for the regeneration of activated carbon. *Chemical Engineering and Technology*, 37(9), pp.1447–1459.

Zhang, L., Chai, L., Liu, J., Wang, H., Yu, W., & Sang, P., 2011. pH Manipulation : A Facile Method for Lowering Oxidation State and Keeping Good Yield of Poly (m - phenylenediamine) and Its Powerful Ag + Adsorption Ability. *Langmuir*, (27)pp.13729–13738.

Zhao, S.L., Chen, F. S., Zhang, J., Ren, S. B., Liang, H. D., & Li, S. S., 2015. On-line flame AAS determination of traces Cd(II) and Pb(II) in water samples using thiol-functionalized SBA-15 as solid phase extractant. *Journal of Industrial and Engineering Chemistry*, 27, pp.362–367.

Zhou, D.M., Dai, Y.Q. & Shiu, K.K., 2010. Poly(phenylenediamine) film for the construction of glucose biosensors based on platinized glassy carbon electrode. *Journal of Applied Electrochemistry*, 40(11), pp.1997–2003.

Zhu, K., Gao, Y., Tan, X., & Chen, C., 2016. Polyaniline-Modified Mg/Al Layered Double Hydroxide Composites and Their Application in Efficient Removal of Cr(VI). *ACS Sustainable Chemistry and Engineering*, 4(8), pp.4361–4369.

CHAPTER 3

RESEARCH OBJECTIVES AND APPROACH

3.1 Research objectives

The primary focus of this research was to fabricate poly(phenylenediamine) and clay-functionalized adsorbents (containing poly(phenylenediamine), polyprrole, or metal salts) with high affinity for oxo-anions ie. Cr(VI) and phosphate ions in water. The specific objectives were therefore:

- To determine the ability of the synthesized pristine poly(phenylenediamine) and native clays as adsorbents for the removal of Cr(VI) and phosphate ions from synthetic wastewater.
- To develop poly(phenylenediamine)-clay and polypyrrole- clay composite adsorbents to improve the performance of clay and effectiveness in removing Cr(VI) and phosphate ions.
- To fully characterise the developed adsorbents and investigate the efficiency of the adsorbents in removing oxo-anions from binary and ternary anionic mixtures in synthetic water solutions.
- To modify clay particles with Fe, Co and Ni metal salts to enhance phosphate removal in water.
- To model the adsorption processes using isothermal and kinetic models.
- To identify and optimize regeneration process for the possibility of re-using the adsorbents for several cycles.

3.2 Research approach

In papers I-II, and III clay-based composite adsorbents were synthesized using poly(*p*-phenylenediamine) (P*p*PD) (Figure 3.1) and polyprrole (PPy) (Figure 3.2) respectively as the functional component for Cr(VI) adsorption. Phytotoxicity studies were carried out in paper II to determine the presence or absence of seed germination for P-*p*-PD and P-*p*-PD-MMT before and after Cr(VI) adsorption and to confirm the impact of Cr(VI) reduction to Cr(III) on the adsorbents surface. The P*p*PD-clay composite was synthesized via a simple *in situ* chemical oxidation polymerization following the scheme in Figure 3.3 using ammonium peroxydisulphate an oxidant. For Ppy-clay composite synthesis, ferric oxide oxidant was used for *in situ* chemical polymerization. The polymer matrices were incorporated into the clay particles to influence the interlayer distance of clay as presented, as well as provide new functional groups for adsorption of the oxyanions. The composites were applied for Cr(VI) remediation and regeneration.

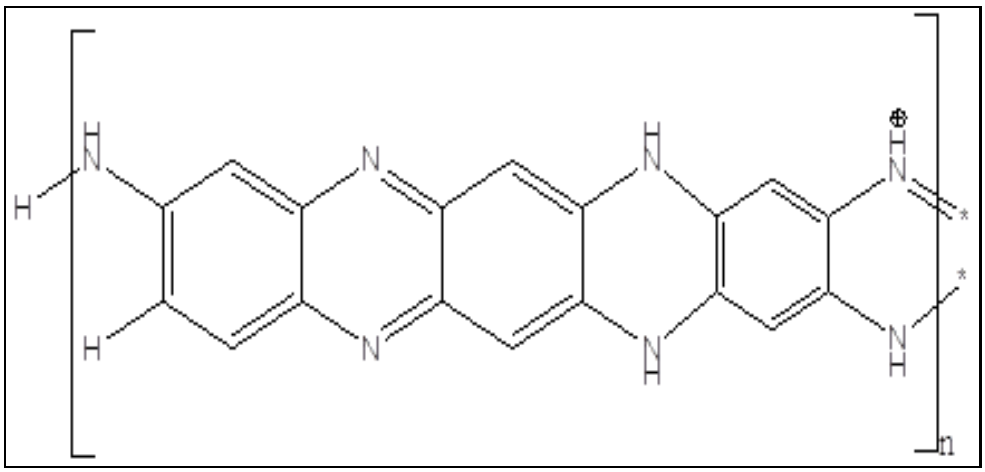

Fig. 3.1 Chemical structure of poly(*p*-phenylenediamine)

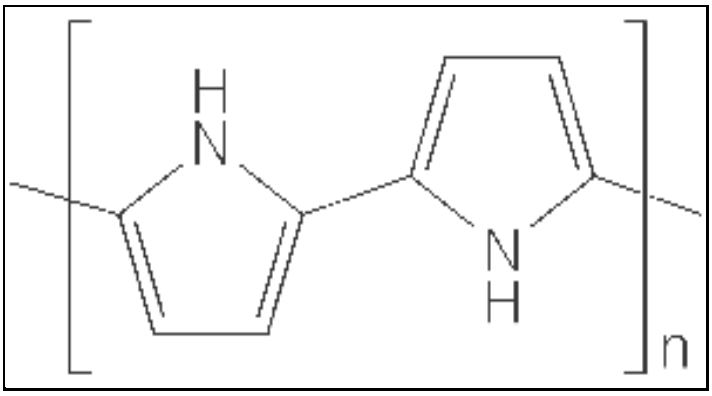

Fig. 3.2 Chemical structure of polypyrrole

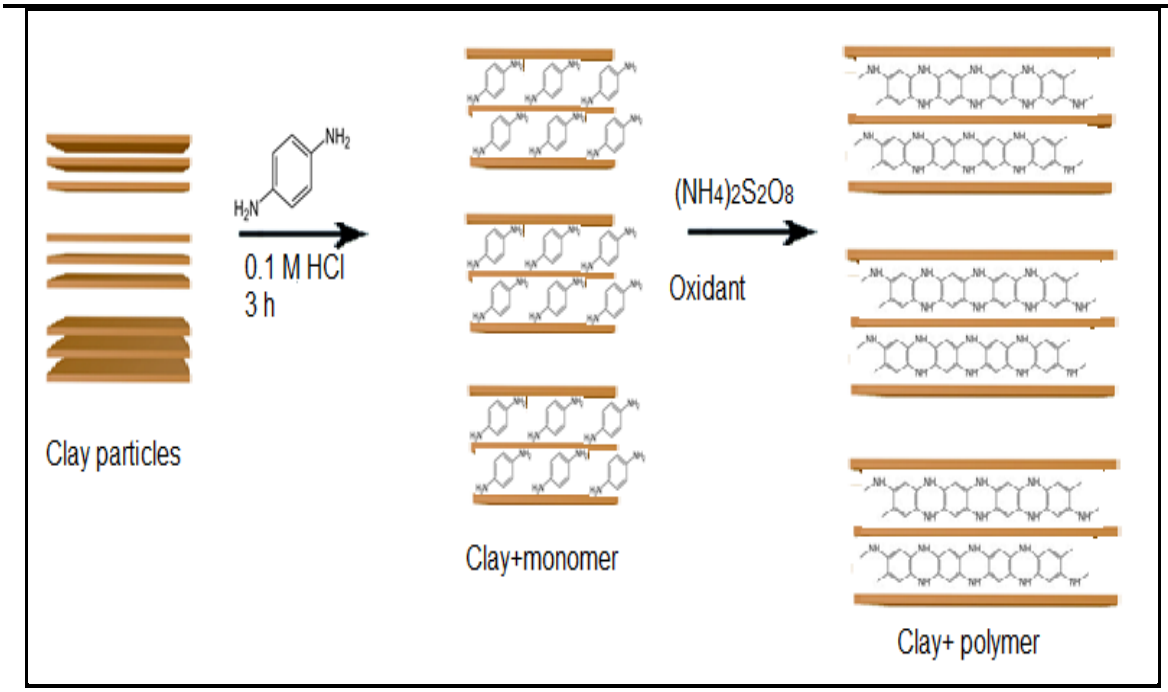

Fig. 3.3: Synthetic pathway of P*p*PD-clay composite

In paper IV, PD isomers (o, m, p) were synthesized through chemical oxidation polymerization, using ammonium peroxydisulphate and potassium dichromate ($K_2Cr_2O_7$) as oxidants. $K_2Cr_2O_7$ produced Cr^{3+} on the surface of the adsorbents which has high affinity to phosphate ions through complexation. The reaction scheme for polymerization is proposed in Figure 3.4.

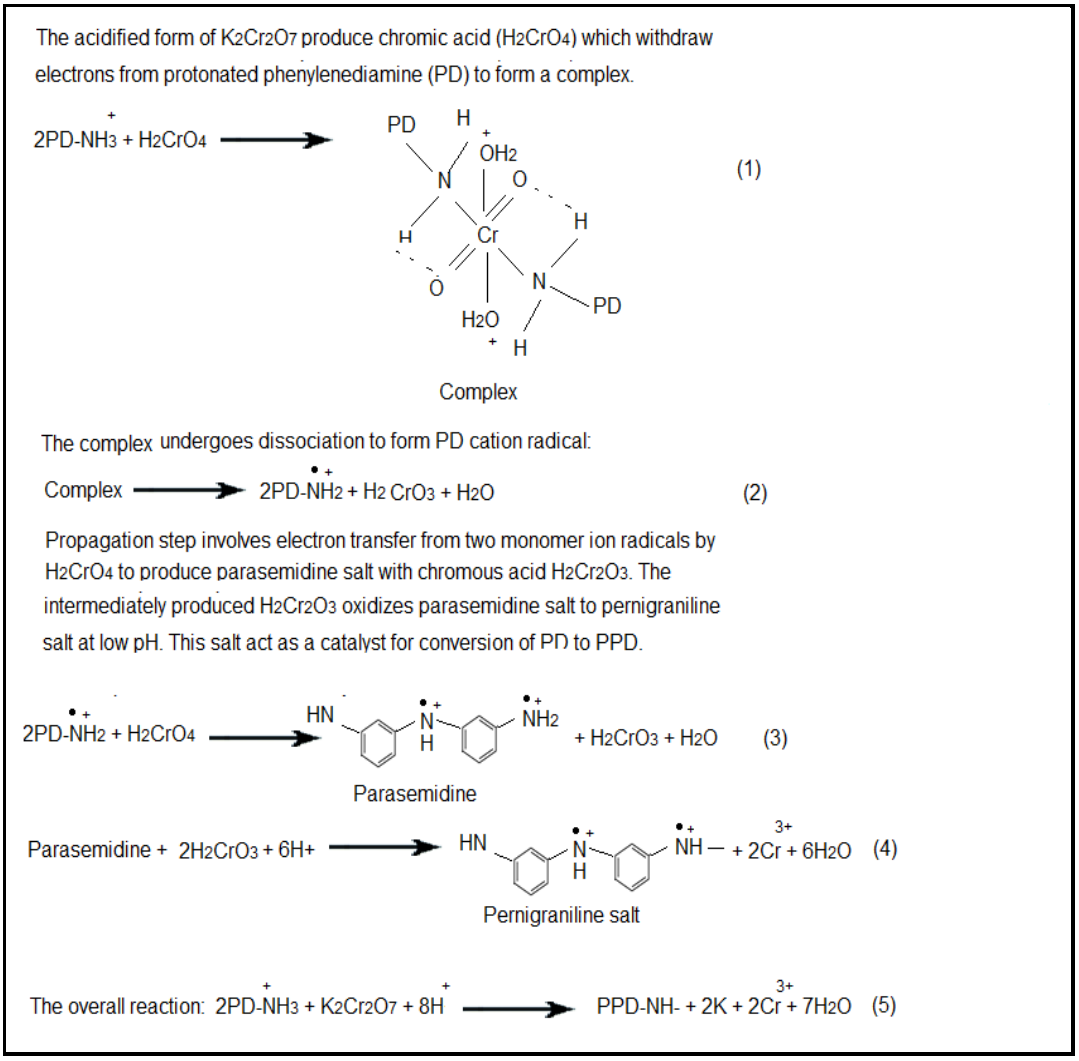

Figure 3.4 Proposed reaction scheme for PD polymerization using $K_2Cr_2O_7$ (Chowdhury & Saha, 2005)

Smectite clays are widely reported for heavy metals adsorption in water (Oehmen et al., 2007). They are abundant in nature and also major components of the soil. This has encouraged paper V where bentonite clay was implemented for phosphate ions adsorption. Since the ligand strength of phosphates is significantly greater with transition metals than other inorganic anions commonly present in water, bentonite was modified with iron, cobalt and nickel salts to improve its affinity to phosphates ions.

The general flow chart of this overall research is shown in Figure 3.5.

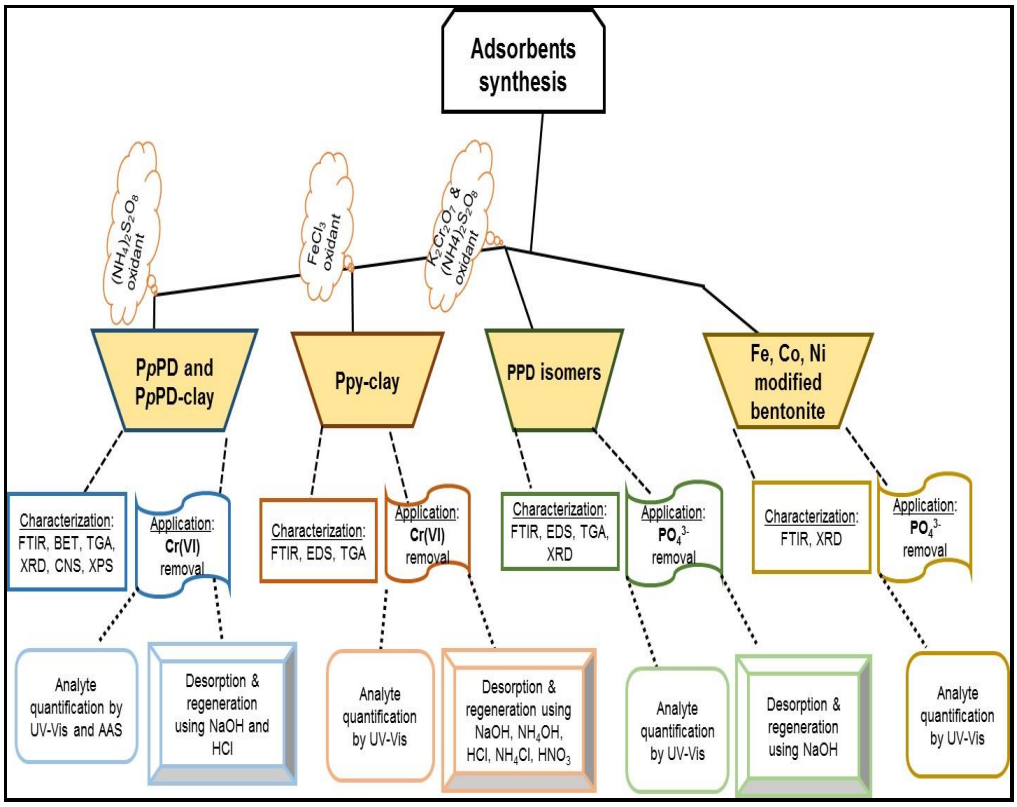

Figure 3.5 General flowchart of the research: Synthesis and adsorption process

3.3 Interpretation of data and quality control

Data treatment including kinetic and isothermic modelling have been included in the manuscripts. For quality control, parameters such as reproducibility and precision, measured data was recorded in triplicate and average values were reported with the standard deviations. Limit of detection was determined on the analytical instruments used for analytes that were used in the study.

References

Chowdhury, P. & Saha, B., 2005. Potassium dichromate-initiated polymerization of aniline. *Indian journal of Chemical Technology*, 12, pp.671–675.

Oehmen, A., Lemos, P. C., Carvalho, G.,Yuan, Z.,Keller, J., Blackall, L. L., Reis, M. A., 2007. Advances in enhanced biological phosphorus removal: From micro to macro scale. *Water Research*, 41(11), pp.2271–2300.

CHAPTER 4

Five manuscripts are included in this chapter. Paper I has already been published, papers II and IV have been submitted and paper III and V are compiled for submission

Paper I

Synthesis, characterisation and optimisation of poly(*p*-phenylenediamine)-based organoclay composite for Cr(VI) remediation

Applied Clay Science 139 (2017) 72–80

Contents lists available at ScienceDirect

Applied Clay Science

journal homepage: www.elsevier.com/locate/clay

Research paper

Synthesis, characterization and optimization of poly(p-phenylenediamine)-based organoclay composite for Cr(VI) remediation

Lindani Mdlalose [a,b,], Mohammed Balogun [a], Katlego Setshedi [a], Matshawe Tukulula [a], Luke Chimuka [b], Avashnee Chetty [a]

[a] Polymers and Composites, Materials Science and Manufacturing, Council for Scientific and Industrial Research, P.O Box 395, 0001 Pretoria, South Africa

[b] Molecular Sciences Institute, School of Chemistry, University of the Witwatersrand, P/Bag 3, WITS, 2050 Johannesburg, South Africa

ARTICLE INFO

Article history:
Received 7 September 2016
Received in revised form 10 January 2017
Accepted 11 January 2017
Available online xxxx

Keywords:
Adsorption
Cr(VI) reduction
Composite materials
Poly(phenylenediamines)

ABSTRACT

The contamination of the water supply with high levels of heavy metals from various human and industrial ac-tivities continues to present a major environmental problem. Heavy metals such as hexavalent chromium (Cr(VI)) are of particular concern since they pose serious health and environmental risks. Many polymeric mate-rials with remarkable anion adsorbing properties have been developed and reported in the literature. However, there is still need to reduce the cost and/or improve the performance of these materials for environmental reme-diation. We report here the synthesis, characterization and application of a poly(para-phenylenediamine) (poly-pPD) organoclay-based composite for removal of Cr(VI) complexes from wastewater. Adsorption capacity of the composite was evaluated at different sample pH, contact time, adsorbent dose and initial concentration. The poly-pPD-based organoclay adsorbent with ƀ55% of the polymer showed similar superior performance to pure polymer over a wide pH range compared to pristine organoclay. Adsorption was better described by the pseudo second-order kinetic model and Langmuir isotherm model, suggesting that chemisorption was the main mechanism of the adsorption process. The Langmuir maximum adsorption capacity for Cr(VI) was 217.4 mg/g and 185.2 mg/g whereas for total Cr it was 193.3 mg/g and 148.8 mg/g for poly-pPD and poly-pPD-organoclay, respectively. Using XPS, it was proven that the adsorbent also reduces Cr(VI) to Cr (III). The prepared poly-pPD-organoclay showed reuse over seven times but still retaining 80% of the recovery for Cr(VI). The composite also performed excellently in batch application to real industrial wastewater containing high levels of Cr(VI) ions and competing anions such as nitrates and sulfates.

© 2017 Elsevier B.V. All rights reserved.

1. Introduction

Industrial activities generate large volumes of effluent containing inorganic and organic pollutants, which pose a health hazard to living organisms. Heavy metals are non-biodegradable; hence those released into the environment persist in soil and ground water. These inevitably find their way through the food supply chain. Hexavalent chromium (Cr(VI)), is one of the most toxic industrially produced heavy metals. It ranks among the top 16 toxic pollutants due to its carcinogenic and teratogenic characteristics (Kawasaki et al., 2006). Industrial sources of Cr(VI) include electroplating, metal finishing, iron and steel manufacturing and chemical production industries (Zadaka et al., 2007). Due to its toxicity, the allowable discharge limit for Cr(VI) into surface and potable water are 0.1 mg/L and 0.05 mg/L, respectively (Wojcik et al., 2011).

Many technologies have been developed to remove heavy metal contaminants from wastewater before release into the environment. These techniques have been widely reported and reviewed (Bhatnagar and Minocha, 2006). Adsorption is arguably a promising alternative, and one of the most effective technologies for water treatment due to its simplicity and low capital cost (Bhaumik et al., 2011). Activated carbon has been the water purification industry's standard adsorbent because of its versatility for removal of organic contaminants (Rivera-Utrilla et al., 2011). It is much less efficient against inorganic contami-nants (Owlad et al., 2010). There is therefore a need to develop a low cost adsorbent to remove inorganic contaminants like Cr(VI).

The application of conducting polymers like polyaniline (PANI) for the adsorption of Cr(VI) has become an active area of research (Karthik and Meenakshi, 2015). PANI is a low cost, stable conjugated polymer with reversible acid/base doping/de-doping characteristics (Wang et al., 2009). Although it has shown impressive performance

Corresponding author at: Polymers and Composites, Materials Science and Manufacturing, Council for Scientific and Industrial Research, P.O Box 395, 0001 Pretoria, South Africa.

E-mail address: lmdlalose1@csir.co.za (L. Mdlalose).

http://dx.doi.org/10.1016/j.clay.2017.01.015 0169-1317/© 2017 Elsevier B.V. All rights reserved.

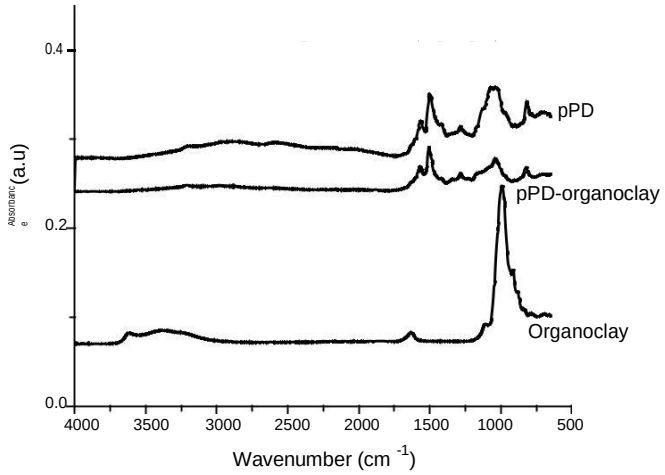

Fig. 1. FT-IR spectra of organoclay, poly-pPD and poly-pPD-organoclay composite.

for Cr(VI) removal, studies have shown its susceptibility to degradation in highly concentrated Cr(VI) solutions (N100 mg/L) due to oxidation of the polymer by the high oxidative potential of Cr(VI) (Olad and Nabavi, 2007). Additionally the use of composites comprising conducting polymers and inorganic layered materials has gained extensive interest nowadays to improve the polymer bulk properties (Setshedi et al., 2013).

Poly(phenylenediamine) homopolymers with 2,3-diaminophenazine or quinoraline repeat units exhibit high thermostability and have al-ready found many applications (Li et al., 2002). These polymers are less conductive than PANI and are mostly used in biomedical applica-tions where the potential toxicity of aniline and its oligomers is un-acceptable (Guimard et al., 2007). Their ability to remove metal ions has been demonstrated (Zhang et al., 2012).

Poly(o-phenylenediamine) possesses a strong adsorption ability for Pb(II) and Hg(II) ions in aqueous solutions through chelation reactions (Han et al., 2011; Li et al., 2009). Among the family of poly(phenylenediamines), extensive research has focused on poly(m-phenylenediamine). This is due to its properties of Cr(VI) adsorption and reduction (Yu et al., 2013). The third isomer, poly(p-phenylenediamine) (poly-pPD) has also shown good adsorption of Pb(II) (Huang et al., 2006; Wang et al., 2008).

Pristine polymers show several limitations to practical field applications. They are susceptible to chemical attacks, oxidation and have poor mechanical strengths. They have low densities which can cause a significant pressure drop in adsorption columns (Stejskal, 2015). Recently, composites of layered materials and polymers have been extensively prepared in order to improve polymer bulk properties (Nascimento et al., 2010). As a result, clay materials have received a great level of interests because of their abundant availability, mechanical stability and benign non-toxic nature (Chen et al., 2013). Montmorillonite (Mt) belongs to a smectite group of clay minerals. It has lamellae which are constructed from octahedral silica sheets with a net negative charge on the surface (Li et al., 2014). This polyanionic character stabilizes insertion of positively charged polymer chains. Although Mt. has been used industrially in environmental remediation, it has low adsorption capacity for Cr(VI) (Setshedi et al., 2013). To overcome this, organoclay was functionalized with poly-pPD through intercalation. The present work aimed to develop a poly-pPD organoclay based composite and describe its properties and application in Cr(VI) remediation.

2. Experimental procedure

2.1. Materials and methods

All reagents were of analytical grade. Ammonium peroxydisulfate and para-phenylenediamine (pPD) were purchased from Sigma Aldrich (Johannesburg, South Africa). Potassium dichromate ($K_2Cr_2O_7$) was obtained from Sigma Aldrich (Johannesburg, South Africa). Organically modified (Mt) clay, commercially known as C20A which is an ion ex-changed Mt. clay modified with dimethyl dehydrogenated Tallow ammonium salt was supplied by Southern Clay Products, Inc., (Johannesburg, South Africa). Hydrochloric acid (HCl) and sodium hydroxide (NaOH) were purchased from Merck (Johannesburg, South Africa) and were used without further purification.

2.2. Characterization techniques

Fourier transform infrared (FTIR) spectrometer Perkin–Elmer Spectrum100 (London, UK) spectrometer was used for functional group identification. Thermal stability was measured by thermogravimetric analysis (TGA) on a Perkin Elmer TGA 400 (Massachusetts, USA). XRD patterns were obtained on X-ray diffractometer (Bruker AXS D8 Advance) using Cu-Kα as the radiation source (Karlsruhe, Germany). Sur-face and fracture morphology was examined with a LEO Zeiss scanning electron microscope with a field emission gun (FE-SEM) (Hillsboro, USA). The specific surface area was measured using Brunauer-Emmett-Teller (BET) instrument (Gemini 2360) by isothermal nitrogen

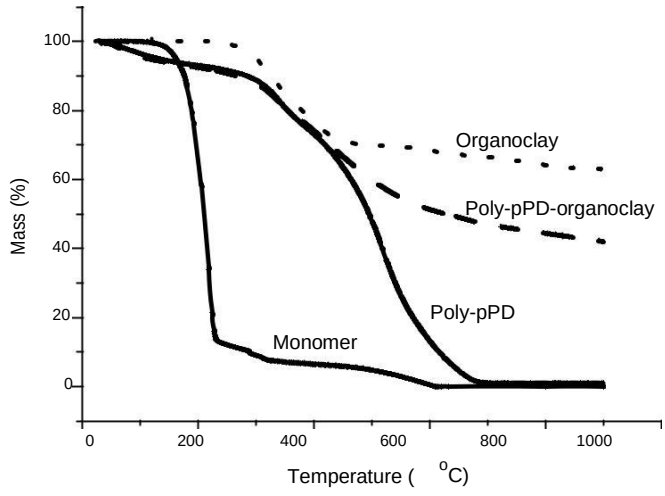

Fig. 2. TGA thermograms of the monomer (pPD), poly-pPD, organoclay and poly-pPD-organoclay.

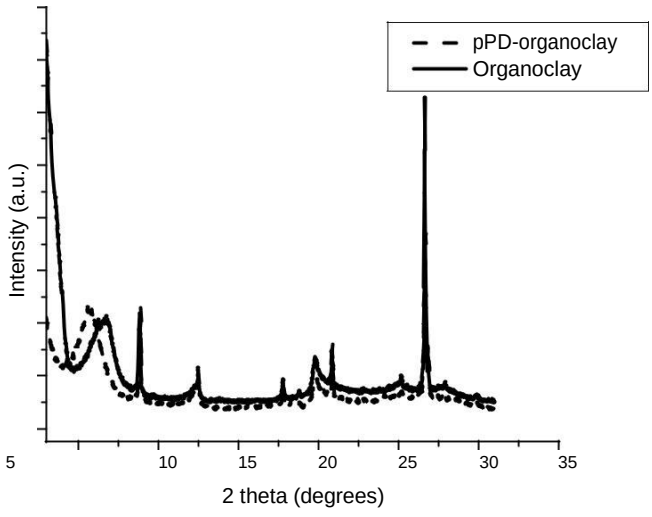

Fig. 3. XRD pattern of (a) organoclay, poly-pPD-organoclay composite.

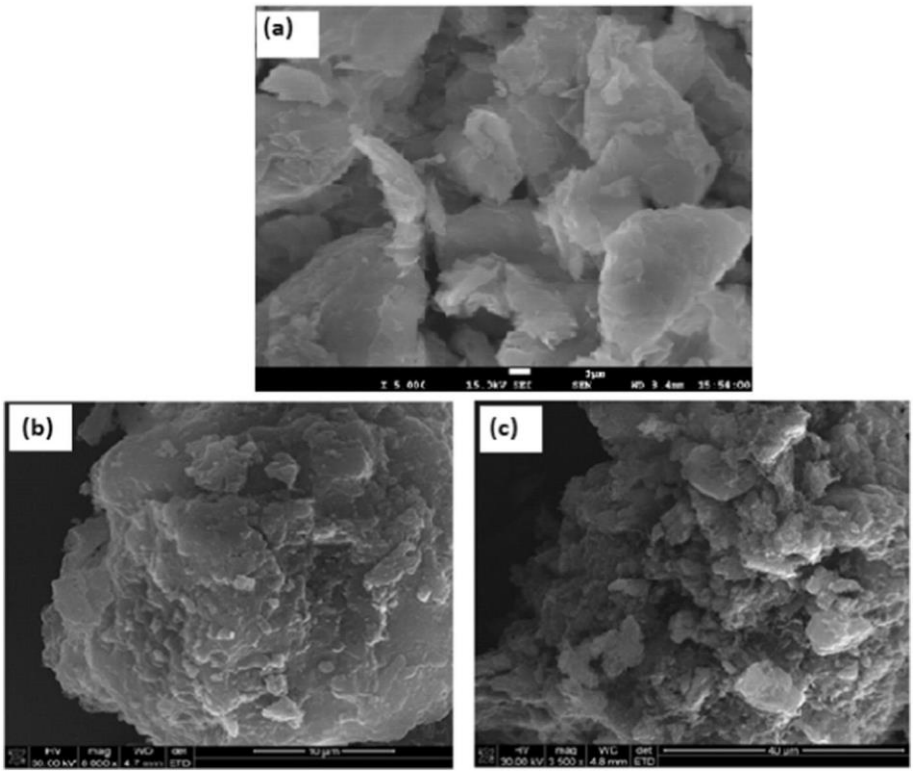

Fig. 4. FE–SEM micrographs of (a) organoclay, (b) pristine poly-pPD and (c) poly-pPD-organoclay composite.

gas adsorption (Norcross, USA). The surface chemistry of the polymers was measured using X-ray spectroscopy (XPS) Thermo Fisher Scientific K-Alpha 1063 (East Grinstead, UK).

2.3. Adsorbent preparation

2.3.1. Poly(p-phenylenediamine) preparation

Poly-pPD was synthesized by a modified method (Pham et al., 2011). Briefly, pPD (1.62 g, 0.015 mol) was dissolved in HCl (50 mL, 0.1 M) and stirred for 3 h on an ice bath. Next, the pPD polymerization was initiated by a dropwise addition of the freshly prepared oxidant solution of ammonium persulfate (3.42 g) in HCl (25 mL, 0.1 M) for 30 min. The resulting mixture was stirred for 24 h at room temperature to ensure complete polymerization of the pPD monomer. The reaction was quenched by adding acetone and the resulting crude product was washed with de-ionized water and dried under vacuum at 60 °C for 24 h.

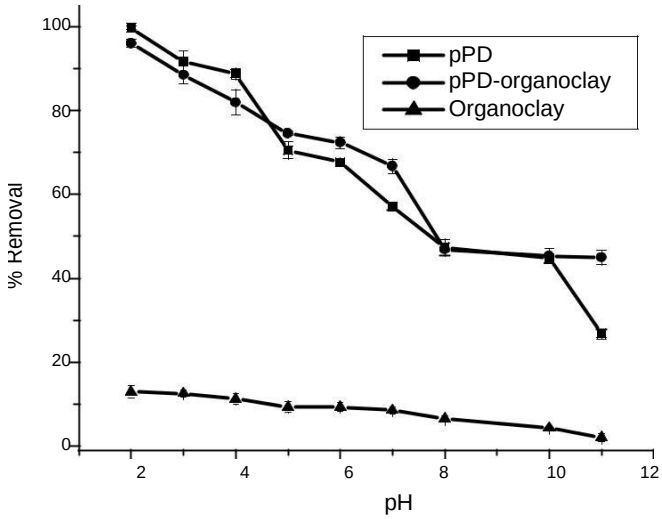

Fig. 5. The effect of pH on the adsorption of Cr(VI) on organoclay, poly-pPD and poly-pPD-organoclay composite.

2.3.2. Poly-pPD-organoclay composite preparation

The poly-pPD-organoclay composite was prepared via in situ chemical oxidative polymerization technique. In a typical procedure, organoclay (2 g) was dispersed in a pPD solution as prepared above and stirred on an ice bath. The ammonium persulfate oxidant solution was added dropwise to the mixture and left to stir for 24 h under ambient conditions. The resulting slurry was then filtered, washed with de-ionized water and dried at 60 °C under vacuum for 24 h. Concurrently, the poly-pPD loading within the poly-pPD-organoclay was varied from 10 to 70% so as to evaluate and determine the minimum optimum loading percentage necessary required for complete removal of Cr(VI).

2.4. Batch adsorption studies

2.4.1. Effect of pH and adsorbent dosage

The effect of pH on Cr(VI) sorption onto poly-pPD, poly-pPD-organoclay and organoclay was evaluated by varying the initial pH of the Cr(VI) solution within the pH range of 2–11, using either NaOH or

Table 1
Optimization of poly-pPD amount in the poly-pPD-ogarnoclay composite for Cr(VI) removal.

Poly-pPD (%)	Cr(V) removal (%)
10	71.0
20	84.8
30	94.1
40	99.4
50	99.9
60	99.8
70	99.9

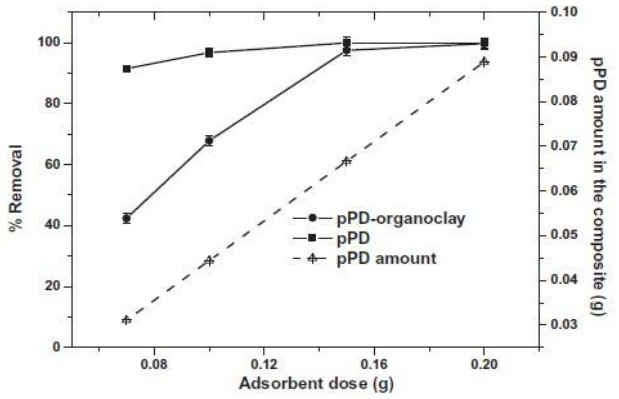

Fig. 6. The effect of adsorbent dose on the adsorption of Cr(VI) on poly-*p*PD and poly-*p*PD-organoclay composite with the amount of poly-*p*PD in the composite indicated separately.

HCl (0.1 M). The adsorbents (0.15 g) were added to Cr(VI) (200 mg/L) solution (50 mL) and agitated for 24 h in a thermostatic shaker. The samples were then filtered through syringe filters (0.45 μm) and the residual Cr(VI) concentrations were measured on a Perkin Elmer Lambda UV–vis spectrometer at 540 nm using 1,5 diphenylcarbazide reagent (Yalcin and Apak, 2004). Furthermore, the effect of poly-*p*PD % loading for Cr(VI) adsorption was assessed in batch adsorption mode, whereby a fixed amount (0.15 g) of poly-*p*PD-organoclay with varying poly-*p*PD % loading were each agitated with 50 mL of 200 mg/L Cr(VI) solution at pH 2 for 24 h, followed by filtration and analysis. Subsequently, the effect of poly-*p*PD and poly-*p*PD-organoclay doses on Cr(VI) removal was evaluated in a batch mode by varying their respective masses from 0.07–0.2 g using 50 mL of 200 mg/L Cr(VI) at pH 2. The residual Cr(VI) or total Cr was then measured and the Cr(VI) removal percentages were determined by using the following Eq. (1):

$$\%\text{Removal} = \frac{(C_o - C_e)}{C_0} \times 100 \quad (1)$$

where C_o and C_e are the initial and the equilibrium concentrations (mg/L) of Cr(VI), respectively.

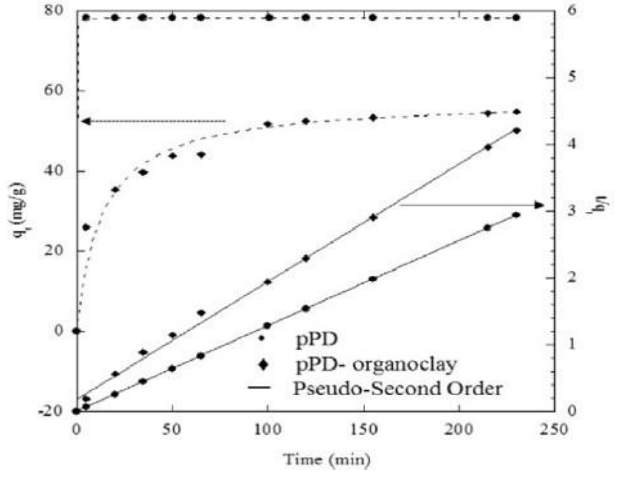

Fig. 7. Effect of contact time on Cr(VI) uptake from aqueous solution by *p*PD and *p*PD-organoclay composite.

2.4.2. Equilibrium isotherms and kinetics

The kinetics of Cr(VI) adsorption onto poly-*p*PD and poly-*p*PD-organoclay were carried out in a batch reactor with an overhead stirrer operated at 200 rpm at room temperature. The Cr(VI) concentration and solution volume were fixed at 200 mg/L and 200 mL, while the poly-*p*PD and poly-*p*PD-organoclay dosages were both fixed at 0.6 g. Samples (3 mL) were taken from the reactor at predetermined time intervals, followed by filtration and analysis. The amounts (q_t) of Cr(VI) ions adsorbed per unit mass of poly-*p*PD or poly-*p*PD-organoclay at any given time were calculated by the following Eq. (2):

$$q_t = \frac{(C_o - C_t)V}{m} \quad (2)$$

where q_t is the time-dependent amount of Cr(VI) adsorbed per unit mass of adsorbent (mg/g) and C_t (mg/L) is the bulk-phase Cr(VI) concentration (mg/L) at any time *t*. Adsorption isotherm data were generated in a batch mode using 100 mL plastic bottles. In a typical trial, 0.15 g of poly-*p*PD or poly-*p*PD-organoclay were contacted with 50 mL of varying concentrations (100–700 mg/L) of Cr(VI) solutions and agitated in a thermostatic shaker for 24 h at 200 rpm. Subsequently, samples were filtered and the residual Cr(VI) concentrations were analyzed. Total Cr was determined using AAS spectrometer (PerkinElmer AAnalyst 200). The equilibrium adsorption capacity (q_e) was determined using the following Eq. (3):

$$q_e = \frac{(C_o - C_e)V}{m} \quad (3)$$

where q_e is the equilibrium amount of Cr(VI) adsorbed per unit mass (m) of adsorbent (mg/g) and V is the sample volume (L).

Isotherm data were analyzed using the Langmuir and the Freundlich isotherm models. The Langmuir isotherm employed to characterize a monolayer adsorption process is represented by Eq. (4)

$$\frac{C_e}{q_e} = \frac{C_e}{q_o} + \frac{1}{q_o b} \quad (4)$$

where q_o (mg/g) is the maximum amount of Cr(VI) ions per unit mass of adsorbent to form a complete monolayer on the adsorbent surface and b (L/mg) is the binding energy constant. An essential characteristic of the Langmuir isotherm used to define the favourability of an adsorption process, the dimensionless separation factor (R_L) is given by Eq. (5):

$$R_L = \frac{1}{(1 + bC_o)} \quad (5)$$

The values of R_L range between 0 and 1 to confirm a favourable adsorption process. The Freundlich isotherm, which assumes sorption processes onto heterogeneous surfaces, is expressed by Eq. (6):

$$\ln q_e = \ln K_F + \frac{1}{n} \ln C_e \quad (6)$$

where K_F (mg/g) and $1/n$ constants are related to the adsorption capacity and intensity of adsorption, respectively.

2.4.3. Regeneration studies

Adsorption-desorption studies of Cr(VI) ions on the poly-*p*PD and poly-*p*PD-organoclay were carried out in a batch mode to evaluate the practical reusability of the adsorbents. Initially, 78 mg/g of Cr(VI) was loaded on poly-*p*PD pristine and poly-*p*PD-organoclay composite with 200 mg/L Cr(VI) at pH 2. Afterwards the residue was treated with 0.05 M of NaOH (25 mL) solution, followed by treatment with 0.1 M HCl (25 mL) solution, respectively. After filtration each eluent solution was kept and reused for the next cycle. The concentrations of the eluents to obtain several cycles were optimized and the optimum concentration was 0.1 M for HCl and 0.05 M for NaOH.

Table 2
Lagergren pseudo-first order, Ho pseudo-second order and Weber-Moris model kinetic parameters for Cr(VI).

Pseudo-first order model				Pseudo-second order model			Intra-particle diffusion model		
C_o (mg/L)	k_1 (1/min)	q_e (mg/g)	R^2	k_2 (g/mg/min)	q_e (mg/g)	R^2	K_p (mg/g $min^{0.5}$)	C (mg/g)	R^2
pPD	0.021	0.08	0.971	0.819	78.1	1.000	0.0032	78.18	0.913
pPD-organoclay	0.010	22.24	0.931	0.001	57.8	0.999	2.69	23.66	0.990

3. Results and discussion

3.1. Characterization

3.1.1. Fourier transform infrared spectroscopy

In the IR spectrum of the pristine poly-pPD (Fig. 1), the broad band around 3000 cm^{-1} suggests the existence of N\\H stretching vibration of the NH\\ group (Pham et al., 2011). The bands at 1566 and 1500 cm^{-1} can be attributed to C\\N and C\\C stretching vibrations of phenazine segments, respectively (Sestrem et al., 2009). A ladder structure was proposed for poly-pPD synthesized via ammonium per-sulfate oxidation contained phenazine rings (Sestrem et al., 2009). The IR spectrum of the composite is dominated by poly-pPD signal bands which confirmed incorporation of polymer into the organoclay particles (Fig. 1). The peak at 1292 cm^{-1} is ascribed to C\\N stretching mode in the benzenoid imine units and the signal at 1029 cm^{-1} is linked to aro-matic C\\H in plane bending mode (Sestrem et al., 2009). There is a minor band shift at the 1029 cm^{-1} region for the composite material which indicates an interface interaction between the polymer and the organoclay particles. The intensities of the bands for the composite were smaller than the pristine polymer bands. This attenuation of IR signals might be due to the formation of the polymeric structures inside the organoclay interlayer spaces.

3.1.2. Thermal stability

TGA was investigated to confirm that polymerization of pPD was successful. The thermal decomposition of the monomer occurred in three steps while for poly-pPD only two stages of decomposition were observed (Fig. 2). The initial mass loss around 100–200 °C with about 7% mass loss is due to the loss of water molecules and oligomers. The second decomposition in the temperature range between 300 and 600 °C is linked to the degradation of the polymer with 90% fall in the mass of the sample (Mano et al., 2003). The monomer decomposition temperature was lower than that of the polymer. This might be attributed to higher content of intermolecular forces which remain intact at high a temperature as a result of nitrogen repeating units in the polymer structure. The lower the molecular mass, the more concentrated are the amine groups which accelerate the thermal instability hence monomers decompose at a lower temperature. This observation is likely to be consistent with a higher initial decomposition temperature observed for a purified polymer (free from a monomer and oligomers) compared to its non-purified counterpart (Cam and Marucci, 1997). The major de-composition phase for organoclay between 300 °C–500 °C (24%) is associated with the release of organic substances present in organoclay and the last stage up to 900 °C is due to the bonded hydroxyl groups. As for poly-pPD-organoclay, the mass loss occurring between 200 °C and 500 °C (32%) is approximately the mass fraction of poly-pPD at the same temperature range. There is no sharp mass loss above 500 °C for poly-pPD-organoclay as observed in the pristine poly-pPD. The compos-ite thermal behaviour confirms the enhanced thermal stability for the intercalated poly-pPD.

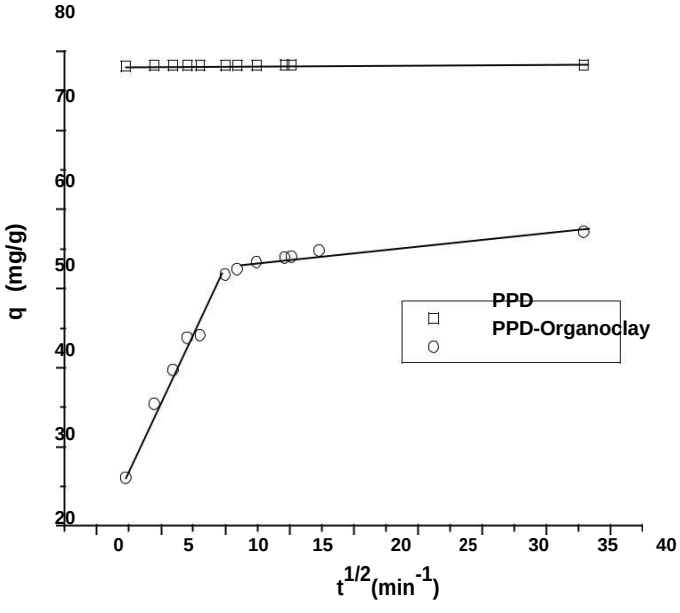

Fig. 8. Intra-particle diffusion plot.

3.1.3. XRD analysis

X-Ray diffraction was used to determine the degree of intercalation or/and exfoliation of the organoclay by poly-pPD, and the diffraction patterns are shown in Fig. 3. The organoclay characteristic peak at 6.7°, with basal spacing of 13.1 Å (Braggs equation) corresponds with the periodicity in the direction of (001). Subsequent to modification with poly-pPD-organoclay, a shift in the organoclay characteristic peak to the lower 2θ region is observed, and furthermore, the basal spacing of organoclay increases to 15.8 Å, which is attributed to the intercalation of the poly-pPD within the organoclay interlayer spaces. These ordered domains are in accord with XRD patterns for intercalated phase of PANI-clay nanocomposite (Jia et al., 2002).

3.1.4. Scanning electron microscope

The surface morphologies of the organoclay, polymer and composite were studied with SEM as indicated in Fig. 4. Photographs of characteristic areas of the samples were taken at 5000× (Fig. 4a), 8000× (Fig. 4b) and 3500× (Fig. 4c) magnifications. SEM micrograph of organoclay exhibited fragments of smaller size with irregular shapes. The surface of the pristine polymer was relatively smooth, but after incorporating organoclay particles a rough texture was evidenced. Also the pristine polymer revealed a well interconnected and dense network structure with flake-like morphology while the poly-pPD-organoclay composite show an altered and uneven surface with globular arrangement.

3.2. Batch adsorption studies

3.2.1. Effect of pH

Pristine poly-pPD and its organoclay composite were tested for Cr(VI) removal. pH is an important parameter in adsorption as it influences the adsorbent's surface charge density, and the ionic species present in the solution (Demiral et al., 2008). In all cases, Cr(VI) absorption was found to be pH–dependent. In Fig. 5, the percent Cr(VI) removal was inversely related to the pH of media pH in a nonlinear but steady trend. The highest removal efficiency of bare organoclay at an optimum pH of 2 was 13%. Such low adsorption on organoclay could mainly be attributed to Mt. enduring continual negative charge from isomorphous substitutions in silanol (Si\\O) and aluminanol (Al\\O) which are not in favour to Cr(VI) anionic species (Yuan et al., 2009). A significant improvement in Cr(VI) adsorption by poly-pPD and poly-pPD-clay is observed, with data displaying a similar adsorption pattern characterized

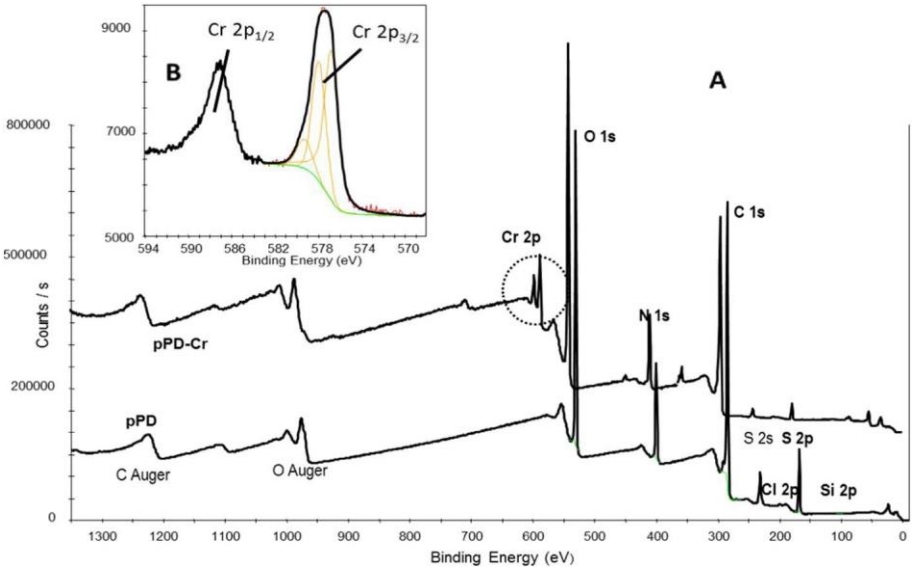

Fig. 9. Full range (A), Cr 2p (B), XPS spectra of poly-pPD and poly-pPD with Cr species adsorbed on polymer surface.

by a gradual decrease in Cr(VI) removal efficiency with increasing solution pH from 2 to 11. Specifically, the Cr(VI) % removal with increasing solution pH (2 −11) decreases from 100% to 27% and 95% to 45% for poly-pPD and poly-pPD-clay, respectively. In view of Cr(VI) removal performance comparison between poly-pPD and poly-pPD-clay, it is no-table that between pH 2 and 7, the poly-pPD-clay lost only about 27% of its Cr(VI) removal performance as compared to about 44% loss for the poly-pPD, and similarly, at the highest pH tested (pH 11) about 45% Cr(VI) removal was achieved with the poly-pPD-clay while only 25% was recorded for poly-pPD. Meanwhile, the performance behaviour with varying solution pH may be attributed various mechanisms such as electrostatic attraction/repulsion, chemical interaction, ion exchange and speciation of Cr(VI), which are responsible for adsorption of adsor-bent surfaces (Setshedi et al., 2013).

According to Cr(VI) speciation diagram (Ciavatta, 2012), the predominant Cr(VI) species in an aqueous solution are $Cr_2O^{2-}_7$ (dichromate), $HCrO^-_4$ (hydrochromate) and CrO^{2-}_4 (chromate) depending on the solution pH. At pH lower than 5.5, Cr(VI) is present either as $HCrO^-_4$ or as $Cr_2O^{2-}_7$, while at pH higher that 5.5 it is present in the form of CrO^{2-}_4 ions (Ciavatta, 2012). As a result, at acidic pH the poly-pPD acquires significant cationic properties due to the presence of H^+ in solution. This readily increases adsorption affinity due to electrostatic attraction between the negatively charged $HCrO^-_4$ and $Cr_2O^{2-}_7$ ions and the positively charged adsorbent. Increasing the solution pH decreases the concentration of H^+ ions and the poly-pPD loses its cationic character. The anionic Cr(VI) complex is less electrostatically attracted to the negatively charged ions, thus resulting in lower Cr(VI) removal at the higher pH ranges.

3.2.2. Adsorbent dose and poly-pPD loading effect

The effect of poly-pPD % loading within the poly-pPD-organoclay was evaluated for Cr(VI) sorption and performance results are presented in Table 1. Data shows a gradual increase in Cr(VI) % removal with an increasing poly-pPD % loading within the composite. A notable increase in Cr(VI) % removal from 71%–99.3% with increasing poly-pPD % loading from 10%–40% is observed, and subsequent complete removal of Cr(VI) with a further poly-pPD loading increments from 50% to 70%. Therefore based on the latter performance results, a minimum of 44% poly-pPD loading content was selected for further experiments.

In succession, poly-pPD showed little variation in adsorption with increase in adsorbent mass between 0.07 g and 2 g at pH 2 (Fig. 6). On the contrary, the poly-pPD-organoclay composite displayed an almost linear correlation between adsorption and adsorbent dose. The amount of poly-pPD present in the composite (represented by dotted line) also

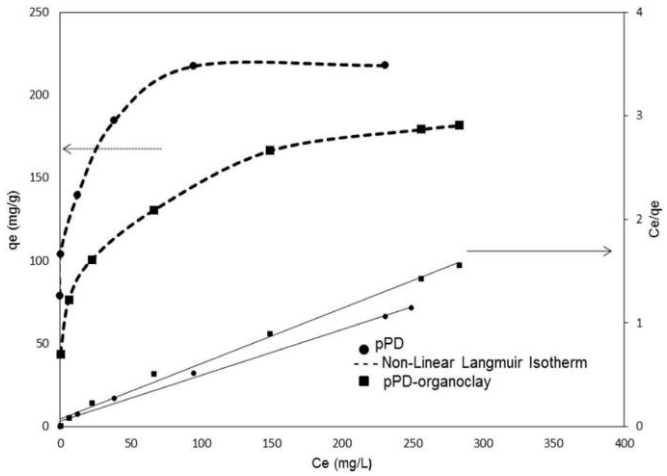

Fig. 10. Adsorption isotherms for Cr(VI).

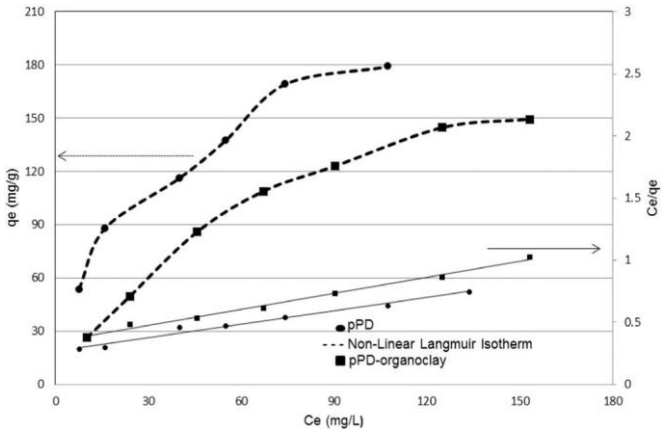

Fig. 11. Adsorption isotherms for total Cr.

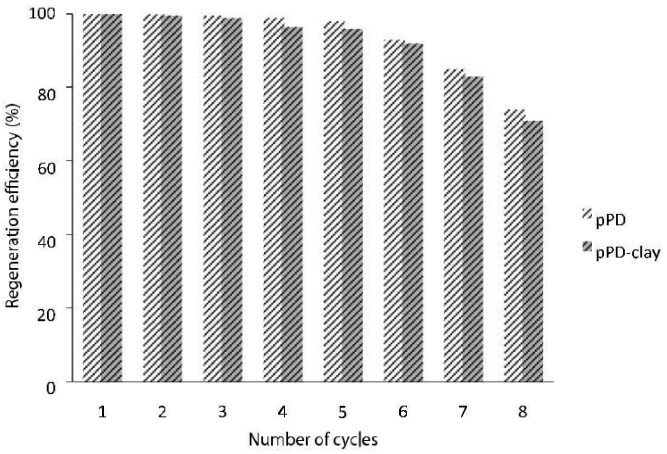

Fig. 12. Adsorption-desorption cycles for poly-pPD and poly-pPD organoclay.

increased linearly such that it required ~45% of the polymer in the composite to achieve 100% Cr(VI) removal just like the pure polymer form. It is evident from this that the poly-pPD is functional component of the composite that is responsible for adsorption as very low adsorption occurs on the organoclay alone.

It has been reported that polymerization of pPD occurs within the organoclay interlayer spaces (Do Nascimento et al., 2010). As these are discrete compartments it can be postulated that the degree of poly-merization will be limited by the confines of the gallery as opposed to the almost unlimited space available during the synthesis of the pristine polymer in solution. The smaller poly-pPD in the interlayer spaces will larger surface areas which could facilitate a more efficient removal of the Cr(VI) anions (Galimberti, 2011). This was supported by the specific surface area of 55.42 m^2/g for poly-pPD and 90.30 m^2/g for pPD-organoclay composite.

3.2.3. Adsorption kinetics

Adsorption kinetics studies offer valuable insights into the reaction pathways and the mechanism of the reactions (Demiral et al., 2008). Kinetic data for Cr(VI) sorption onto poly-pPD and poly-pPD-organoclay is presented in Fig. 7. An interesting rapid Cr(VI) uptake onto poly-pPD and attainment of equilibrium is observed in the first 5 min, with 99.9% of the Cr(VI) removed. The fast adsorption rate of pristine polymer is also revealed by the rate constant value of 0.819 g/mg/min for pseudo second order. Data for poly-pPD-organoclay shows a rapid removal of only 50% Cr(VI) in the first 5 min, which then slows down considerably as the reaction approaches equilibrium. The complete and rapid uptake of Cr(VI) by pristine poly-pPD may be due to the exposed and readily accessible active sites of the 'naked' pristine poly-pPD, while the delayed equilibrium attainment observed for poly-pPD-organoclay may be due to the delayed accessibility to the poly-pPD hidden within the organoclay interlayers.

The kinetic data for Cr(VI) sorption onto poly-pPD and poly-pPD-organoclay were subjected to the Lagergren pseudo-first order and Ho pseudo-second order kinetic models, in order to determine the rate at

Table 3
Isotherm parameters for the removal of Cr(VI) by poly-pPD and poly-pPD-organoclay.

		Langmuir isotherm			Freundlich isotherm		
	q_e (mg/g)	b (L/mg)	R_L	R^2	K_F (mg/g)	1/n	R^2
Poly-pPD	217.4	0.114	0.025	0.986	77.9	0.174	0.918
Poly-pPD-organoclay	185.2	0.038	0.070	0.930	61.1	0.159	0.922

Table 4
Isotherm parameters for total Cr removal by poly-pPD and poly-pPD-organoclay.

		Langmuir isotherm			Freundlich isotherm		
	q_e (mg/g)	b (L/mg)	R_L	R^2	K_F (mg/g)	1/n	R^2
Poly-pPD	193.3	0.081	0.073	0.973	55.7	0.115	0.906
Poly-pPD-organoclay	148.8	0.022	0.121	0.922	32.3	0.101	0.921

which adsorption occurred (Tseng et al., 2014). The linearized forms of the pseudo-first order and pseudo-second order models are given by Eqs. (7) and (8), respectively:

$$\ln (q_e - q_t) = \ln q_e - kt \quad (7)$$

$$\frac{t}{q_t} = \frac{1}{k_2 q_e^2} + \frac{t}{q_e} \quad (8)$$

where k_1 (1/min) and k_2 (g/mg/min) are the pseudo-first order and pseudo-second order rate constants, respectively, q_t is the amount of Cr(VI) adsorbed at any time (mg/g) and q_e is equilibrium adsorption capacity (mg/g).

The rate constants and the correlation coefficients extracted from the linear plots of the pseudo-first order and pseudo-second order (Fig. 7) given in Table 2. Based on correlation coefficients (R^2), the pseu-do-second order kinetic model ($R^2 > 0.999$) is found to give a better description for Cr(VI) sorption onto poly-pPD and poly-pPD-organoclay, as compared to the pseudo-first order model ($R^2 < 0.97$). The agreement between the experimental and calculated pseudo-second order model maximum sorption capacities (q_e) for both poly-pPD and poly-pPD-organoclay validates the applicability of the model for Cr(VI) sorption. This suggests that the rate limiting step may be chemisorption, involving valence forces through sharing or exchange of electrons between Cr(VI) ions and the poly-pPD surface (Setshedi et al., 2013).

3.2.4. Adsorption mechanisms

The oxidation state of the Cr bound to the polymers was characterized using XPS analysis. Fig. 9(A) shows a full range of bare poly-pPD and poly-pPD laden with Cr(VI) in acidic medium. The survey spectrum reveals the presence of Cr on the surface of the polymer after adsorption. Fig. 9(B) demonstrates a high resolution spectra collected from the Cr2p primary region. Quantification of Cr2p binding energy at 577–578 eV and 586–588 eV corresponds to Cr(III) and the characteristics binding energy bands for Cr(VI) are at 580–580.5 eV and 589– 590 eV (Tang et al., 2014). In this case, the Cr2p binding energy peaks of poly-pPD-Cr were obtained at around 578 and 588 eV, which con-firms that the present Cr is in the form of Cr(III). The former band arises from the high spin component, $Cr2p_{3/2}$ and the latter from low spin $Cr2p_{1/2}$ orbital. The absence of Cr(VI) on the polymer surface implies that the adsorbent have reduced the Cr(VI) ions to Cr(III) ions which proves the redox mechanism.

Adsorption processes on porous materials will generally involve multi-steps chemical reactions between surface functional groups on the adsorbent and the solute ions to form inorganic or organic complexes, or ion exchange reactions depending on the nature of the adsorbent. The adsorption dynamics can thus be described in the following three consecutive steps (Unuabonah et al., 2007): (i) Transport of the solute from bulk solution through liquid film to the adsorbent exterior surface, (ii) Solute diffusion into the pore of the adsorbent except for a small quantity of adsorption on the external surface; parallel to this is the intra-particle transport mechanism of the surface diffusion, (iii) Ad-sorption of solute on the interior surfaces of the pores and capillary spaces of the adsorbent.

The rate determining step of an adsorption process, which invariably controls the overall rate of adsorption, is the slowest step which would be either film diffusion or pore diffusion and can be identified using the

intraparticle diffusion model. The intra-particle diffusion model is evaluated by the relationship between the time-dependent adsorption capacity (q_t) and the $t^{1/2}$ represented by Eq. (9):

$$q_t = k_p t^{1/2} + C \quad (9)$$

where k_p is the intra-particle diffusion rate constant ($mg \cdot g^{-1}\ min^{-1/2}$) and C is the intercept (mg/g). The model states that intra-particle diffusion is involved if the plot of q_t versus $t^{1/2}$ is linear, and if the plot passes through the origin, then intra-particle diffusion is the sole rate limiting step. In cases where the plot of q_t versus $t^{1/2}$ is multi-linear, then two or more steps govern the sorption process (Hu et al., 2011). Multi-linear plots of q_t versus $t^{1/2}$ shown in Fig. 8 suggests that more than one pro-cess controlled the adsorption process of Cr(VI) onto poly-pPD-organoclay. For Cr(VI) adsorption onto poly-pPD, a single adsorption process is observed representing surface or film diffusion on the exterior of poly-pPD. Conversely, a two-step adsorption process is observed for Cr(VI) onto poly-pPD-organoclay as represented by the two linear segments of the plot, where the first and the second linear segments indicate surface and intra-particle diffusion, respectively. As result, the multilinear plots for adsorption of Cr(VI) onto poly-pPD-organoclay suggest that the process was governed by more than one step, with intraparticle diffusion as the rate limiting step. The intra-particle diffusion model constants k_p and C are shown in Table 2.

3.2.5. Adsorption isotherms

Adsorption isotherms provide essential information about the capacity of an adsorbent or the amount required to remove a unit mass of Cr(VI) under system conditions (Jeppu and Clement, 2012). The isotherms of Cr(VI) sorption for poly-pPD and poly-pPD-organoclay are given if Fig. 10. The plots for poly-pPD and poly-pPD-organoclay display similar characteristics of an “L” type isotherm curve, shown by a gradual increase in capacity for Cr(VI) with increasing initial concentrations until the curve reaches a strict asymptotic plateau implying equilibrium attainment. The increase in poly-pPD and poly-pPD-organoclay adsorp-tion capacities for Cr(VI) may be attributed to the generated adsorption driving force with increasing Cr(VI) concentration gradient. As a result, increasing moles of Cr(VI) available to the adsorbent's surface area in-creases the number of collisions between the Cr(VI) and the poly-pPD or poly-pPD-organoclay, thus developing a driving force to overcome all mass transfer resistance (Chen et al., 2013).

Fig. 10 displays the linear and nonlinear plots of the Langmuir isotherm, while the extracted parameters from the respective models are given in Table 3. Based on higher correlation coefficients (R^2), the Langmuir isotherm model gave the best description for Cr(VI) sorption onto both poly-pPD and poly-pPD-organoclay, as compared to the Freundlich isotherm. The calculated Langmuir maximum sorption capacities were similar to those determined experimentally, thus validating the applicability of the Langmuir isotherm model for Cr(VI) adsorption onto both poly-pPD and poly-pPD-organoclay. In addition, the R_L values for Cr(VI) sorption onto both the poly-pPD and poly-pPD-organoclay are found to be in the range 0–1, thus confirming the favourability of the ad-sorption process.

The mechanism by which Cr(VI) ions were adsorbed onto poly-pPD and poly-pPD-organoclay was also examined by determining the maxi-mum adsorption capacity of total Cr remaining in the solution at pH 2 as shown in Fig. 11. Langmuir maximum adsorption capacities for total Cr reported in Table 4 are 193.3 mg/g and 148.8 mg/g for poly-pPD and poly-pPD-organoclay, respectively. The lower capacity for total Cr com-pared to Cr(VI) could be attributed to the reduction of Cr(VI) to Cr(III) which partly remains in the aqueous solution or form complexes with the polymer binding groups. In acidic medium Cr(III) easily get released into aqueous phase due to repulsion between positively charged Cr(III) and positively charged adsorbent surface.

Table 5
Comparison of adsorption capacity of poly-pPD and poly-pPD-organoclay with polyaniline derivatives and clay based adsorbents for Cr(VI) removal.

Adsorbents	Adsorption capacity (mg/g)	pH	Reference
Montmorillonite-supported magnetite nanoparticles	15.3	2.0	Yuan et al. (2009)
Chitosan-montmorillonite-Fe_3O_4 microsphere	58.8	2.0	Chen et al. (2013)
Montmorillonite-supported carbon spheres	156.2	2.0	Li et al. (2014)
Dodecyl-benzene-sulfonic acid doped- polyaniline/multi-walled carbon nanotubes	55.5	2.0	Kumar et al. (2013)
Polyaniline coated chitin	24.6	4.2	Karthik and Meenakshi (2015)
Polyaniline ethyl cellulose	38.8	1.0	Qiu et al. (2014)
Polyaniline-magnetic mesoporous silica	193.8	2.0	Tang et al. (2014)
Poly(m-phenylenediamine/palygorskite)	153.8	1.2	Xie et al. (2014)
Poly(m-phenylenediamine)	500	2.0	Yu et al. (2013)
Polypyrrole-organically modified montmorillonite clay	119.3	2.0	Setshedi et al. (2013)
Poly-pPD	217.4	2.0	Present work
Poly-pPD-organoclay	185.2	2.0	Present work

3.3. Regeneration

Fig. 12 indicates the adsorption-desorption cycles of Cr(VI) onto poly-pPD and poly-pPD-organoclay. It has been reported that a certain percentage of Cr(VI) adsorbed on the adsorbent surface is reduced to Cr(III) by the electron rich amino/imino groups on polymers of aniline derivatives in acidic media (Tang et al., 2014). Aqueous NaOH therefore releases anionic Cr(VI) ions, while the HCl leaches out the cationic Cr(III) from the adsorbent's surface. For poly-pPD, maximum adsorption of Cr(VI) was maintained for 7 cycles with >80% regeneration efficiency. A slight drop to about 74% was obtained in the eighth cycle. A similar pattern was observed for the poly-pPD-organoclay where the eighth cycle gave regeneration efficiency of 71%.

3.4. Application to real industrial wastewater

To assess the performance of the composite in real wastewater in the presence of competitive anions, two batch tests of wastewater were used: (i) the industrial wastewater obtained from industrial site with initial Cr(VI) concentration of 140 mg/L. The industrial wastewater pH was adjusted to 2.0 from an initial of 7.5. An adsorbent dosage of 0.15 g per 50 mL of Cr(VI) solution was used. Complete removal of Cr(VI) ions from the industrial effluent and simulated wastewater was achieved for both pristine poly-pPD and the poly-pPD-organoclay composite. This specifies that the presence of coexisting anions like sulfates (270 mg/L) and nitrates (11 mg/L) did not hinder the removal of Cr(VI) ions.

4. Conclusion

Poly-pPD-supported Mt. organoclay readily prepared can be used for Cr(VI) removal. XRD analysis demonstrated that poly-pPD molecules are intercalated into the galleries of the organically modified clay and TGA results confirmed an enhanced thermal stability of poly-pPD-organoclay relative to the pristine poly-pPD. Under a wide range of experimental conditions conducted in the study, pristine poly-pPD and poly-pPD-organoclay composite were found to efficiently remove Cr(VI) from solutions at pH 2. Cr(VI) ions were efficiently adsorbed through redox and chelation reactions. Equilibrium data are well de-scribed by the Langmuir isotherm model, indicating monolayer adsorption for Cr(VI). Also, a greater inter-particle diffusion was obtained o

the composite reaction rate measurements while the pristine polymer was mostly led by external mass transfer. Organoclay solid support is beneficial on tailoring the aggregation performance of poly-pPD, and can thus help with pelletization.

Acknowledgements

This work was supported by the South African Council for Scientific and Industrial Research (CSIR) (Project grant: 88568), and National Re-search Foundation (NRF) PDP. The authors acknowledge the University of the Witwatersrand and the University of Latvia for contributions to this project.

References

Bhatnagar, A., Minocha, A.K., 2006. Conventional and non-conventional adsorbents for re-moval of pollutants from water – a review. Indian J. Chem. Technol. 13, 203–217.

Bhaumik, M., Maity, A., Srinivasu, V.V., Onyango, M.S., 2011. Enhanced removal of Cr(VI) from aqueous solution using polypyrrole/Fe_3O_4 magnetic nanocomposite. J. Hazard. Mater. 190, 381–390.

Cam, D., Marucci, M., 1997. Influence of residual monomers and metals on poly(L-lactide) thermal stability. Polymer 38, 1879–1884.

Chen, D., Li, W., Wu, Y., Zhu, Q., Lu, Z., Du, G., 2013. Preparation and characterization of chitosan/montmorillonite magnetic microspheres and its application for the removal of Cr (VI). Chem. Eng. J. 221, 8–15.

Ciavatta, C., 2012. Chromium-containing organic fertilizers from tanned hides and skins: a review on chemical, environmental, agronomical and legislative aspects. J. Environ. Prot. 3, 1532–1541.

Demiral, H., Demiral, I., Tumsek, F., Karabacakoglu, B., 2008. Adsorption of chromium(VI) from aqueous solution by activated carbon derived from olive bagasse and applicabil-ity of different adsorption models. Chem. Eng. J. 144, 188–196.

Do Nascimento, G.M., Sestrem, R.H., Temperini, M.L.A., 2010. Structural characterization of poly-para-phenylenediamine-montmorillonite clay nanocomposites. Synth. Met. 160, 2397–2403.

Galimberti, M., 2011. Rubber-Organoclay Nanocomposites: Science, Technology and Ap-plications. John Wiley & Sons (Chapter 4).

Guimard, N.K., Gomez, N., Schmidt, C.E., 2007. Conducting polymers in biomedical engi-neering. Prog. Polym. Sci. 32, 876–921.

Han, J., Dai, J., Guo, R., 2011. Highly efficient adsorbents of poly(o-phenylenediamine) solid and hollow sub-microspheres towards lead ions: a comparative study. J. Colloid Interface Sci. 356, 749–756.

Hu, X.J., Wang, J.S., Liu, Y.G., Li, X., Zeng, G.M., Bao, Z.L., Long, F., 2011. Adsorption of chro-mium (VI) by ethylenediamine-modified cross-linked magnetic chitosan resin: iso-therms, kinetics and thermodynamics. J. Hazard. Mater. 185, 306–314.

Huang, M., Peng, Q., Li, X., 2006. Rapid and effective adsorption of lead ions on fine poly(phenylenediamine) microparticles. Chem. Eur. J. 12, 4341–4350.

Jeppu, G.P., Clement, T.P., 2012. A modified Langmuir-Freundlich isotherm model for sim-ulating pH-dependent adsorption effects. J. Contam. Hydrol. 129–130, 46–53.

Jia, W., Segal, E., Kornemandel, D., Lamhot, Y., Narkis, M., Siegmann, A., 2002. Polyanilinine-DBSA/organophilic clay nanocomposites: synthesis and characteriza-tion. Synth. Met. 128, 1–6.

Karthik, R., Meenakshi, S., 2015. International journal of biological macromolecules syn-thesis, characterization and Cr (VI) uptake study of polyaniline coated chitin. Int. J. Biol. Macromol. 72, 235–242.

Kawasaki, N., Bun-ei, R., Ogata, F., Nakamura, T., Tanei, S., Tanada, S., 2006. Water treat-ment technology using carbonaceous materials produced from vegetable biomass. J. Water Environ. Technol. 4, 73–82.

Kumar, R., Ansari, M.O., Barakat, M., 2013. DBSA doped polyaniline/multi-walled carbon nanotubes composite for high efficiency removal of Cr(VI) from aqueous solution. Chem. Eng. J. 228, 748–755.

Li, X., Huang, M., Duan, W., Yang, Y., 2002. Novel multifunctional polymers from aromatic diamines by oxidative polymerizations. Chem. Rev. 102, 2925–3030.

Li, X., Ma, X., Sun, J., Huang, M., 2009. Powerful reactive sorption of silver (I) and mercury (II) onto poly (o-phenylenediamine) microparticles. Langmuir 25, 1675–1684.

Li, T., Shen, J., Huang, S., Li, N., Ye, M., 2014. Hydrothermal carbonization synthesis of a novel montmorillonite supported carbon nanosphere adsorbent for removal of Cr (VI) from waste water. Appl. Clay Sci. 93–94, 48–55.

Mano, J.F., Koniarova, D., Reis, R.L., Azure, C.D., Gualtar, C., 2003. Thermal properties of thermoplastic starch/synthetic polymer blends with potential biomedical applicabil-ity. J. Mater. Sci. Mater. Med. 14, 127–135.

Nascimento, G.M., Sestrem, R.H., Temperini, M.L., 2010. Structural characterization of poly-para-phenylenediamine-montmorillonite clay nanocomposites. Synth. Met. 160, 2397–2403.

Olad, A., Nabavi, R., 2007. Application of polyaniline for the reduction of toxic Cr(VI) in water. J. Hazard. Mater. 147, 845–851.

Owlad, M., Aroua, M.K., Wan, W.M., 2010. Hexavalent chromium adsorption on impreg-nated palm shell activated carbon with polyethyleneimine. Bioresour. Technol. 101, 5098–5103.

Pham, Q.L., Haldorai, Y., Nguyen, V.A., Tuma, D., 2011. Facile synthesis of poly (p-phenylenediamine)/MWCNT nanocomposites and characterization for investigation of structural effects of carbon nanotubes. Bull. Mater. Sci. 34, 37–43.

Qiu, B., Xu, C., Sun, D., Yi, H., Guo, J., Zhang, X., Wei, S., 2014. Polyaniline coated ethyl cel-lulose with improved hexavalent chromium removal. Sustain. Chem. Eng. 2, 2070–2080.

Rivera-Utrilla, J., Sanchez-Polo, M., Gomez-Serrano, V., Alvarez, P.M., Alvim-Ferraz, M.C.M., Dias, J.M., 2011. Activated carbon modifications to enhance its water treat-ment applications. An overview. J. Hazard. Mater. 187, 1–23.

Sestrem, R.H., Ferreira, D.C., Landers, R., Temperini, M.L., Nascimento, G.M., 2009. Struc-ture of chemically prepared poly-(para-phenylenediamine) investigated by spectro-scopic techniques. Polymer 50, 6043–6048.

Setshedi, K.Z., Bhaumik, M., Songwane, S., Onyango, M.S., Maity, A., 2013. Exfoliated poly-pyrrole-organically modified montmorillonite clay nanocomposite as a potential ad-sorbent for Cr(VI) removal. Chem. Eng. J. 222, 186–197.

Stejskal, J., 2015. Polymers of phenylenediamines. Prog. Polym. Sci. 41, 1–31.
Tang, L., Fang, Y., Pang, Y., Zeng, G., Wang, J., Zhou, Y., Chen, J., 2014. Synergistic adsorption and reduction of hexavalent chromium using highly uniform polyaniline–magnetic mesoporous silica composite. Chem. Eng. J. 254, 302–312.
Tseng, R.L., Wu, P.H., Wu, F.C., Juang, R.S., 2014. A convenient method to determine kinetic parameters of adsorption processes by nonlinear regression of pseudo-nth-order equation. Chem. Eng. J. 237, 153–161.
Unuabonah, E.I., Adebowale, K.O., Olu-Owolabi, B.I., 2007. Kinetic and thermodynamic studies of the adsorption of lead (II) ions onto phosphate-modified kaolinite clay. J. Hazard. Mater. 144, 386–395.
Wang, B.J., Jiang, J., Hu, B., Yu, S., 2008. Uniformly shaped poly (p-phenylenediamine) mi-croparticles: shape-controlled synthesis and their potential application for the re-moval of lead ions from water. Adv. Funct. Mater. 18, 1105–1111.
Wang, J., Deng, B., Chen, H., Wang, X., Zheng, J., 2009. Removal of aqueous Hg (II) by polyaniline: sorption characteristics and mechanisms. Environ. Sci. Technol. 43, 5223–5228.
Wojcik, G., Neagu, V., Bunia, I., 2011. Sorption studies of chromium(VI) onto new ion ex-changer with tertiary amine, quaternary ammonium and ketone groups. J. Hazard. Mater. 190, 544–552.
Xie, A., Ji, L., Luo, S., Wang, Z., Xu, Y., Kong, Y., 2014. Synthesis, characterization of poly(m-phenylenediamine)/palygorskite and its unusual and reactive adsorbability to chromium(vi). New J. Chem. 38, 777–783.
Yalcin, S., Apak, R., 2004. Chromium(III, VI) speciation analysis with preconcentration on a maleic acid-functionalized XAD sorbent. Anal. Chim. Acta 505, 25–35.
Yu, W., Zhang, L., Wang, H., Chai, L., 2013. Adsorption of Cr(VI) using synthetic poly(m-phenylenediamine). J. Hazard. Mater. 260, 789–795.
Yuan, P., Fan, M., Yang, D., He, H., Liu, D., Yuan, A., Chen, T., 2009. Montmorillonite-sup-ported magnetite nanoparticles for the removal of hexavalent chromium [Cr(VI)] from aqueous solutions. J. Hazard. Mater. 166, 821–829.
Zadaka, D., Mishael, Y., Polubesova, T., Serban, C., Nir, S., 2007. Modified silicates and po-rous glass as adsorbents for removal of organic pollutants from water and compari-son with activated carbons. Appl. Clay Sci. 36, 174–181.
Zhang, L., Wang, H., Yu, W., Su, Z., Chai, L., Li, J., Shi, Y., 2012. Facile and large-scale synthe-sis of functional poly(m-phenylenediamine) nanoparticles by Cu^{2+}-assisted method with superior ability for dye adsorption. J. Mater. Chem. 22, 18244–18251.

PAPER II

ADSORPTION MECHANISM OF Cr(VI) ON TO POLY(*p*-PHENYLENEDIAMINE)-ADSORBENT FROM WASTEWATER

Adsorption mechanism of Cr(VI) on to poly(*p*-phenylenediamine)-based adsorbent from wastewater

Lindani Mdlalose[a,b*], Mohammed Balogun[a], Maris Klavins[c], Christopher Deeks[d], Jon Treacy[d], Luke Chimuka[b], Avashnee Chetty[a]

[a]Polymers and Composites, Materials Science and Manufacturing , Council for Scientific and Industrial Research, Pretoria, South Africa, P.O Box 395, Pretoria, 0001

[b]Molecular Sciences Institute, School of Chemistry, University of the Witwatersrand, Johannesburg, South Africa P/Bag 3, WITS, 2050

[c]Department of Environmental Science, University of Latvia, Raina Blvd 19, Riga LV-1586, Latvia

[d]Thermo Fisher Scientific, Birches Industrial Estate, East Grinstead, West Sussex, RH19 1UB, United Kingdom

ABSTRACT

Water pollution due to industrial processes has necessitated and spurred robust research into the development of adsorbent materials for remediation. Polyphenylenediamines (PPD) have attracted significant attention because of their dual cationic and redox properties. They are able to reduce Cr(VI) to Cr(III) in solution. Interrogation of the chemical processes involved in the Cr(VI) adsorption of the *para*-PPD was primarily by XPS and FT-IR. It was confirmed that the underlying oxidation of the amino groups to imines during the reduction of Cr(VI) to Cr(III) was irreversible. This process occurred at both acidic and alkaline conditions. Reduction was accompanied by Cr(III) chelation on the adsorbent surface. Further, regeneration with dilute aqueous NaOH and HCl extended the polymer's adsorptive capacity beyond exhaustion of its redox potentials. For phytotoxicity analysis, P*p*PD-MMT loaded and unloaded with Cr(VI) performed way better than pristine P*p*PD with a highest %GI of 99%.

GRAPHICAL ABSTRACT

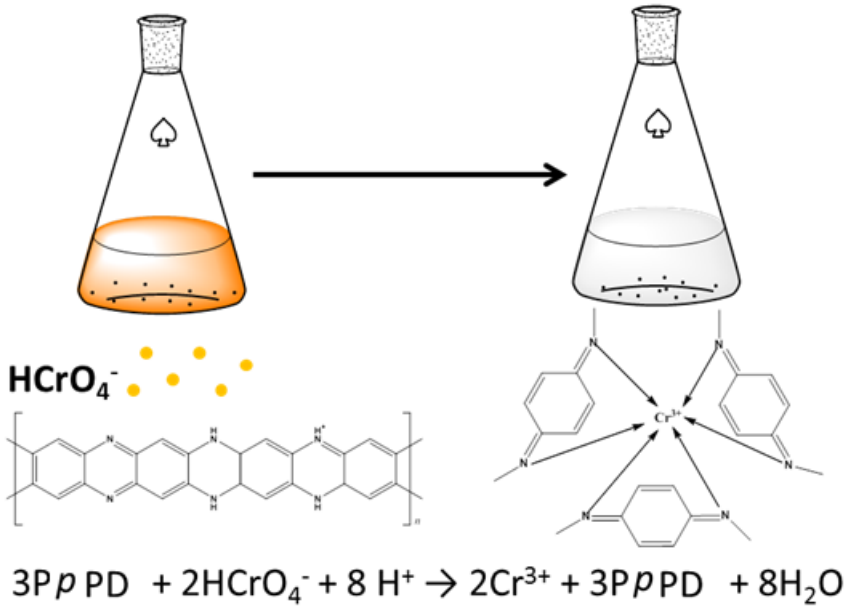

1. Introduction

Industrialization has brought huge pressure on available water resources globally. Many industrial processes are heavily water intensive and, post-use, the effluents are often not suitable for direct discharge to the environment. Strict environmental contamination limits are set by local and international regulatory bodies which must be complied with by the industrial users. This has spurred intense scientific research into technologies for removal of contaminants.

Several established technologies for the removal and recovery of hazardous metal ions from wastewater, but usually with imitated successes, include chemical precipitation, electrolysis, ion exchange, reverse osmosis, membrane separation and adsorption (Li et al., 2009, Tian et al., 2015). Adsorption is attractive and effective methods for its simplicity of design, ease of operation and wide choice of adsorbents (Zhu et al., 2016). To date, more efforts have been contributed to the development of new adsorbents with activated carbon being frequently used for adsorption technology (Ihsanullah et al., 2016). In spite of its

prolific applications, activated carbon is still expensive and is applied mostly in organic compounds adsorption rather than heavy metal ions (Aboua et al., 2015).

Recently, aromatic amine polymers have attracted much interest due to their wide range of applications, strong electroactivities, and high environmental and thermal stabilities. Polyaniline (PANI) has been investigated as a potential adsorbent for metallic pollutants because of its facile synthesis and excellent redox reversibility (Kumar et al., 2013, Qiu et al., 2014). Poly(phenylenediamine) (PPD), a cheaper diamine derivative of PANI, has drawn interest due to its high oxidative polymerization yield and large numbers of amine and imine functional groups (Stejskal, 2015). PPDs have shown high affinity to metal ions through redox reactions and chelations by the amino/imino groups. Poly(meta-phenylenediamine) (P*m*PD)-palygorskite composite was demonstrated to bear a maximum adsorption capacity of 153 mg/g for Cr(VI) removal (Xie et al., 2014). The adsorption capacity of poly(ortho-phenylenediamine) (P*o*PD) microparticles for Pb^{2+} reached 533 mg/g (Han et al., 2011). Wang et al. (2008) reported that poly(para-phenylenediamine) (P*p*PD) microparticles gave a superior Pb^{2+} removal of 2890 mg/g .

Polymers containing abundant amine groups like PPD can act as electron donors and therefore reduce the valence states of metallic pollutants (Li et al., 2009). These polymers consist of three idealized oxidation states (leucoemeraldine, emeraldine and pernigraniline) which correspond to the reduced, doped and oxidized states of the polymer chain, respectively. This intriguing multi-functionality is the most important scavenger of metals including trace metals as a result of dominant adsorptive strength.

We and other authors have reported on the use of PPD as an adsorbent for Cr(VI) removal (Mdlalose et al., 2017, Wang et al., 2008). In aqueous solution, Cr primarily exists as Cr(III) and Cr(VI) steady states. Cr(VI) exists predominantly as H_2CrO_4, $HCrO_4^-$, and CrO_4^{2-} at pHs less than 1.0, from 1.0 to 6.0, and greater than 6.0, respectively (Dionex, 1996). It is one of the most toxic industrially-produced heavy metals while Cr(III) is considered non-toxic.

PPD does not only adsorb Cr(VI) through electrostatic interactions, it also reduces Cr(VI) to Cr(III) followed by complexation on the adsorbent surface (Xie et al., 2014) . There is, however, a paucity of information on the chemical interactions occurring on the surface of

the polymer. Here, we report on the use of various analytical tools to interrogate and understand the adsorption process on the surface of P*p*PD. We also investigated the effect of two regenerants, NaOH and HCl, used separately and in tandem on the regeneration of P*p*PD and P*p*PD-clay composite.

2. Material and Methods

2.1. Chemicals

Montmorillonite (MMT) clay, para-phenylenediamine (*p*PD), potassium dichromate ($K_2Cr_2O_7$) and ammonium peroxydisulphate ($(NH_4)_2S_2O_8$) were purchased from Sigma Aldrich, Germany. Hydrochloric acid (HCl) and sodium hydroxide (NaOH) were purchased from Merck, Germany and were used without further purification.

2.2. Synthesis of P-*p*-PD and P-*p*-PD-MMT composite

In general, the synthesis protocols of both the pristine P*p*PD and the composite have been described elsewhere (Mdlalose et al., 2017). Briefly, the P*p*PD-MMT composite, was prepared via in situ chemical oxidation polymerization method. MMT clay (2 g) was dispersed in a *p*PD solution (1.62 g, 0.015 mol) in HCl (0.1 M) and stirred for 3 hrs. The ammonium peroxydisulfate oxidant solution (3.42 g, 0.015 mol) in 25 mL of HCl (0.1 M) was added dropwise to the mixture and left to stir for 24 hrs under ambient conditions. The resulting slurry was then filtered, washed with de-ionized water and dried at 60 °C under vacuum for 24 hrs.

2.3. Characterization of P*p*PD and P*p*PD-MMT composite

Elemental analyser (Carlo Erba 1108) was used to determine the amount of C, N and H content in the composite. The specific surface area was measured using Brunauer-Emmett-Teller (BET) instrument (Gemini 2360) by isothermal nitrogen gas adsorption. Thermal was performed on themogravimetry thermal analyser (TG), Exstar 6000 TG/DTA 6300 using nitrogen gas. The presence of functional groups was determined using Fourier transform infrared (FT-IR) spectroscopy (Spectrum One Apparatus, Perkin Elmer) using

KBr pellets. The surface chemistry of the polymer was also analysed by X-ray photoelectron spectroscopy (XPS) (K-Alpha$^+$ spectrometer) to determine the binding energies of the elements present.

2.4. Adsorption-desorption experiments

All adsorption experiments were carried out on a shaker at 120 rpm and an ambient temperature of 25 °C. Suspensions of P*p*PD (0.15 g) and the composite P*p*PD-MMT (0.15 g) in aqueous Cr(VI) solutions (50 mL, 100 mg/L, pH 2) were agitated for 24 h on the shaker. The solid adsorbent particles were filtered and air dried at room temperature after the experiments. The particles were then transferred into another container, and 25 mL of the regeneration solution (either 0.05 M NaOH or 0.1 M HCl) was added, followed by shaking for 1 h to allow for complete desorption of the bound Cr ions. The adsorbent particles were then filtered from the solution and air dried at room temperature. The adsorption-desorption cycle was repeated multiple times. The filtrates obtained from adsorption and desorption were measured using a UV–Vis spectrophotometer (PerkinElmer Lambda) at 540 nm using 1,5 diphenylcarbazide reagent to determine Cr(VI) concentration. Atomic absorption spectrometer (AAS) (PerkinElmer AAnalyst 200) was used to determine total Cr. The equilibrium adsorption capacity (qe) was calculated using equation (1).

$$qe = \frac{(Co - Ce)V}{m} \qquad (1)$$

where:

m is the mass of the adsorbent (g)

V is the volume of the solution (L)

Co and Ce represent the initial and final concentrations of Cr(VI) (mg/L), respectively

$$\%\text{Removal} = \left(\frac{Co - Ce}{Co}\right)100\% \qquad (2)$$

Regeneration efficiency was calculated using:

$$\%\,\text{Regeneration} = \frac{qe}{qo}\,x\,100\% \qquad (3)$$

qe is the adsorption capacity of regenerated adsorbent and qo is the adsorption capacity of the initial adsorption cycle.

2.5. Phytotoxicity experiment

Toxicity of the adsorbents before and after Cr(VI) adsorption were studied against Lepidium sativum (L. sativum) seeds. Seeds were placed in Petri dishes lined with germination sheets soaked in P-p-PD and P-p-PD-MMT laden with a range of Cr(VI) concentration. Cr(VI) solution before treatment and control sample were also tested. Plates were incubated at 25 °C for 7 days. After incubation, growth parameters were determined according to the formula

where:
Gi: germination index, G0 and L0 are respectively mean seed germination and root length in the control, G and L are mean seed germination and root length in the stabilized mixture.

3. Results and Discussion

3.1. Characterization of P-*p*-PD and P-*p*-PD-MMT composite

The synthesis of the pristine polymer and MMT composite yielded 99.86% and 97.64% of the respective products. Elemental analysis of the composite gave an organic composition of 21.9% carbon, 4.3% nitrogen and 2.1% hydrogen based on the elements' stoichiometries indicating that the composite consisted of more than 70% of MMT clay.

The specific surface areas were found to be 10.13 m^2/g for MMT, 55.42 m^2/g for P-*p*-PD and 90.30 m^2/g for P*p*PD-MMT composite. The incorporation of P*p*PD into MMT interlayers significantly increased the surface area of the adsorbent composite. This translates into greater exposure of the adsorbent to the contaminated water.

TGA curves for P*p*PD-MMT with P*p*PD before and after Cr(VI) adsorption in Fig. S1 (Supplementary Materials) indicate similar mass loss behaviour between the two materials. A small loss of mass before 120 °C is attributed to the evaporation of absorbed water. According to this analysis, there was an insignificant mass loss for P*p*PD from the onset decomposition temperature up until the maximum mass loss which occurred at 566 °C. This indicates that P*p*PD has a good thermal stability. When comparing P*p*PD and P*p*PD-MMT composite, the composite exhibited a higher thermal stability because of the interaction between P*p*PD and MMT components. Although the onset decomposition temperature was almost the same for pristine polymer before and after adsorption, drastic maximum mass loss for the latter was obtained at a low decomposition temperature of 180 °C which was almost 10% less than the polymer before adsorption. This is attributed to more benzenoid structural units on bare P*p*PD with better thermal stability than the quinoid arrangements that occur after Cr(VI) adsorption (Zeng & Ko, 1998).

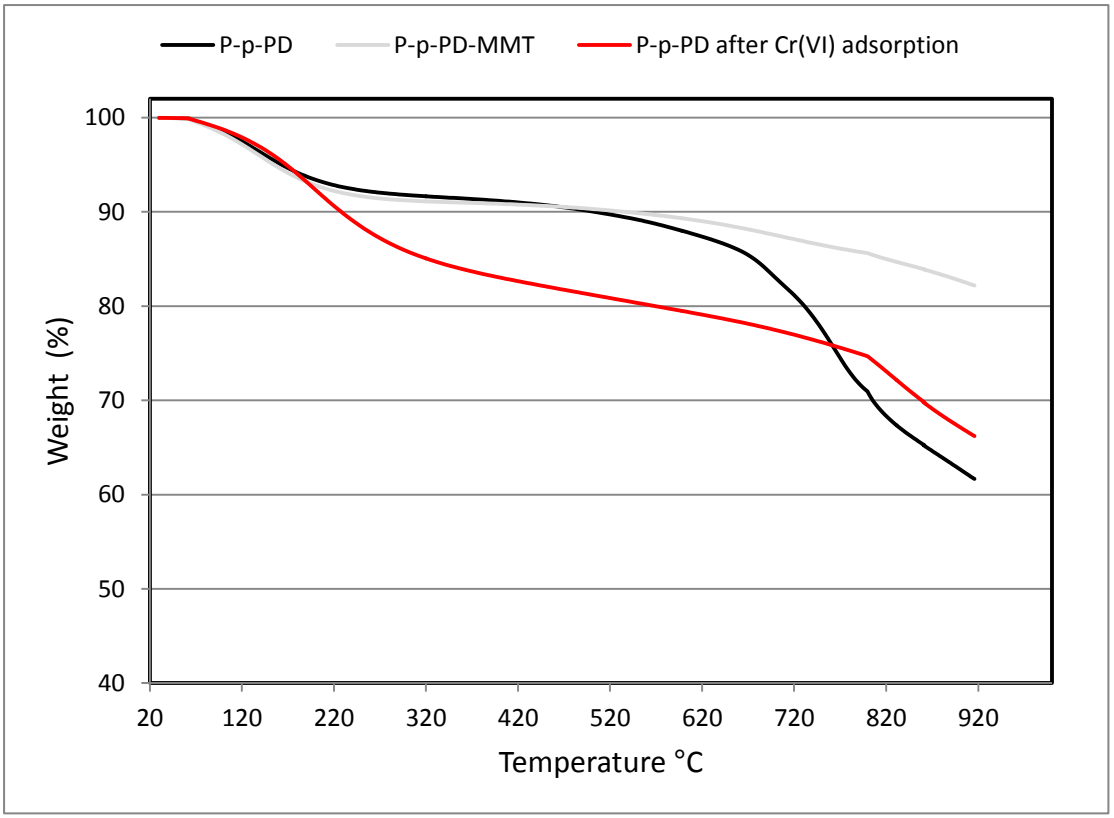

Fig. S1. TGA of P*p*PD-MMT and P*p*PD before and after Cr(VI) adsorption

3.2. Adsorption and desorption of Cr(VI)

P*p*PD and P*p*PD-MMT removed Cr(VI) with high efficiency at low pH but this decreased as the acidity of the medium decreased (Fig. 1). The mechanism of removal was a redox process. The removal and reduction capacities were investigated. The amount of Cr(VI) removed was determined experimentally while the total Cr was determined by calculating the Cr(III) remaining in the solution. Both the pristine P*p*PD and the composite P*p*PD-MMT showed excellent reduction efficiencies of Cr(VI) at acidic pH such that there was almost no detectable amount of Cr(VI) between pH 2 and 3.

Total Cr removal was 81% for pristine P*p*PD at pH 2 and this increased to 96% at pH 3. This suggests that Cr(VI) was reduced to Cr(III) and was released into the solution again as 18% and 4% of Cr(III) ions were detected at pH 2 and pH 3, respectively. A similar observation was made for the composite which suggests that the Cr(VI) reduction property is inherent in the polymer and was not affected by incorporation into clay.

The percentage of Cr(III) present in the solution after adsorption was observed not to be equivalent to the initial Cr(VI). This can be explained by the very low solubility of Cr(III). This explanation is supported by the high recovery of Cr(III) after desorption of the adsorbent [*vide infra*].

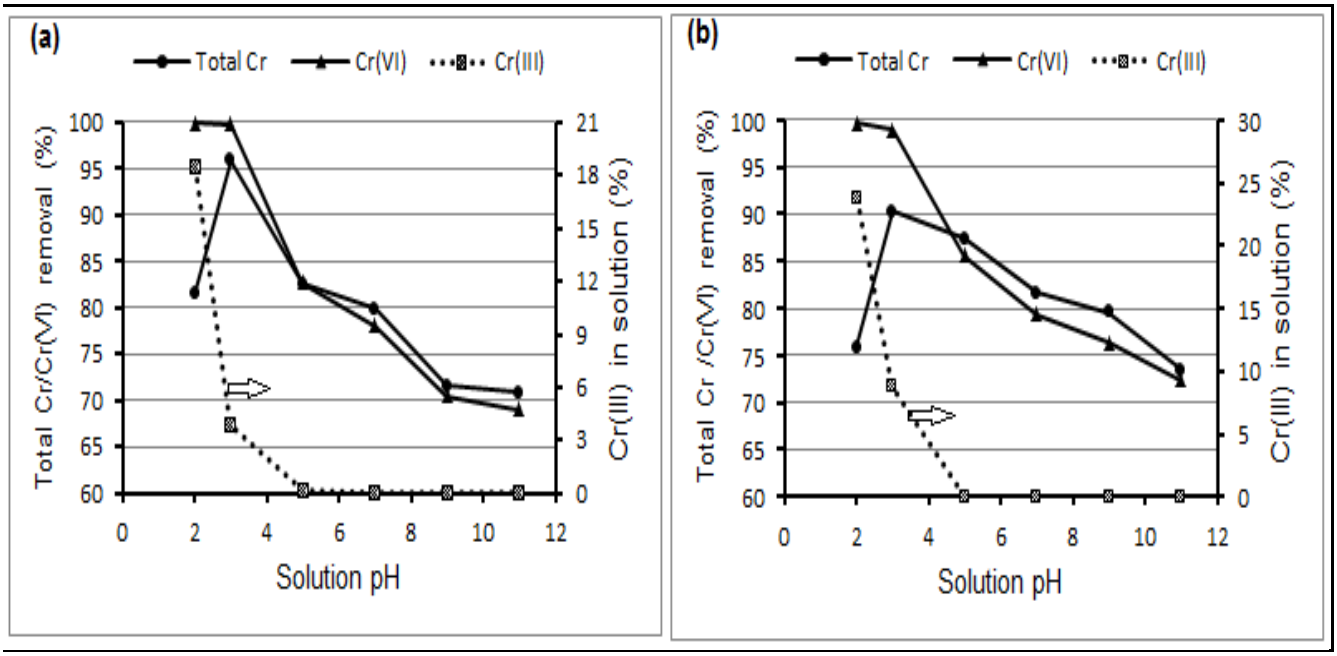

Fig. 1. Effect of solution pH for total Cr and Cr(VI) removal with Cr(III) in solution: (a)

P*p*PD and (b) P*p*PD-MMT. (Temperature = 25 °C, time = 24 h, adsorbent dose = 0.15 g/50 mL, initial concentration = 100 mg/L).

To further understand the chemical redox reaction occurring during the adsorption process, P*p*PD was examined using XPS. XPS spectra of N1s and Cr2p shown in Fig. 2 determined the valence state of nitrogen and chromium functional groups present on the polymer surface before and after been treated with Cr(VI) solution at pH 2 and pH 8 for one cycle. In general, N1s XPS and XANES spectrum of P*p*PD is deconvoluted into two discrete curves located at 399.2 eV, and 401.8 eV which are attributed to amine (-NH-) and charged nitrogens (-N^+=) which are referred to as radical –N^+= and dictation –N^+= nitrogens (Sestrem et al., 2009).

Figure 2(a) shows high resolution N1s spectra of bare P*p*PD with two high resolution peaks at 399 eV for –NH- and 402 eV for –N^+ = with molar ratios of 47.8 and 52.2, respectively. After Cr(VI) adsorption at pH 2 (shown in Fig. 2(b)) the charged –N^+= group signal disappeared and a typical imine (-N=) band appeared at a binding energy of 398.5 eV with a molar ratio of 6.3%. However, after Cr(VI) adsorption at pH 8 three bands were observed at 398 eV (2.7%), 399 eV (86%) and 401 eV (11.3%), which correspond to the functionalities –N=, -NH- and charged –N^+=, respectively. This indicates that the oxidation state of P*p*PD decreased in basic medium, verified by the oxidized imine (-N=) band of 2.7% at pH 8 and 6.3% at pH 2. The occurrence of redox adsorption was also confirmed by the FT-IR spectra in Fig. 4, where the intensity of the benzenoid peak (1510 cm^{-1}) decreased after adsorption indicating the enhancement of polymer-oxidized state through Cr(VI) reduction.

Significant bands with binding energies between 577-578 eV and 586-588 eV are observed in the Cr2p spectra (Fig. 2(d) and (e)). These energy bands correspond to the Cr2p3/2 and Cr2p1/2 orbitals of Cr(III). The higher binding energies between 580-580.5 eV and 589-590 eV correspond to Cr(VI) forms (Biesinger et al., 2011). The Cr2p3/2 and Cr2p1/2 peaks that are respectively centred at 578 eV and 588 eV for adsorption at pH 2 and pH 8 are entirely contributed by Cr(III). No Cr(VI) was detected on the polymer surface.

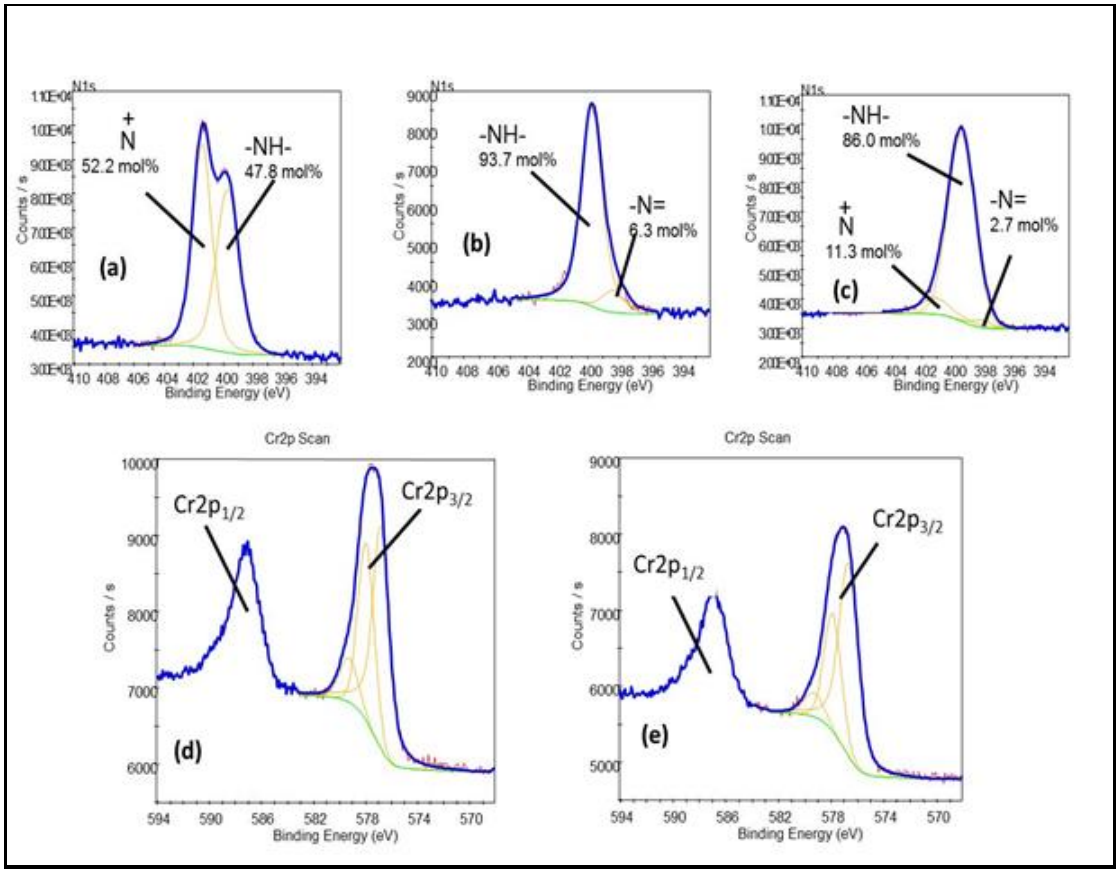

Fig. 2. XPS N1s of P*p*PD before (a) and after adsorption at pH 2 (b) pH 8 (c). XPS Cr2p of P*p*PD after adsorption at pH 2 (d) and pH 8 (e).

It is known that the adsorption free energy of $HCrO_4^-$ (the major oxochromium species present at pH 2) is -2.5 to -0.6 kcal/mol whereas for CrO_4^{2-} (the major oxochromium species present at pH 8) it is -2.1 to -0.3 kcal/mol (Hu et al., 2005). The higher free adsorption energy for CrO42- makes it less favourable for adsorption than $HCrO_4^-$. Further, the reduction potential of $HCrO_4^-$ (+1.33 eV) is higher than the reduction potential of CrO_4^{2-} (-0.12) which makes the former preferential for reduction by P*p*PD. It was observed that above pH 2 the Cr(VI) removal process was predominantly reduction accompanied by complexation of Cr(III) to the polymer.

Because of the pH dependency of the Cr(VI) removal process the P*p*PD could be regenerated and recycled for re-use of the adsorbents by changing the pH of the solution (Wang et al., 2015). Using an aqueous NaOH (0.05 M) solution (to desorb Cr(VI) and HCl (0.1 M) the adsorption capacity was restored for seven cycles (Fig. 3). The Cr(VI) desorption capacity increased significantly between the first and fourth cycles and

remained relatively constant thereafter. Beyond the 7th cycle only Cr(VI) was desorbed implying that the polymer was fully, and probably irreversibly, oxidized. The adsorption of Cr(VI) from the solution was still maintained at about 49 mg/g (98. 8% efficiency). This continued removal of Cr(VI) might be due to the ionic interactions between the 'NH' groups of the polymer and the anion.

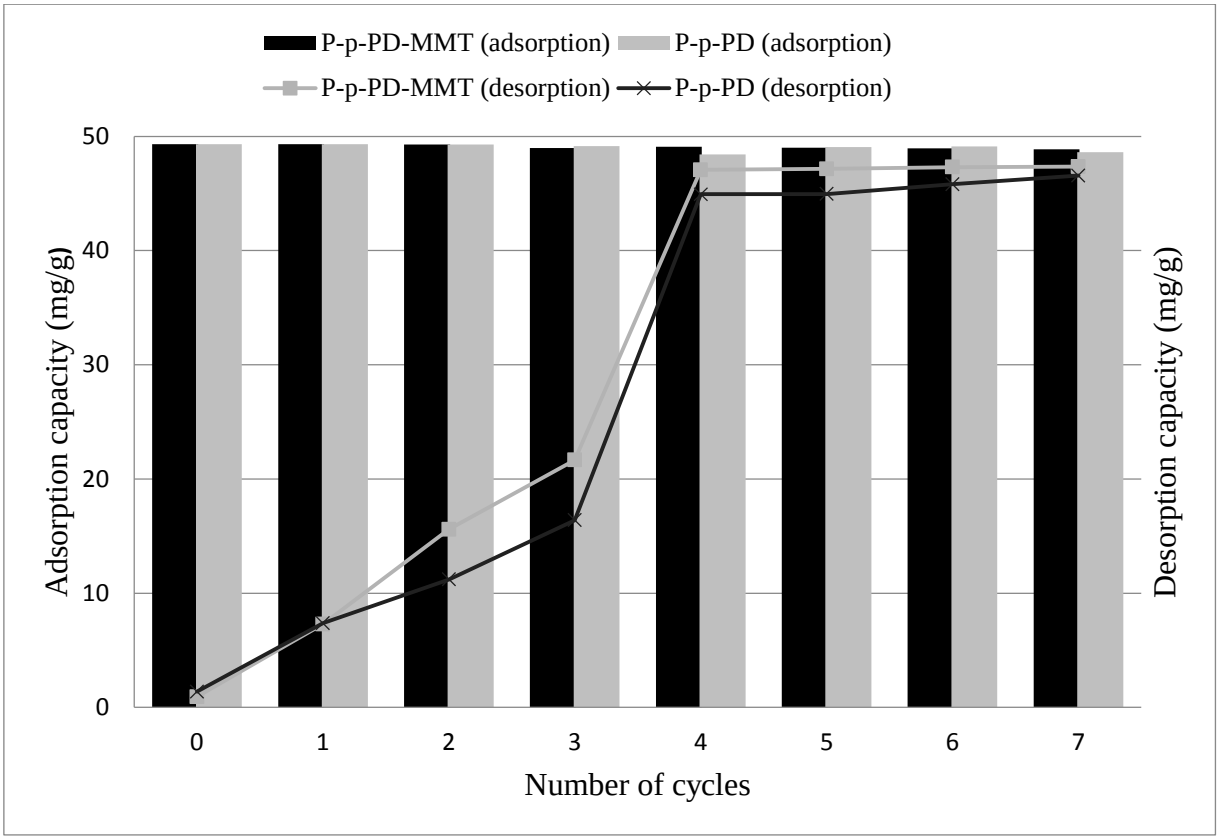

Fig. 3. Adsorption-desorption cycles and regeneration of adsorbents using NaOH (0.05 M) and HCl (0.1 M). (Temperature = 25 °C, adsorption time = 24 h, desorption time = 1 h adsorbent dose = 0.15 g/50 mL, initial concentration = 100 mg/L).

FT-IR was used to monitor the adsorption of Cr(VI) onto the functional P*p*PD (Fig. 4). The typical functional groups of the pristine P*p*PD is well described in literature (Sestrem, et al., 2009). The major peaks located around 3500, 1590, 1509 and 1200 cm^{-1} are attributed to N-H stretching vibration, stretching mode of quinoid imine, benzenoid amine and the C-N band, respectively (Fig. 4). The benzenoid amine (1509 cm^{-1}) of the polymer before adsorption has high intensity relative of its quinoid imine (1590 cm^{-1}). After Cr(VI)

adsorption, there was a decline in the benzenoid amine band while there was a noticeable broadening of the quinoid imine to 1625 cm^{-1}. These signal variations correspond to a redox reaction between P*p*PD and Cr(VI) with a resultant oxidation of the polymer to the quinoid imine form after adsorption. There was no significant reversal of this process when the adsorbent was repeatedly regenerated.

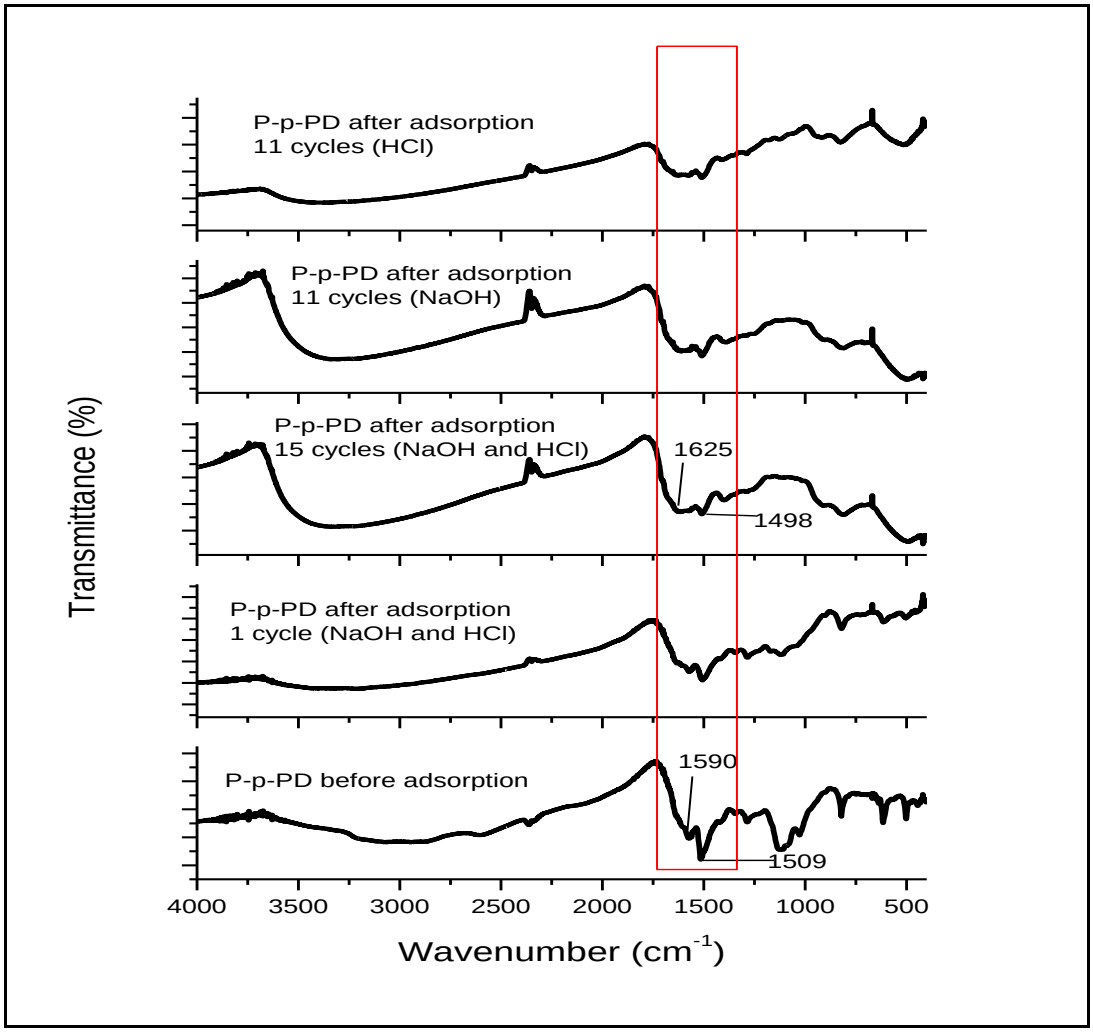

Fig. 4. FT-IR spectra of P*p*PD before and after Cr(VI) adsorption.

3.3. Effect of regenerants on continual adsorption cycles

An economically viable and environmentally suitable adsorbent is one that can be re-used several times through a facile regeneration process. Many papers have reported on various regeneration methods, often using aqueous solutions of acids, bases or salts (Huang et al., 2007, Lata et al., 2015).

The effect of aqueous regenerants on the performance of P*p*PD as a pristine polymer and as a clay composite in a cyclical adsorption-desorption-regeneration process was investigated. Unlike what has predominantly been reported in the literature, emphasise of Cr(VI) desorption for each cycle was investigated instead of just the number of regeneration cycles. NaOH, HCl and a combination of the two were used as regenerants. Maximum capacity of the Cr(VI)-adsorbed polymer could not be restored even after just the first regeneration cycle when NaOH was used as the only regenerant (Fig. 5(a)). The capacity continued to drop progressively until more than 50% of the adsorption efficiency was lost by the 10^{th} cycle, the terminal cycle of this investigation. Regeneration with HCl alone resulted in a similar loss of adsorption capacity by the 10^{th} cycle (Fig. 5(b)). However, the adsorbent showed resilience up to three regeneration cycles with more than 90% adsorption capacity remaining in the first three cycle times.

Zhang & Bai (2003) reported that treatment of adsorbents with aqueous HCl exponentially increases the hydronium ions (H^+) on the material's surface. As a result, the positive zeta potential of the material increases gradually as the amino nitrogen atoms on the polymer get protonated. As the polymer's amino group content depreciates due to conversion to the imines, protonation from HCl had limited impact on the positive charge content of the adsorbent.

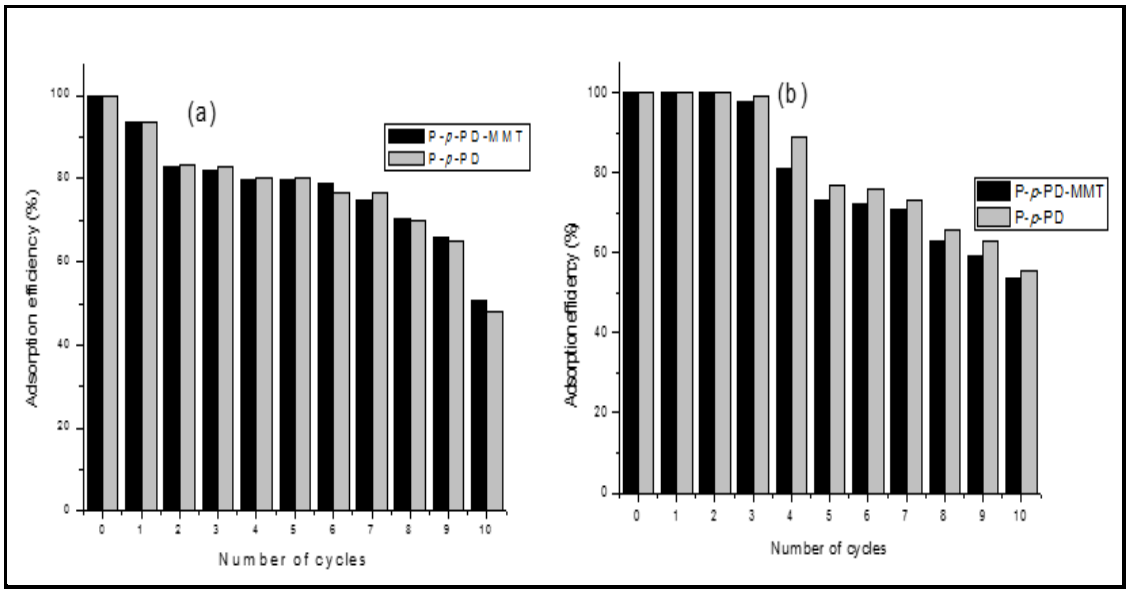

Fig. 5. Successive regeneration cycles using NaOH (0.05 M) (a) and HCl (0.1 M) (b). (Temperature = 25 °C, adsorption time = 24 h, desorption time = 1 h, adsorbent dose = 0.15 g/50 mL, initial concentration = 100 mg/L).

A different scenario was observed when regeneration was carried out with both regenerants. A synergy appears to have occurred in initially treating the adsorbent with NaOH (0.05 M) and following this with HCl (0.1 M). The polymer performed optimally for eight cycles of adsorption-desorption-regeneration (Fig. 6). A gradual decline was only observed after the eighth cycle and even then about 80% adsorption efficiency was obtained at the 10^{th} cycle, a significant contrast to 50% efficiency when the regenerants were used individually. An explanation for this remarkable synergy is that NaOH is able to release bound Cr(VI) adsorbates from the material's surface while HCl is able to desorb Cr(III) (Setshedi et al., 2013). Hence, used together, these processes avail more adsorption sites for the next cycle than when used separately.

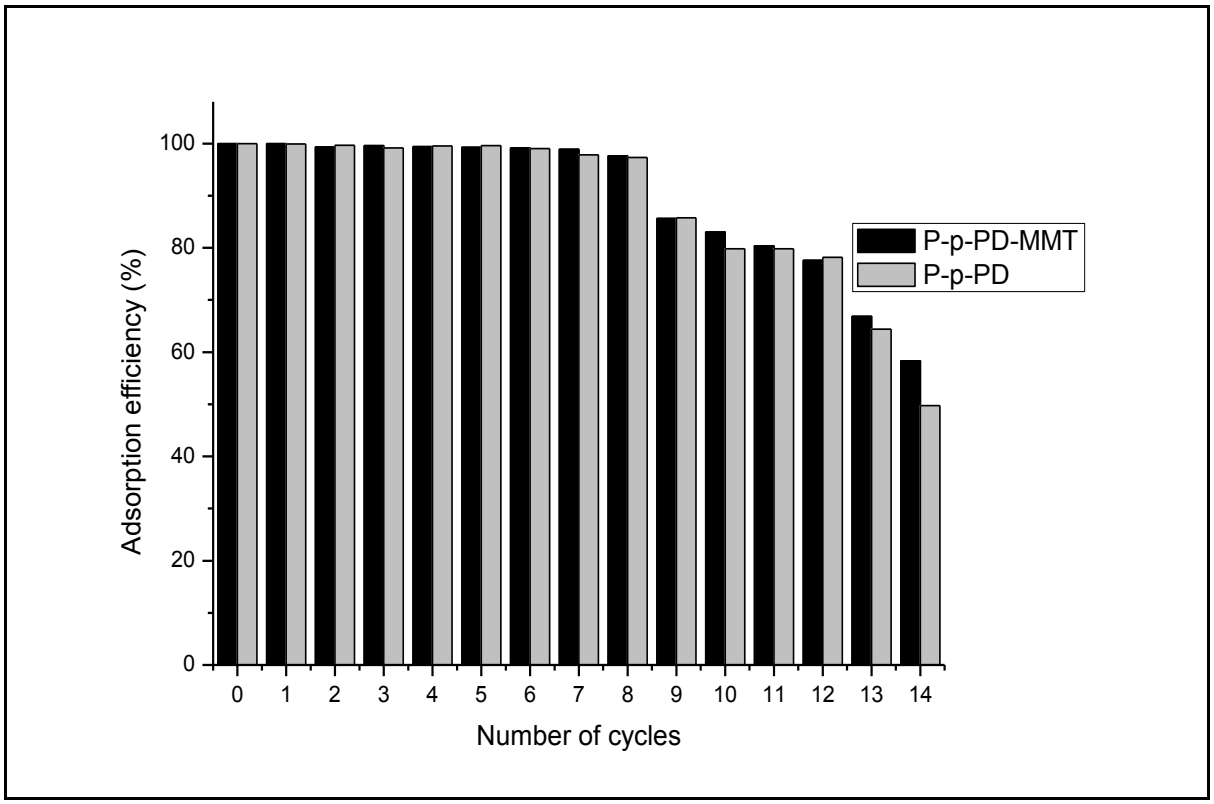

Fig. 6. Successive regeneration cycles using NaOH (0.05 M) and HCl (0.1 M). (Temperature = 25 °C, adsorption time = 24 h, desorption time = 1 h adsorbent dose = 0.15 g/50 mL, initial concentration = 100 mg/L).

3.4. Phytotoxicity test

To protect the ecological risks of soil contamination for used adsorbents, phytotoxicity test was implemented. Stable oxidation states of chromium which are Cr(VI) and Cr(III) present different toxicological characteristics as regulated by EPA. Cr(VI) is a powerful tissue irritant and considered toxic to many plants, aquatic animals and microorganisms while Cr(III) is generally not harmful. Phytotoxicity studies were carried out to determine the presence or absence of seed germination for P*p*PD and P*p*PD-MMT before and after Cr(VI) adsorption and to confirm the reduction of Cr(VI) to Cr(III) on the adsorbents surface. Initially, a range of Cr(VI) (50 mg/L – 200 mg/L) solution was exposed to *L. sativum* seed and incubated for 10 days to assess growth. No germination was observed for the entire period, instead there was radicles growth inhibition when they were starting to emerge (Fig 10 (f)).

Seed germination severely diminished to 35% and 14% (respective to control) in the presence of P*p*PD-MMT and P*p*PD, respectively as shown in Fig 9. From this observation, it was clear that the germination medium was sensitive plant growth even before adsorbing Cr (Fig 10). With respect to Cr(VI) reduction on adsorbents, seed germination increased with the increase in Cr(VI) initial concentration (Fig 9). Although that was the case, P*p*PD-MMT performed way better than the pristine P*p*PD with the maximum Cr(VI) of 200 mg/L reaching a GI% of 99%. The manifested negative influence of pristine P*p*PD might be attributed to its high oxidation state which then hinders the seed germination and root growth due to oxidative stress (Foyer & Shigeoka 2011). P*p*PDMMT consists of only 44% of the polymer matrix hence it performed better. Given the need of sustainable development, P*p*PD-MMT has proven to show great features as a potential adsorbent.

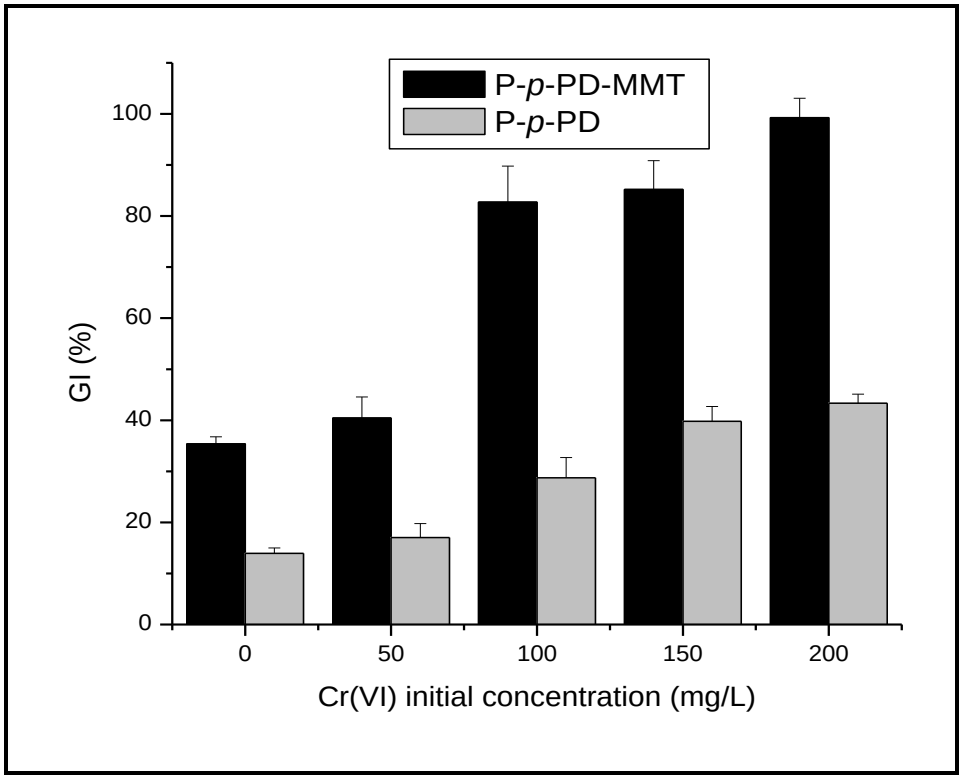

Fig. 7. Effect of Cr(VI) initial concentration on P*p*PD-MMT and P*p*PD for seed germination of *L. sativum*.

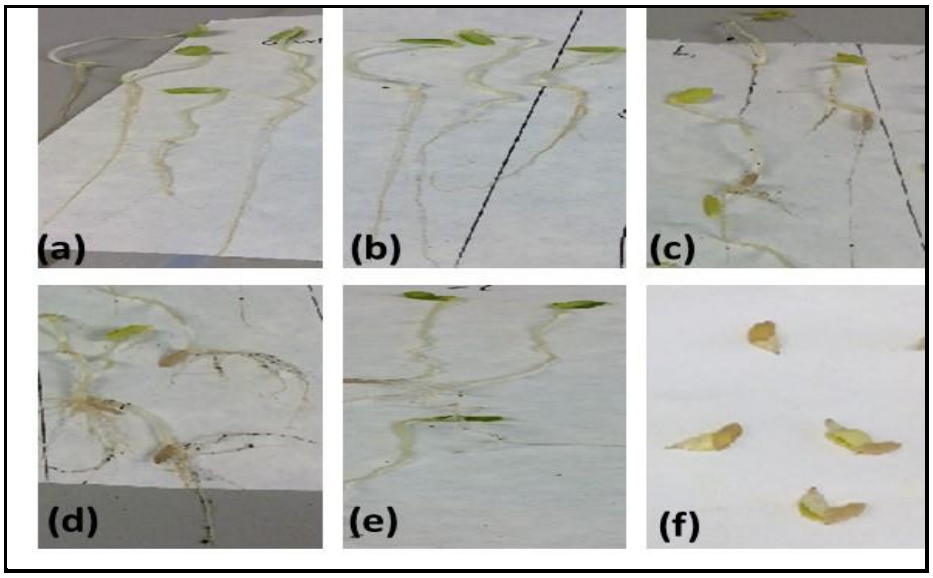

Fig. 8. Seed germination and root growth of *L. sativum* for (a) control, (b) P*p*PD-MMT after Cr(VI) adsorption, (c) P*p*PD after Cr(VI) adsorption, (d) P*p*PD-MMT before adsorption, (e) P*p*PD before adsorption and (f) Cr(VI) solution.

4. Conclusion

The polymer P*p*PD and its clay composite P*p*PD-MMT were facilely synthesized and used to remove Cr(VI) from wastewater as have been previously reported. Phenylenediamine-based polymers have redox potentials and we deliberately investigated, by FT-IR and XP spectroscopies, the role of this property in the adsorption process. Both the pristine polymeric and composite materials showed effective Cr(VI) removal performance through a combination of metal reduction and chelation. The Cr(VI) adsorption efficiency was mainly affected by the solution pH with the maximum adsorption at pH 2. The adsorbents were regenerated and reused using NaOH and/or HCl as regenerants. Treatment with the regenerants showed irreversible oxidation reaction for adsorbents while still removing Cr(VI) for several cycles.

Acknowledgements

This work was supported by the South African Council for Scientific and Industrial Research (CSIR) (Project grant: 88568), National Research Foundation (NRF) PDP and Erasmus Mundus (Aesop project). The authors acknowledge the University of the Witwatersrand and the University of Latvia for contributions to this project.

References

Aboua, K.N., Yobouet, Y. A., Yao, K. B., Gone, D. L. and Trokourey, A, 2015. Investigation of dye adsorption onto activated carbon from the shells of Macore fruit. *Journal of Environmental Management*, 156, pp.10–14.

Mark C. Biesingera, Brad P. Paynec, Andrew P. Grosvenord, Leo W.M. Laua,c, Andrea R. Gersonb, Roger St.C. Smartb

Biesinger, M.C., Payne, B. P., Grosvenor, A. P., Lau L. W., Gerson A. R., Smart, G. R., 2011. Resolving surface chemical states in XPS analysis of first row transition metals , oxides and hydroxides : Cr , Mn , Fe , Co and Ni. *Applied Surface Science*, 257(7), pp.2717–2730.

Dionex, 1996. Determination of Cr(VI) in water, wastewater and solid waste extracts. *Dionex Corporation*, (VI), pp.1–5.

Foyer, C.H. & Shigeoka, S., 2011. Understanding oxidative stress and antioxidant functions to enhance photosynthesis. *Plant physiology*, 155(1), pp.93–100.

Han, J., Han, J., Dai, J. and Guo, R., 2011. Journal of Colloid and Interface Science Highly efficient adsorbents of poly (o -phenylenediamine) solid and hollow sub-microspheres towards lead ions : A comparative study. *Journal of Colloid And Interface Science*, 356(2), pp.749–756.

Hu, J., Chen, G., and Lo, I. M. C, 2005. Removal and recovery of Cr(VI) from wastewater by maghemite nanoparticles. *Water Research*, 39(18), pp.4528–4536.

Huang, M.-R., Lu H.-J., Li, X.-G., 2007. Efficient multicyclic sorption and desorption of lead ions on facilely prepared poly(m-phenylenediamine) particles with extremely strong chemoresistance. *Journal of colloid and interface science*, 313(1), pp.72–9.

Ihsanullah, A., Al-Amer, A. M., Laoui, T., Al-Marri, M. J., Nasser, M. S., Khraisheh, M., Atieh, M. A., 2016. Heavy metal removal from aqueous solution by advanced carbon nanotubes: Critical review of adsorption applications. *Separation and Purification Technology*, 157, pp.141–161.

Kumar, R., Ansari, M. O. and Barakat, M. A., 2013. DBSA doped polyaniline/multi-walled carbon nanotubes composite for high efficiency removal of Cr(VI) from aqueous solution. *Chemical Engineering Journal*, 228, pp.748–755.

Lata, S., Singh, P. K. and Samadder, S. R., 2015. Regeneration of adsorbents and recovery of heavy metals: a review. *International Journal of Environmental Science and*

Technology, 12(4), pp.1461–1478.

Li, X.G., Ma, X. L, Sun, J., and. Huang, M. R., 2009. Powerful Reactive Sorption of Silver (I) and Mercury (II) onto Poly (o-phenylenediamine) Microparticles. *Langmuir*, 25(3), pp.1675–1684.

Mdlalose, L., Balogun, M., Setshedi, K., Tukulula, M., Chimuka, L., and Chetty, A., 2017. Synthesis, characterization and optimization of poly(p-phenylenediamine)-based organoclay composite for Cr(VI) remediation. *Applied Clay Science*, 139, pp.72–80.

Qiu, B., Xu, C., Sun, D., Yi, H., Guo, J. Zhang, X., Qu, H., Miguel Guerrero, M., Wang, X., Noel, N., Luo, Z., Guo, Z., and Wei, S., 2014. Polyaniline Coated Ethyl Cellulose with Improved Hexavalent Chromium Removal. *ACS Sustainable Chemistry & Engineering*, 2, pp.2070-2080.

Sestrem, R.H., Ferreira, D. C., Landers, R., Temperini, M. L. A. and do Nascimento, G. M., 2009. Structure of chemically prepared poly-(para-phenylenediamine) investigated by spectroscopic techniques. *Polymer*, 50(25), pp.6043–6048.

Setshedi, K.Z., Bhaumik, M., Songwane, S., Onyango, M. S. and Maity, A., 2013. Exfoliated polypyrrole-organically modified montmorillonite clay nanocomposite as a potential adsorbent for Cr(VI) removal. *Chemical Engineering Journal*, 222, pp.186–197.

Stejskal, J., 2015. Polymers of phenylenediamines. *Progress in Polymer Science*, 41(C), pp.1–31.

Tian, Z., Yang, B., Cui, G., Zhang, L., Guo, Y. and Yan, S., 2015. Synthesis of poly(m-phenylenediamine)/iron oxide/acid oxidized multi-wall carbon nanotubes for removal of hexavalent chromium. *RSC Advances*, 5(3), pp.2266–2275.

Wang, B.J., Jiang, J., Hu, B., and Yu, S., 2008. Uniformly Shaped Poly (p - phenylenediamine) Microparticles : Shape-controlled Synthesis and Their Potential Application for the Removal of Lead Ions from Water. *Advanced Functional Materials*,18, pp.1105–1111.

Wang, T., Zhang, L., Li, C., Yang, W., Song, T., Tang, C., Meng, Y., Dai, S., Wang, H., Chai, L., and Luo, J., 2015. Synthesis of Core−Shell Magnetic Fe_3O_4 @poly(m-Phenylenediamine) Particles for Chromium Reduction and Adsorption. *Environmental Science & Technology.*, 49, pp.5654-5662.

Xie, A., Ji, L., Luo, S. , Wang, S. Xu, Y. and Kong, Y., 2014. Synthesis, characterization of poly(m-phenylenediamine)/palygorskite and its unusual and reactive adsorbability

to chromium(VI). *New Journal of Chemistry*, 38(2), pp.777.

Zeng, X.-R. & Ko, T.-M., 1998. Structures and properties of chemically reduced polyanilines. *Polymer*, 39(5), pp.1187–1195.

Zhang, X. & Bai, R., 2003. Surface electric properties of polypyrrole in aqueous solutions. *Langmuir*, 19(26), pp.10703–10709.

Zhu, K., Gao, Y., Tan, X. and Chen, C., 2016. Polyaniline-Modified Mg/Al Layered Double Hydroxide Composites and Their Application in Efficient Removal of Cr(VI). *ACS Sustainable Chemistry and Engineering*, 4(8), pp.4361–4369.

PAPER III

CHEMICAL REGENERATION OF POLYPYRROLE-MONTMORILLONITE CLAY FOR Cr(VI) REMOVAL IN WASTEWATER

Abstract

Ppy-based materials have been studied in many adsorption processes related to trace elements removal, more especially Cr(VI) from the water phase. The progressive accumulation of Cr(VI) onto the material surface reduces their adsorption capacity before the adsorbent becomes exhausted. This factor limits the application of these adsorbents due to high cost and environmental impact related to disposal after use. Here, we report a feasible recycling procedure to recover the adsorbed Cr from a Ppy-MMT composite and to restore the initial adsorption capacity of the adsorbent. The resultant adsorbent was characterized by FTIR, TGA and EDS analysis. At low solution pH, Ppy-MMT is protonated resulting in high adsorption capacity for Cr(VI) through electrostatic attraction and ion exchange while simultaneously reducing Cr(VI) to less toxic Cr(III). The spent adsorbent was reversibly subjected to sequential adsorption-desorption cycles between adsorbent neutral state and the oxidized state using eluents (NaOH, NH_4OH) and regenerants (HCl, NH_4Cl, HNO_3) respectively. The results suggested that with 0.01 M NaOH and 0.5 M HCl, Ppy-MMT could be used for over five cycles for Cr(VI) removal with more than 80% regeneration efficiency showing good promise as potential adsorbent for chromium remediation.

1. Introduction

The commonly used techniques for chromium ions removal are focused on chemical precipitation, ion exchange, electrochemical, membrane and adsorption (Minocha, 2006). Most of these are expensive, produce large volumes of sludge and not sensitivity to lower pollutants concentrations. Among them adsorption has gained interested because it is easy to use and has wider applicability from concentrated to diluted pollutants in aqueous systems (Rivera-Utrilla et al., 2011). This process alone implies the presence of a solid adsorbent which is capable of binding molecules through numerous mechanisms such as electrostatic interaction, ion exchange, and complexation. It is recommended that the material should be of large adsorption capacity, quick adsorption velocity, easily produced in large quantities and can be regenerated.

Activated carbon and polymer resins are most frequently used adsorbents in industrial scale (Rivera-Utrilla et al., 2011). Although they are extensively used, they are regarded expensive, have low mass transfer rate and difficult to be regenerated (Zanella et al., 2014; Berenguer et al., 2010). Nevertheless the adsorption capacity of chromium ion using activated carbon is generally low (Owlad et al., 2010). Polypyrrole (Ppy)-based composites has proven to be an effective adsorbent to remove a wide variety of inorganic pollutants dissolved in aqueous solutions including chromium (Wang et al., 2013).

Nanocomposite materials derived from Ppy linked with layered inorganic solid substances are of interest for producing improved mechanical structure and development of new functional materials (Setshedi et al., 2013). Clay minerals for example have been largely implemented in the nanocomposite field because of their small particle size, abundancy and intercalation properties for reinforcement of materials with polymers (Jafari et al., 2014). Ppy-clay nanocomposite exhibit new synergistic properties, which cannot be attained from individual ingredients. Since this composite consist of high surface area and surface functional groups responsible for most adsorption mechanism, it is used for remediation of pollutants in wastewater (Setshedi et al., 2013). Despite its widespread use in adsorption processes, additional drawback to its industrial application will essentially depend on the pollutants nature and the ease with which they can be desorbed.

One of the adsorption technique challenges is the disposal of adsorbents once their adsorption capacity has been exhausted. With more stringent environmental standards, the disposal of hazardous waste in landfills is becoming intolerable. This has inspired the development of adsorbents restoration practices to allow broader application and ensure its economic viability and environmental security. The commonly used regeneration techniques are thermal and chemical methods (Zanella et al., 2014). Thermal regeneration requires high energy for excessive burnout of the adsorbent which leads to adsorbent being lost particularly for carbonaceous materials (Zanella et al., 2014). Chemical regeneration on the other hand involves inorganic and organic chemicals which may be difficult to separate in the completion step. However, chemical methods have a number of benefits which include recovery of valuable adsorbates and re-using chemical regenerants without the loss of carbon resulting from thermal treatment.

Ultrasound process has also been used to improve desorption of pollutants in various systems. Investigations done mainly focus on organic pollutants or heavy metals with low valance state (such as lead, cadmium) (Jing et al., 2011).Although there are limited ultrasound desorption studies on metal ions with high valance state, such as hexavalent chromium, an investigation was carried out to improved desorption rates of Cr(VI) onto activated carbon however, there was no significant impact using this method (Jing et al., 2011).

Ppy-based composites have to some extent been investigated for regeneration post Cr(VI) adsorption (Setshedi et al., 2013; H. Wang et al., 2015). Based on the overall results obtained, chemical adsorption occurred. This was supported by Cr(VI) maximum recovery of less than 20% using eluents at different concentrations. However, it was found that the regenerated composite could be recycled for the removal of Cr(VI) without substantial loss of adsorption efficiency even after the partial recovery. Observations made indicated that adsorbent treatment with NaOH released Cr(VI) ions but also changed the surface charge of the composite creating an imbalance between ionized Cr(VI) and adsorbent surface leading to adsorption process being unfavourable (Bhaumik et al., 2011). To counteract this, the material was further exposed to dilute HCl solution to recover Cr(III) ions proven to be a reduced Cr(VI) as a result of electron rich Ppy moieties in acidic media and to further re-dope with chloride ions (Bhaumik et al., 2011). Thereafter, the obtained material was further examined for sequential adsorption-desorption cycles to verify reusability. Regeneration experiments revealed that Ppy-based composites can be re-used for three consecutive cycles in acidic media (Setshedi et al., 2013).

According to literature, Ppy undergo protonation and deprotonation reactions when immersed in acidic or alkaline solutions, causing the change in its surface charge (Zhang & Bai, 2003). The existence of positively charged nitrogen atoms particularly in acidic media provide a good prospect for its adsorption application for negatively charge Cr(VI) ions.

Considering the importance of restoring the adsorption capacity of Ppy-MMT composite, particularly for Cr(VI) removal, the influence of different eluents were studied for regeneration of the composite. The variations in adsorption capacity of the composite upon

Cr(VI) removal are examined in relation to changes in Cr(VI) speciation, material microstructure and mechanisms involved between eluents-composite interaction.

2. Experimental

2.1. Chemicals

Pyrrole and iron (III) chloride hexahydrate ($FeCl_3$. $6H_2O$) were purchased from Sigma Aldrich, South Africa. Pyrrole was freshly distilled before use and kept in a refrigerator. Montmorillonite (MMT) clay was provided by Biocentric, South Africa. All other reagents were used as provided without further purification. Hydrochloric (HCl), nitric acid (HNO_3), ammonium chloride (NH_4Cl), ammonium hydroxide (NH_4OH) and sodium hydroxide (NaOH) were procured from Merck, South Africa. Analytical grade salt of potassium dichromate ($K_2Cr_2O_7$) was obtained from Sigma Aldrich, Germany. Deionized water was used as a solvent.

2.2. Preparation of Ppy-MMT composite

The MMT clay was dispersed in aqueous medium by adding 2.0 g clay into a known volume of deionized water under constant stirring. After an hour of insertion, pyrrole (0.4 mL) was added to the above dispersion while stirring. This was followed by the addition of $FeCl_3.6H_2O$ (3.0 g) oxidant and the reaction mixture was kept for 24 hours at ambient temperature. The resulting black Ppy-MMT composite was collected by filtration, washed with acetone and deionized water several times until the filtrate became colourless. Finally, the residue product was reaction mixture was kept for 24 hours and the obtained black residue was dried in a vacuum oven at 60 ˚C for 24 hours. The obtained yield of the product was > 98%.

2.3. Characterization techniques

In order to determine the functional groups of the composite, Fourier transform infrared (FTIR) spectrometer Perkin-Elmer Spectrum (London, UK) was used. Thermal stability was examined using thermographic analysis (TGA) Perkin Elmer TGA 400

(Massachusetts, USA). Elemental composition was determined using Scanning electron microscope (SEM) equipped with energy dispersive X-ray spectroscopy (EDS), FEI Quanta 200 ESEM (Hillsboro, USA).

2.4. Adsorption/ desorption batch experiments

The reusability of Ppy-clay composite was carried out in three steps: (1) adsorption of Cr(VI) ions on Ppy-clay, (2) desorption of Cr(VI) from the adsorbent using NaOH, NH_4OH and deionized water, (3) adsorbent regeneration with selected regenerants namely, HCl, NH_4Cl and HNO_3. A series of experiments involved Ppy-MMT (0.15 g) suspension in 50 mL Cr(VI) (100 mg/L) solution at pH 2. The solution was then stirred on a mechanical shaker (200 rpm) until equilibrium was reached. After the Ppy-MMT was separated from the solution by filtration. The residual concentration of Cr(VI) solution was measured by UV-Vis spectrometer (Perkin Elmer Lambda) at 540 nm using 1.5 diphenylcarbazide reagent method. The Ppy-MMT composite loaded with Cr(VI) was air dried and saved for the next step.

For desorption experiments, Ppy-MMT adsorbent from the previous step was treated with NaOH, NH_4OH (0.01 M – 0.5 M) and deionized water for three hours using a mechanical shaker. Eluent solutions were reused for multi-desorption cycles while measuring solution pH change for each cycle. The adsorbent was separated from the solution, air dried and stored for the next step.

Adsorbents were regenerated by treatment with 0.5 M concentrations of HCl, NH_4Cl and HNO_3 while stirring on a mechanical shaker for three hours. The regenerant solutions were separated and stored for reuse. The residual adsorbent product was then dried for 24 hours to obtain a constant mass for the next adsorption cycle. The amounts of adsorbed metal species (qe) were calculated using equation (1).

$$qe = \frac{(Ci - Ce)V}{m} \qquad (1)$$

where:

m is the mass of the adsorbent (g)

V is the volume of the solution (L)

C_i and C_e represent the initial and final concentrations (mg/L), respectively

Regeneration efficiency was calculated using:

$$\%\text{Regeneration} = \frac{qe}{qi} x100\% \qquad (2)$$

qe is the adsorption capacity of regenerated composite and *qi* is the adsorption capacity of the initial composite

3. Results and discussion

3.1. Characterization of Ppy-MMT composite before and after adsorption

The FTIR Ppy-MMT composite (before and after adsorption) are respectively shown in Fig 1-3. Fig. 1 (a) is the composite before Cr(VI) demonstrated characteristic peaks at 1551 cm^{-1}, 1461 cm^{-1}, 1112 cm^{-1} and 960 cm^{-1} which are reflected to arise from stretching of pyrrole ring, conjugated C-N vibration and C-H in plane stretching and out-plane bending vibration (Setshedi et al., 2013). The strong peak at 1016 cm^{-1} corresponds to Si-O stretching vibration of MMT clay (Chen et al. 2014). Most typical Ppy peaks appeared on the composite which indicates the integration of Ppy moieties in the material. Fig. 1(b) represent the composite adsorbent laden with Cr(VI). It was noted that Ppy-MMT bands shifted towards higher values after Cr(VI) adsorption. This feature indicated that $HCrO_4^-$ and $Cr_2O_7^{2-}$ (which are the most present ions in acidic medium) behaved as doping ions to Ppy backbone and hence the skeletal vibrations were affected (Bhaumik et al., 2011) (Setshedi et al., 2013). The obtained red shift as a result of limited charge delocalization of polymer chains after Cr(VI) adsorption agree well with the FTIR results from other Ppy-based composites (Ballav et al., 2012).

Fig. 1 (c-e) shows FTIR spectra for Ppy-MMT after Cr(VI) desorption using different concentrations of NaOH (0.05 M- 0.5 M). No significant changes were observed on the Ppy bands which indicated that the material was intact after treatment with NaOH with no detectable new generated species. However, upon increasing the NaOH concentration to 0.5 M, the 1551 cm^{-1} initial intensity was reduced at 1585 cm^{-1}. This was presumed to be a result of polymer backbone undergoing some degradation (Neoh et al., 1996). For further studies, 0.05 M NaOH/NH_4OH was implemented. The NaOH or NH_4OH treated

composites were further exposed to 0.1 M regenerants (HCl, NH_4Cl and HNO_3), respectively as shown in Fig. 2 and Fig. 3.

Noticeable changes were observed with the base and acid treatment in the skeletal stretching of the Ppy ring specifically around 1551 cm^{-1} region. A closer look in Fig. 2 (b, d, e) and Fig. 3 (b, c) around the 1461 cm^{-1} region, specified a lower band intensity compared to the spectra of the bare composite. This may be associated with oxidation of the polymer by strong oxidants (HCl, HNO_3) which are likely to interfere with the effective conjugation of the polymer (Neoh et al., 1996).

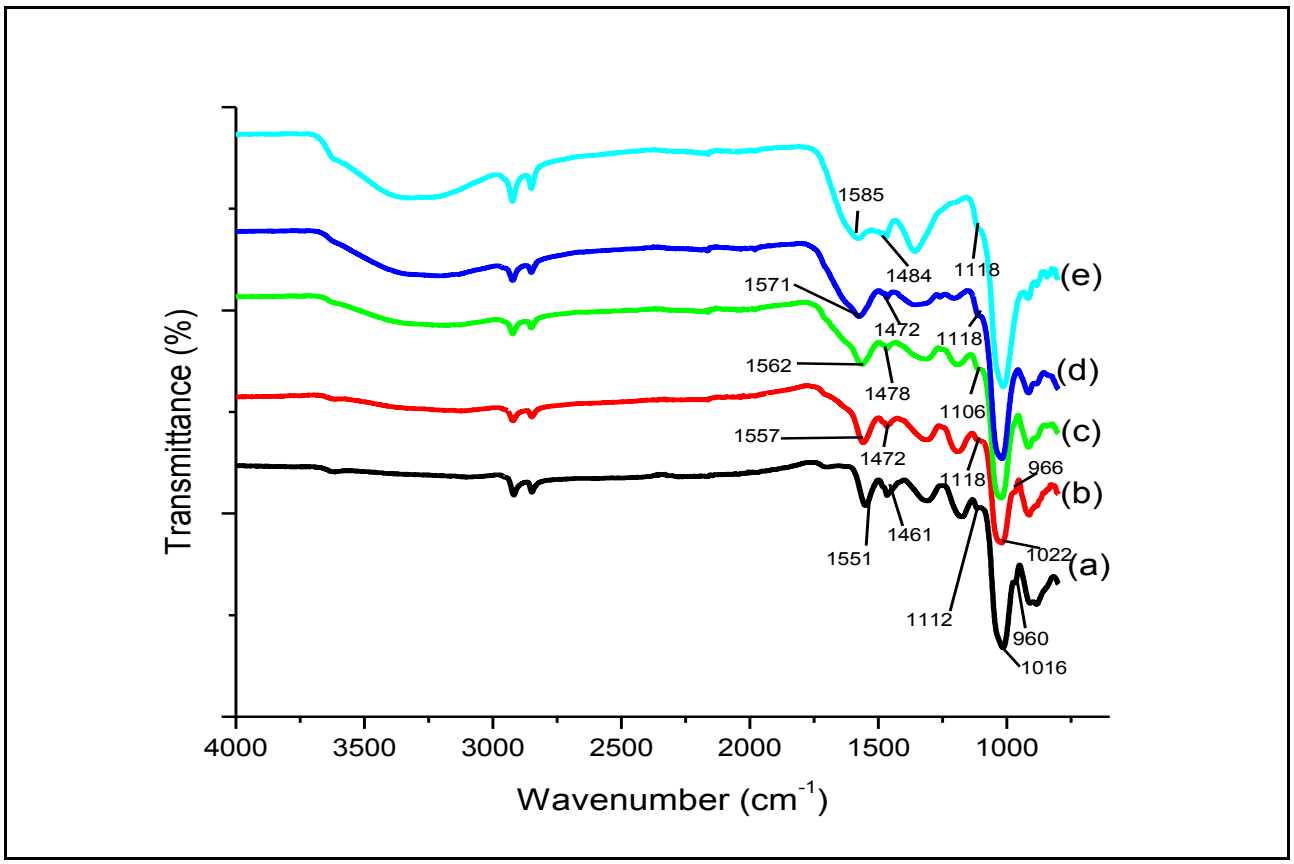

Fig. 1: The FTIR spectra of (a) Ppy-MMT before adsorption, (b) after Cr(VI) adsorption, (c) desorption with 0.05 M NaOH, (d) 0.1 M NaOH and (e) 0.5 M NaOH.

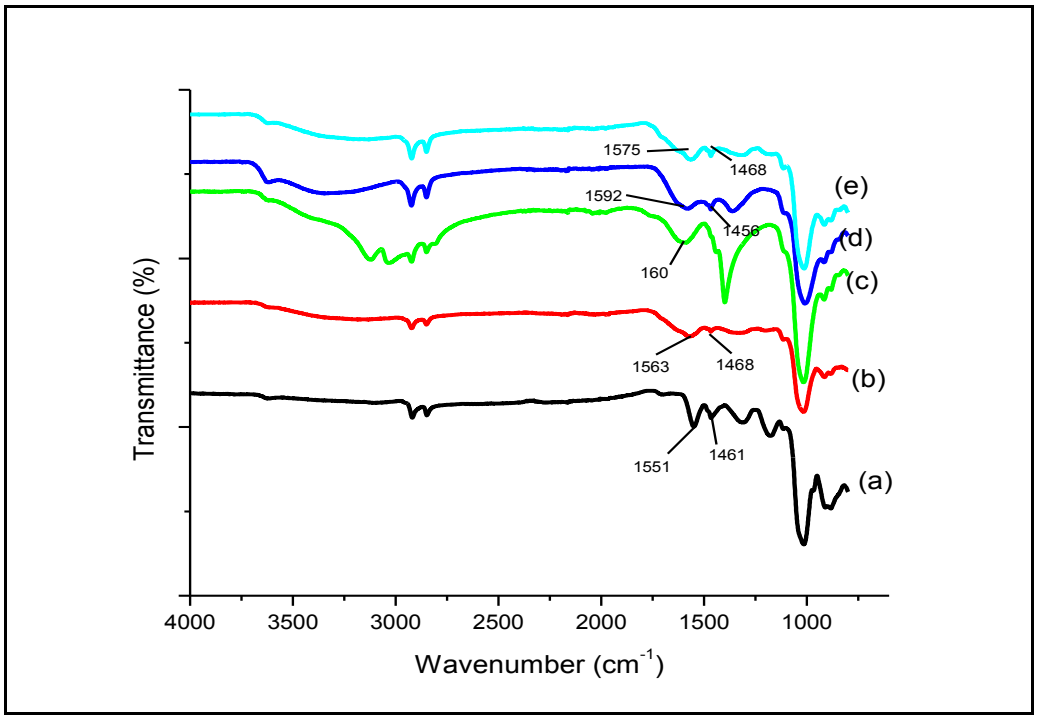

Fig. 2: The FTIR spectra of (a) Ppy-MMT before adsorption, (b) regeneration with NaOH/HCl, (c) NaOH/NH_4Cl, (d) NaOH/HNO_3, and (e) H_2O/HCl.

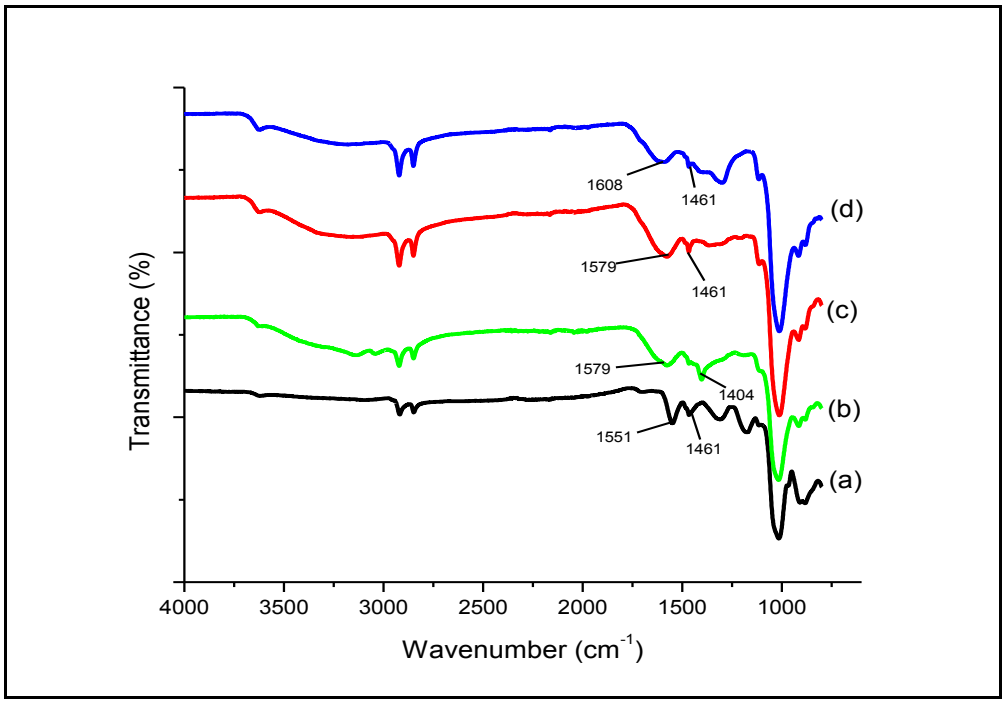

Fig. 3: The FTIR spectra of (a) Ppy-MMT before adsorption, (b) regeneration with NH_4OH/HCl, (c) NH_4OH /NH_4Cl and (d) NH_4OH /HNO_3.

Fig. 4 compared the TGA curves of Ppy-MMT before Cr(VI) adsorption, after adsorption and when treated with regenerants for one cycle and 5 cycles. The initial mass loss before 120 °C is presumably attributed to the release of water on the adsorbent surface (Bagreev et al., 2001). The second significant mass loss between 120-300 °C was 7%, 6%, 9% and 12% for the bare Ppy-MMT, after Cr(VI), one cycle treated with NaOH/HCl and 5 cycles treated with NaOH/HCl. This shows that the thermal stability of the composite is weakened by treatment with the eluents.

This was also supported by the change in thermal stability with a severe mass loss for the composite between 300-500 °C , went down to 285-432 °C after Cr(VI) adsorption and decreased even further to 250-400 °C after five adsorption cycles. At the mentioned regions, the mass loss is conceivably related to the degradation of any doped ions in the polymer structure and it is the decomposition area of the Ppy chain (Yao et al., 2014). It is worth noting that five adsorption cycles of the composite gave the highest residue of over 50%. This is probably ascribed to over oxidation of the composite and hence some by-products of the destroyed polymer are formed.

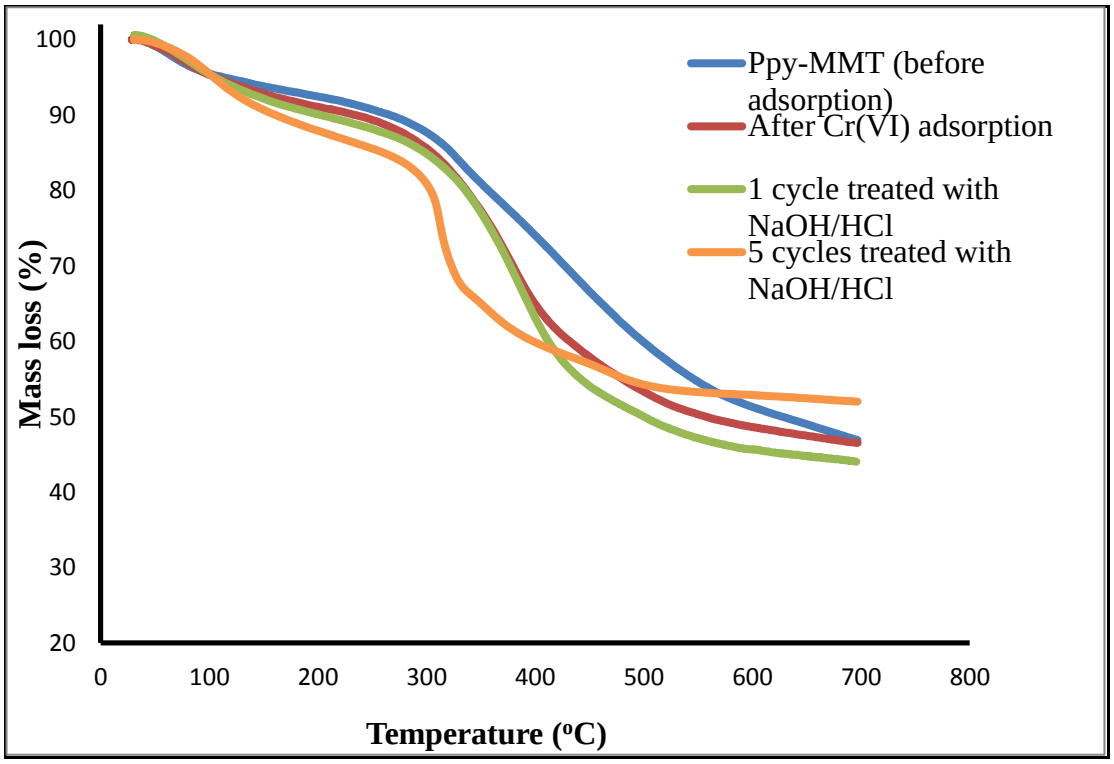

Fig 4: TGA plots of Ppy-MMT before and after Cr(VI) adsorption and regeneration.

Elemental components of Ppy-MMT before and after Cr(VI) adsorption were determined by EDS as shown in Fig. 4. Both materials revealed similar elements, particularly intense peaks of C and O. After exposing Ppy-MMT to Cr(VI), EDS presented a greater O% from 25% to 30%. This indicated oxidation of the material by $Cr_2O_7^{2-}$ and $HCrO_4^-$ at pH 2. Additionally, Cl content after adsorption decreased to about 1% from 5% of the native Ppy-MMT. This is agreement with the reported adsorption mechanism where Cr(VI) removal was partly driven by ion exchange through replacement of doped Cl by $HCrO_4^-$ ions (Setshedi et al., 2013). It has also been reported that Cr(VI) adsorption onto electron rich Ppy-based materials under acidic conditions involve the reduction of Cr(VI) to Cr(III) (Bhaumik et al., 2011). Cr ions were not detectable by EDS analysis but the amount of O was around 25% before adsorption and increased to about 30% after Cr(VI) adsorption, which could be attributed to the presence of $HCrO_4^-$ on the adsorbent surface. This was probably due to low concentration of Cr on the adsorbent as the reduced form (Cr(III)) is likely to leach out in acidic solution (Setshedi et al., 2013).

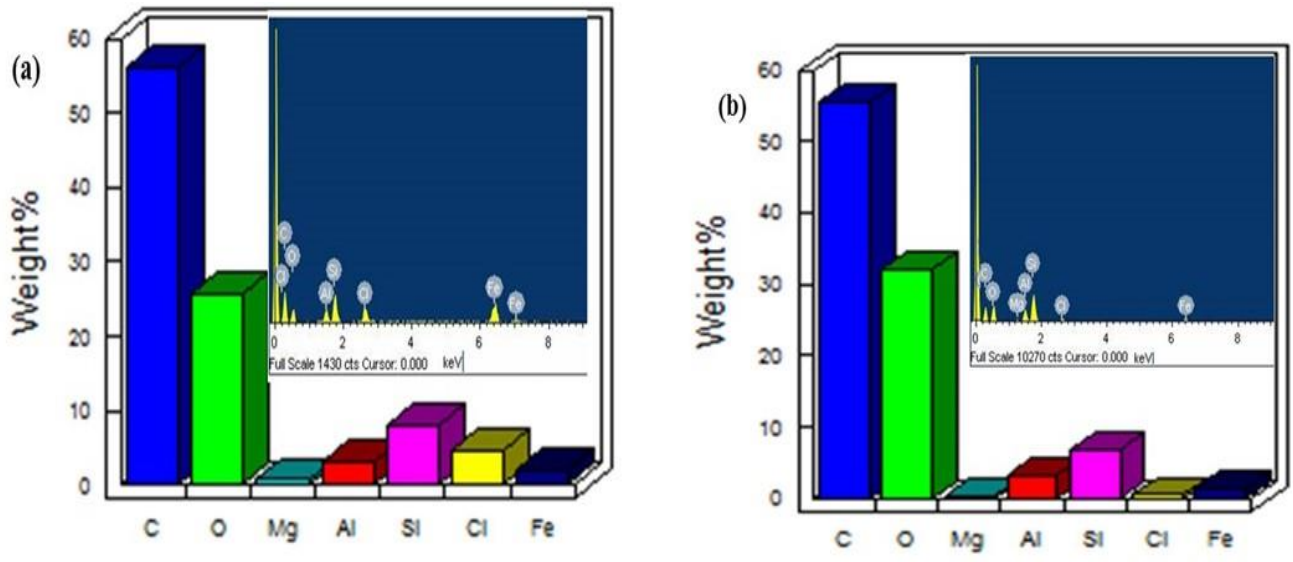

Fig 4: Elemental composition and EDX spectra of (a) Ppy-MMT before and (b) after Cr(VI) adsorption.

3.2. Batch experiments

Solution pH is one of the vital parameters that influences metal adsorption. It controls the surface charge density of the adsorbent and the existing charge of the metallic species. For

Ppy-based adsorbents, it has been reported that Cr(VI) removal is partly through electrostatic attraction where the negatively charged Cr(VI) forms below the pH 6 interact with the protonated nitrogen moieties of Ppy (Wang et al., 2015; Ballav et al., 2012). Besides electrostatic attraction, the Cr(VI) removal in this manner also involve ion exchange and chemical reduction behaviour (Setshedi et al., 2013).

This was verified in Fig. 5 where efficient Cr(VI) removal was achieved at pH 2 and gradually decreased with increasing the pH. The high adsorption efficacy at low pH is attributed to synergistic adsorption which includes electrostatic attraction as a result of protonated adsorbent. Secondly, the reduction of Cr(VI) to Cr(III) is mostly favoured in acidic condition considering the oxidizing power of Cr(VI) to be the function of pH (Lei et al., 2012). Lastly Cr(VI) could be adsorbed through ion exchange between the negatively charged metal ions and the present chloride ions in the polymer chain. This was supported by chloride ions reduction after Cr(VI) adsorption in Fig. 4 for EDS spectra. For efficient Cr(VI) uptake, solution pH of 2 was used throughout.

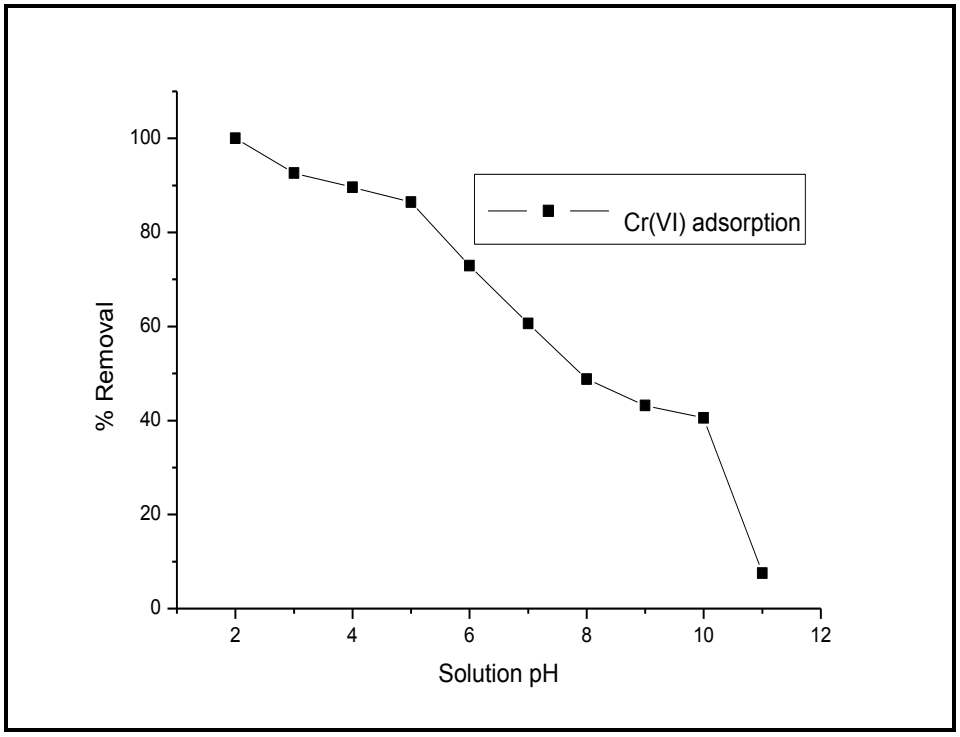

Fig. 5: Effect of solution pH on Cr(VI) adsorption using Ppy-MMT. (Temperature = 25 °C, adsorption time = 24 h, adsorbent dose = 0.15 g/50 mL, initial concentration = 100 mg/L).

To test the reusability of the adsorbent, desorption experiments were conducted in a batch mode where 42 mg/g of Cr(VI) was loaded on Ppy-MMT. The detailed procedure was defined in section 2.4. Interestingly, it was observed that less 15% of Cr(VI) could be extracted from the adsorbent after the first adsorption cycle. The remaining Cr could be the reduced form of Cr(VI) to Cr(III) ions which may resist to leach out in alkaline solution.

In Fig. 6, the regeneration efficiency of adsorbent using 0.5 M of NaOH and NH_4OH showed poor performance for second cycle with more than 40% and 20% drop respectively. After regenerating the spent adsorbent with HCl, NH_4Cl and HNO_3, regeneration efficiency improved for when NH_4OH was used as an eluent (Fig. 6). This showed that 0.5 M NaOH harshly reacted with the adsorbent in such a way that even treatment with doping agents could not restore the adsorbent. This supported the FTIR spectra in Fig. 1 where characteristic peak of Ppy stretching was affected by 0.5 M NaOH. NH_4OH solution at the very same concentration as NaOH was less harsh to the adsorbent due to its partial dissociation is solution. From the obtained experimental results, HCl, NH_4Cl and HNO_3 assisted in releasing the bound Cr(III) ions and re-doping Ppy-MMT with the chloride ions.

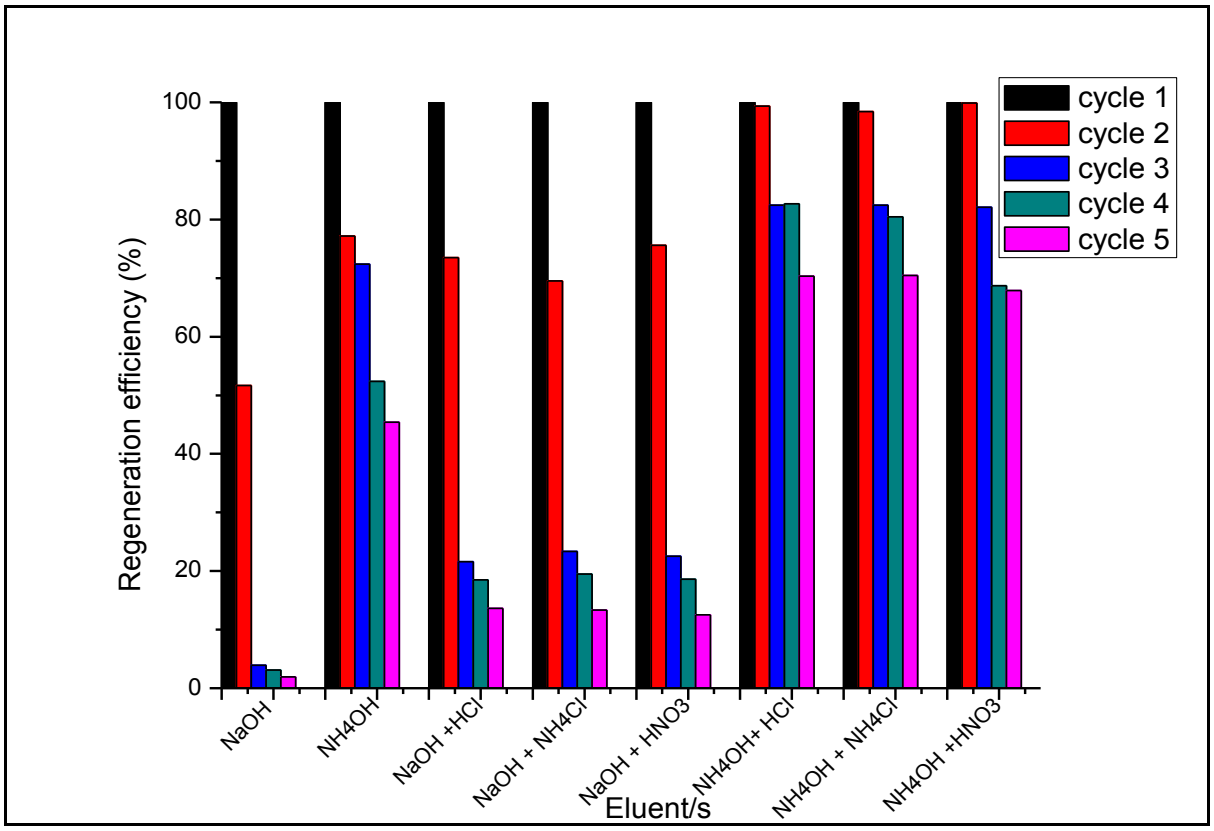

Fig. 6 Adsorption-desorption cycles using 0.5 M (NaOH, NH_4OH) and 0.5 M (HCl, NH_4Cl, HNO_3). (Temperature = 25 °C, adsorption time = 24 h, desorption time = 1 h adsorbent dose = 0.15 g/50 mL, initial concentration = 100 mg/L).

In Fig.7 the concentration of NaOH and NH_4OH was reduced to 0.1 M while keeping HCl, NH_4Cl and HNO_3 constant. Regeneration efficiency was maintained for atleast three cycles under the mentioned conditions and slightly decreased on the forth cycle with about 80% recovery. Fig. 8 shows that the regeneration efficiency using 0.01 NaOH and NH_4OH was successful for over four cycles even when water was used as an eluent. However, it is very important to note that re-adsorption capacity decreased significantly after the second cycle when NH_4Cl was implemented as a dopant. This could be associated with some precipitation of chromium salt on the adsorbent surface which hindered the adsorption sites for the next cycle. The distinctive feature obtained here is supported by the change in pH (Fig. 9) after each adsorption cycle showing a drastic decrease in solution pH of 0.01 M NaOH after the second cycle. The concentration of the regenerant on the sixth cycle (Fig. 8) was increased to 0.05 M as indicated. Major improvements were observed for regeneration using NH_4Cl dopant where efficiency increased from 63% to 98% and 58% to 88% for NaOH and NH_4OH eluents, respectively.

In overall, the best performance was obtained for 0.01/0.05 M NaOH with HCl with regeneration efficiency of greater than 90% for all the six cycles that were done. NH_4OH is not frequently used for adsorbents recycling due to its unpleasant smell and weak alkaline nature which may require higher concentrations than NaOH (Wang et al., 2013).

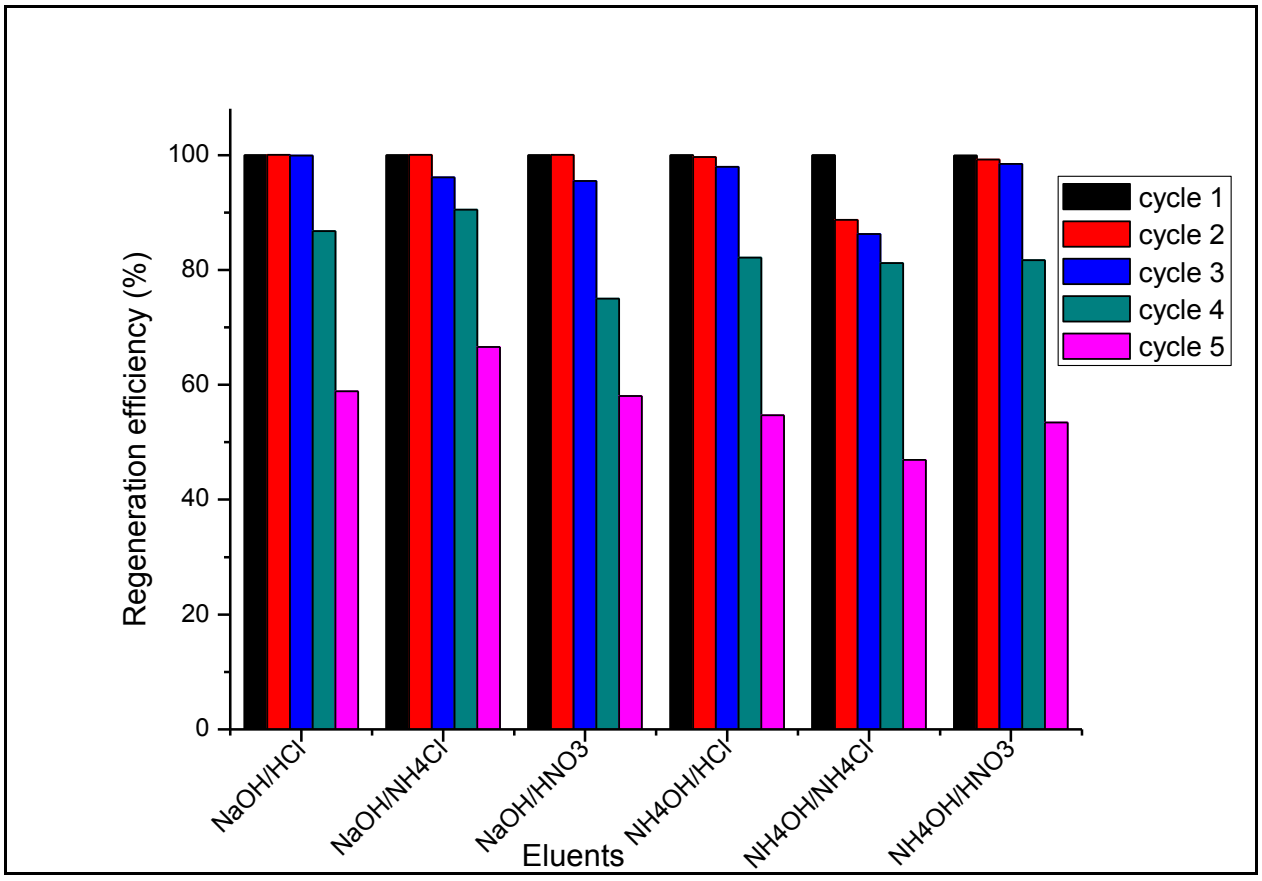

Fig 7 Adsorption-desorption cycles using 0.1 M (NaOH, NH_4OH) and 0.5 M (HCl, NH_4Cl, HNO_3). (Temperature = 25 °C, adsorption time = 24 h, desorption time = 1 h adsorbent dose = 0.15 g/50 mL, initial concentration = 100 mg/L).

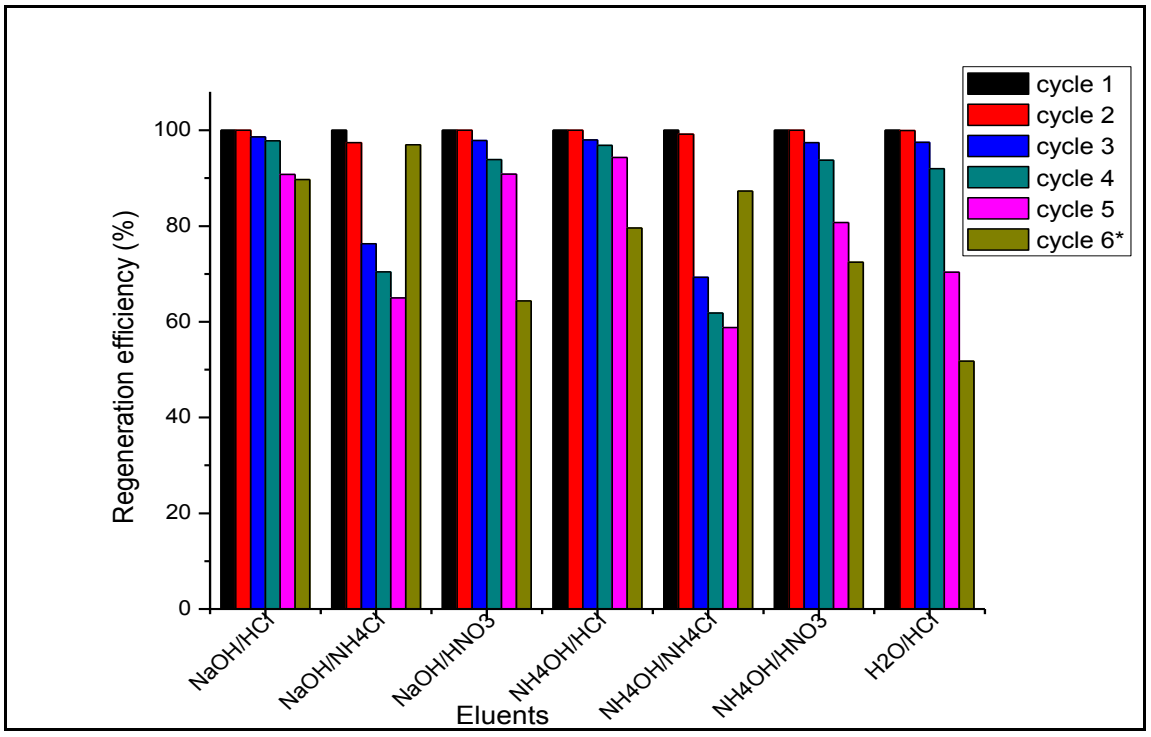

Fig. 8: Adsorption-desorption cycles using 0.01-0.05* M (NaOH, NH_4OH) and 0.5 M (HCl, NH_4Cl, HNO_3). (Temperature = 25 °C, adsorption time = 24 h, desorption time = 1 h adsorbent dose = 0.15 g/50 mL, initial concentration = 100 mg/L).

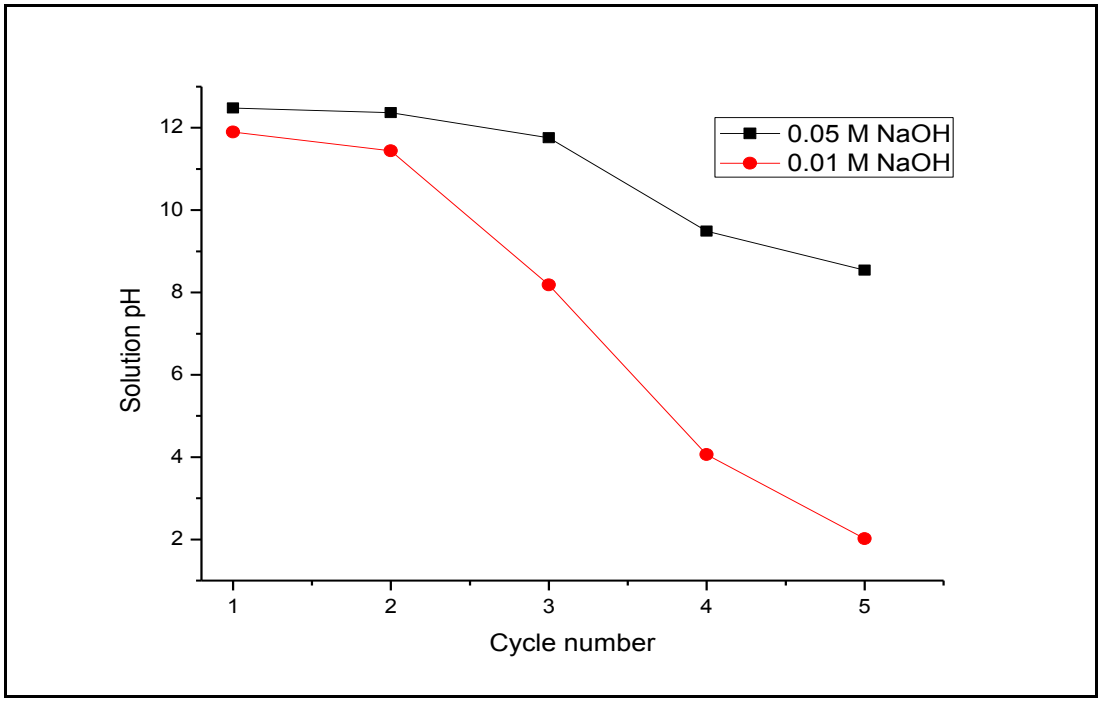

Fig. 9: Changes in pH after successive adsorption / regeneration runs for 0.01 M and 0.05 M NaOH.

4. Conclusion

Ppy-MMT composite was successfully prepared for Cr(VI) removal in acidic aqueous solution. Mostly, the application of adsorption with subsequent regeneration by desorption results in secondary pollutant production which requires further treatment. Here the synthetic material showed not only excellent removal capability but also reduced Cr(VI) to less toxic Cr(III). The adsorbent could be generated for more than five cycles with the regeneration efficiency of greater than 80% by 0.01 NaOH and 0.5 M HCl while re-using the basic eluent. Thus, it can be concluded that Ppy-MMT is a cost effective adsorbent that has a great potential in Cr(VI) contained wastewater treatment plant.

References

Bagreev, A., Rahman, H. & Bandosz, T.J., 2001. Thermal regeneration of a spent activated carbon previously used as hydrogen sulfide adsorbent. *Carbon*, 39(9), pp.1319–1326.

Ballav, N., Maity, A. & Mishra, S.B., 2012. High efficient removal of chromium(VI) using glycine doped polypyrrole adsorbent from aqueous solution. *Chemical Engineering Journal*, 198–199, pp.536–546.

Berenguer, R., Marco-Lozar, J. P., Quijada, C., Cazorla-Amoros, D., Morallo, E., 2010. Electrochemical regeneration and porosity recovery of phenol-saturated granular activated carbon in an alkaline medium. *Carbon*, 48(10), pp.2734–2745.

Bhaumik, M., Maity, A., Srinivasu, V. V., & Onyango, M. S., 2011. Enhanced removal of Cr(VI) from aqueous solution using polypyrrole/Fe3O4 magnetic nanocomposite. *Journal of Hazardous Materials*, 190(1–3), pp.381–390.

Chen, Y., Xu, H., Wang, S., & Kang, L., 2014. Removal of Cr(vi) from water using polypyrrole/attapulgite core–shell nanocomposites: equilibrium, thermodynamics and kinetics. *RSC Adv.*, 4(34), pp.17805–17811.

Jafari, M.T., Saraji, M. & Sherafatmand, H., 2014. Polypyrrole/montmorillonite nanocomposite as a new solid phase microextraction fiber combined with gas chromatography-corona discharge ion mobility spectrometry for the simultaneous determination of diazinon and fenthion organophosphorus pesticides. *Analytica Chimica Acta*, 814, pp.69–78.

Jing, G., Zhou, Z., Song, L., & Dong, M., 2011. Ultrasound enhanced adsorption and desorption of chromium (VI) on activated carbon and polymeric resin. *Desalination*, 279(1–3), pp.423–427.

Minocha, A.K., 2006. Conventional and non-conventional adsorbents for removal of pollutants from water – A review. , 13(May), pp.203–217.

Neoh, K.G., Lau, K. K. S., Wong, V. V. T., Kang, E. T., & Tan, K. L., 1996. Structure and Degradation Behavior of Polypyrrole Doped with Sulfonate Anions of Different Sizes Subjected to Undoping - Redoping Cycles. *Chemistry of Materials*, 8(15), pp.167–172.

Owlad, M., Aroua, M.K. & Wan Daud, W.M., 2010. Hexavalent chromium adsorption on impregnated palm shell activated carbon with polyethyleneimine. *Bioresource Technology*, 101(14), pp.5098–5103.

Rivera-Utrilla, J., Sanchez-Poloa, M., Gomez-Seeanob, V., Alvarezc, P. M., Alvim-Ferrazd M. C. M., Diasd, J. M., 2011. Activated carbon modifications to enhance its water treatment applications. An overview. *Journal of Hazardous Materials*, 187(1–3), pp.1–23.

Setshedi, K.Z., Bhaumik, M., Songwane, S., Onyango, M. S., & Maity, A., 2013. Exfoliated polypyrrole-organically modified montmorillonite clay nanocomposite as a potential adsorbent for Cr(VI) removal. *Chemical Engineering Journal*, 222, pp.186–197.

Wang, H., Yuan, X., Wu, Y., Chen, X., Leng, L., Wang, H., Zeng, G., 2015. Facile synthesis of polypyrrole decorated reduced graphene oxide-Fe3O4 magnetic composites and its application for the Cr(VI) removal. *Chemical Engineering Journal*, 262, pp.597–606.

Wang, J., Pan, K., He, Q., & Cao, B., 2013. Polyacrylonitrile/polypyrrole core/shell nanofiber mat for the removal of hexavalent chromium from aqueous solution. *Journal of Hazardous Materials*, 244–245, pp.121–129.

Yao, W., Ni, T., Chen, S., Li, H., & Lu, Y., 2014. Graphene/Fe3O4at polypyrrole nanocomposites as a synergistic adsorbent for Cr(VI) ion removal. *Composites Science and Technology*, 99, pp.15–22.

Zanella, O., Tessaro, I.C. & Féris, L.A., 2014. Desorption- and decomposition-based techniques for the regeneration of activated carbon. *Chemical Engineering and Technology*, 37(9), pp.1447–1459.

Zhang, X. & Bai, R., 2003. Surface electric properties of polypyrrole in aqueous solutions. *Langmuir*, 19(26), pp.10703–10709.

PAPER IV

ADSORPTION OF PHOSPHATES FROM AQUEOUS SOLUTIONS BY POLY(PHENYLENEDIAMINE) ISOMERS

Adsorption of Phosphates from Aqueous Solutions by Poly(phenylenediamine) Isomers

Abstract

The discharge of nutrients such as phosphates has always been identified as a risk to natural environments due to the severe effects of eutrophication. In recent years, new technologies have been investigated over traditional physico-chemical and biological systems to remove nutrients from secondary wastewater. Here we present the development and performance of polyphenylenediamine isomers which were produced through oxidation polymerization using $(NH_4)_2S_2O_8$ and $K_2Cr_2O_7$ as oxidants. Superior performance for phosphate adsorption was observed when using $K_2Cr_2O_7$ as an oxidant. Empirical data from batch trials showed that solution pH, contact time and initial concentration exhibited a remarkable impact on phosphate adsorption with the maximum adsorption capacities of 143 mg/g, 217 mg/g and 69.0 mg/l (about 55.5%, 74.75% and 41.7% adsorption efficiency) for P*o*PD, P*m*PD and and P*p*PD adsorbents, respectively. According to the characterization techniques (TGA and XRD), the outstanding behaviour of P*m*PD is attributed to high amorphous orientation due to low intrachain hydrogen bonding during polymerization. The adsorption rate kinetic model fitted to the pseudo-second order and isotherm data favoured Langmuir model indicating chemisorption process of phosphate removal. P*m*PD displayed high affinity for phosphates removal in the presence of high concentrations of competing anions (nitrates and sulphates) and was amenable to regeneration while maintaining its adsorption capacity for five cycles.

1. Introduction

Phosphorus (P) is an essential macronutrient for most biological tissues and therefore is a vital commodity for nurturing food production (Bajpai et al., 2009). When released into the environment in the form of phosphates from point (eg. sewerage plants) and non-point sources (eg. runoff from farms) it causes eutrophication and profuse algae growth. Dissolved phosphate ions of about 0.02 mg/L are considered sufficient to accelerate eutrophication. The United States Environmental Protection Agency (USEPA) has

recommended discharge levels ranging between 0.1-0.5 mg P L^{-1} (Sowmya & Meenakshi, 2013).

There are numerous physicochemical techniques adopted for phosphate removal in water (Loganathan et al., 2014). The most recognized methods at industrial scale are, physical processes (settling, filtration), chemical precipitation (using aluminium, calcium and iron salts), biological approach which mostly rely on biomass growth (bacteria, algae, plants) and adsorption (Yan et al., 2010). Adsorption technology has been reported to have the potential for pollutants remediation in water due to its simplicity in operation with minimal sludge production (Loganathan et al., 2014) .

Investigations has been carried out on inorganic material adsorbents such as iron-based layered double hydroxides, fly ash, zeolites, blast furnace slag, functionalized mesoporous silica, clays and activated aluminium oxide/hydroxide (Loganathan et al., 2014). These conventional adsorbents often tend to exhibit low selectivity in the presence of other competing ions and low sensitivity at low concentrations of phosphates (Zhao & Sengupta, 1998). Moreover, polymeric ligand exchangers (PLEs) (e.g. made of lanthanum (III) bound to Chelex-100 resin) have been regarded as the possible adsorbent for phosphates removal that is fairly selective with high adsorption capacities (Wu et al., 2007). Theoretically, the mechanism involves appropriate immobilization of metal ions to the polymer phase which act as anion-exchange sites with high affinities to anions with heavy ligand features, like phosphates (Zhao & Sengupta, 1998). However, the challenge with PLE synthesis is that it requires a speciality chelating polymer as a substrate which is relatively expensive, leading to infrequent applications.

In this work, the use of electrical conductive polymers of phenylenediamines (ortho, meta and para isomers) was implemented by synthesized with ammonium peroxydisulphate. For comparison, a metal ion-based oxidant, potassium dichromate, was also used to synthesize the polymers. The materials were compared for removal of phosphate in aqueous solutions. Phenylenediamine polymers (PPDs) are polymers synthesized from the amino-derivatives of aniline. Polyaniline (PANI) is one of the most intensely researched conducting polymers. It has high conductivity, redox activity, and adsorbent characteristics for various heavy and noble metal ions in water (Stejskal, 2015). PPDs possess better processability

and has various properties as compared to PANI due to an extra free amino group per monomeric unit (Xin et al., 2002).

2. Experimental

2.1 Chemicals

Phenylenediamine monomers (*o*-phenylenediamine (*o*PD), *m*-phenylenediamine (*m*PD) and *p*-phenylenediamine (*p*PD)) were purchased from Sigma Aldrich and were used as received. Ammonium persulfate ($(NH_4)_2S_2O_8$), potassium dichromate ($K_2Cr_2O_7$) and potassium dihydrogen phosphate (KH_2PO_4) were purchased from Sigma Aldrich. All reagents were analytical grade. The working solutions of different phosphate concentrations were prepared in de-ionized water.

2.2 Preparation of adsorbents

Two experimental routes related to chemical oxidative polymerization of phenylenediamine isomers in 0.1 M HCl solution were investigated. One route included radical polymerization using a previously reported method, where equimolar (0.015 mol) of phenylenediamine and $(NH_4)_2S_2O_8$ oxidant were used to initiate polymerization (Mdlalose et al., 2017). For the other approach 0.015 mol of phenylenediamine and 0.03 mol of $K_2Cr_2O_7$ were used. The temperature of the reactions was maintained at 25 °C. The oxidants were added dropwise and the reaction was continued for 24 h. The polymers were collected by filtration and washed with de-ionized water. The product was collected by filtration and washed with dilute NaOH (0.01 M) solution, de-ionized water and dried in a vacuum oven at 60 °C for 24 h. Polymers obtained from $(NH_4)_2S_2O_8$ as an oxidant are denoted with an –S suffix and the ones from $K_2Cr_2O_7$ with –Cr suffix.

2.3 Characterization techniques

The Fourier transform infrared (FT-IR) analysis for functional group identification was carried out using KBr pellets on Spectrum One Apparatus, PerkinElmer. Thermal stability was performed on themogravimetry thermal analyser (TG), Exstar 6000 TG/DTA 6300

using nitrogen gas. X-ray diffraction (XRD) patterns were performed using Bruker AXS D8 Advance with Cu-Kα as the radiation source. Elemental spectra were obtained using energy dispersive X-ray spectroscopy (EDX) on JEOL model (JED-2300) analyser.

2.4 Batch adsorption tests and regeneration

A stock solution of phosphate (1000 mg/L) was prepared by dissolving anhydrous KH_2PO_4 in deionized water. To investigate the pH effect, adsorption studies were carried out by adjusting the pH of a 100 mg/L phosphate solution from pH 2 to 9 using either dilute NaOH or HCl. The adsorbent (0.1 g) was suspended in phosphate solution and agitated at 120 rpm at ambient temperature for 24 h. The filtrate was analysed by the molybdenum blue method in which the absorbance was measured at a wavelength of 880 nm in Hach Lange DR 2800 spectrometer. The extent of Cr leaching off the polymer after adsorption was determined by atomic absorption spectroscopy (AAS) for total Cr and 1,5 diphenylcarbazide method for Cr(VI).The analyte was measured and the percentage removals of phosphate were determined by using the following Eq. (1):

$$\% \text{ Removal} = \frac{(C_o - C_e)}{C_0} \times 100 \quad (1)$$

where C_o and C_e are the initial and the equilibrium concentrations (mg/L) of PO_4^{3-}, respectively.

The equilibrium adsorption capacity (q_e) was determined using the following Eq. (2):

$$q_e = \frac{(C_o - C_e)V}{m} \quad (2)$$

where q_e is the equilibrium amount of PO_4^{3-} adsorbed per unit mass (m) of adsorbent (mg/g) and V is the sample volume (L).

The effect of contact time was examined at pre-determined time intervals for 50 mg/L and 100 mg/L phosphate solutions at an optimum pH of 2. The adsorption kinetics experiment data was used to determine the linearized forms of the pseudo-first order and pseudo-second order models given in Eqs. (3) and (4), respectively (Tseng, & Juang, 2014):

$$ln(q_e - q_t) = ln - kt \quad (3)$$

$$\frac{t}{q_t} = \frac{1}{k_2 q_e^2} + \frac{t}{q_e} \quad (4)$$

(4)

where k_1 (1/min) and k_2 (g/mg/min) are the pseudo-first order and pseudo-second order rate constants, respectively, q_t is the amount of PO_4^{3-} adsorbed at any time (mg/g) and q_e is equilibrium adsorption capacity (mg/g).

The effect of initial concentration was varied between 2-700 mg/L to study the adsorption capacity of the adsorbents. Langmuir and Freundlich isotherms models were used to fit the adsorption isotherm parameters (Jeppu & Clement, 2012). For the Langmuir isotherm monolayer adsorption process was described as presented by Eq. (5)

$$\frac{C_e}{q_e} = \frac{C_e}{q_o} + \frac{1}{q_o b} \quad (5)$$

where q_o (mg/g) is the maximum amount of PO_4^{3-} ions per unit mass of adsorbent to form a complete monolayer on the adsorbent surface and b (L/mg) is the binding energy constant. An essential characteristic of the Langmuir isotherm used to define the favourability of an adsorption process, the dimensionless separation factor (R_L), is given by Eq. (6):

$$R_L = \frac{1}{(1 + bC_o)} \quad (6)$$

The values of R_L range between 0 and 1 to confirm a favourable adsorption process. The Freundlich isotherm, which predicts adsorption onto heterogeneous surfaces, is expressed by Eq. (7):

$$\ln q_e = \ln K_F + \frac{1}{n} \ln C_e \quad (7)$$

where K_F (mg/g) and $1/n$ constants are related to the adsorption capacity and affinity of adsorption, respectively.

To investigate the stability of the adsorbent for multiple use cycles, the polymers were regenerated using 0.05 M NaOH solution. The optimum time was fixed and adsorbents were re-used for several cycles.

3. Results and Discussion

3.1 Characterization

Radical polymerization reactions of the three phenylenediamine isomers using $(NH_4)_2S_2O_8$ and $K_2Cr_2O_7$ oxidants yielded uniform powdered polymer particles. However, the yield strongly depends on the monomer structure, polymerization medium and the chosen oxidant (Li et al., 2009). As listed in Table 1, the polymerization yields were above 95% for all the polymers except P*o*PD when $(NH_4)_2S_2O_8$ was used. Additionally P*m*PD-S and P*p*PD-S gave much higher yields than P*o*PD-S. The poor polymerization yield for P*o*PD-S is attributed trimer compound formation hence lower molecular weight. Polymerization of *o*-PD in strong acid medium with a high reduction potential oxidant like $(NH_4)_2S_2O_8$ (2.01 eV) produces some nitrogen dioxide (NO_2) (Sestrem etal., 2010). The standard reduction potential of $K_2Cr_2O_7$ is 1.33 eV and was less harsh in preparing the ladder phenazine polymer of P*o*PD-Cr.

Table 1: Synthetic yield

Adsorbent	Polymerization yield (%)
P*o*PD-Cr	96.94
P*m*PD-Cr	97.04
P*p*PD-Cr	96.28
P*o*PD-S	40.05
P*m*PD-S	99.73
P*p*PD-S	99.86

3.1.1 FT-IR Analysis

Two distinctive peaks around 1510 cm^{-1} and 1620 cm^{-1} (Figure 1) were observed in the FT-IR spectra of the prepared polymers which corresponded to the stretching mode of the benzenoid amine and the quinoid imine of PPD, respectively, with the latter being the oxidised form of the polymer (Yu et al., 2013). It was observed that when $(NH_4)_2S_2O_8$ was used as the oxidant, P*o*PD and P*p*PD exhibited much stronger benzenoid amine bands as compared to the oxidised quinoid imine form, while oxidation with $K_2Cr_2O_7$ gave stronger quinoid imine signals. This is interpreted as an indication that the oxidation process was

more efficient with the latter metallic oxidant. All the polymers prepared with $K_2Cr_2O_7$ showed better oxidized characters and less intense band was obtained around 1510 cm^{-1} than that at 1618 cm^{-1} for P*m*PD (S and Cr) spectra. The similarities in the spectra of P*o*PD and P*p*PD is attributable its comparable arrangement in their chemical structures. Although *p*PD monomer is a 1,4-substituted benzene, both polymers are organized by 1,2-substituted benzene rings (as compared to 1,2,3 tri-substituted in the case of P*m*PD) giving phenazine segment molecules (Sestrem et al., 2009) (Huang et al., 2006).

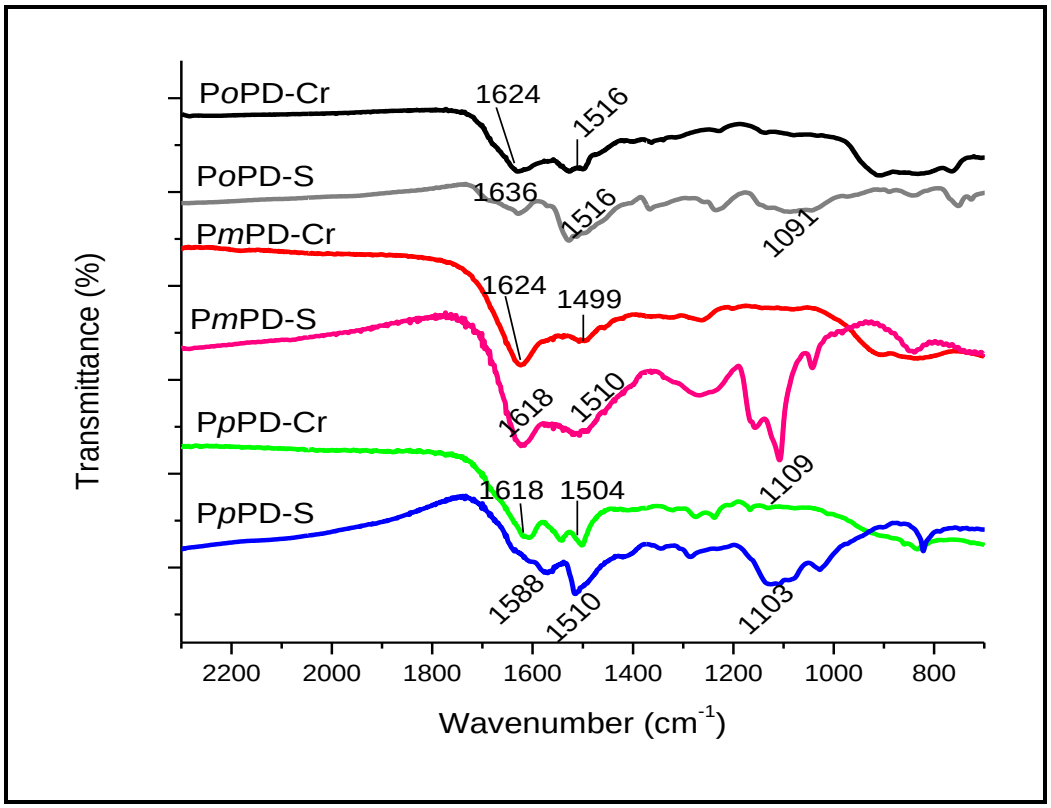

Figure 1. FT-IR spectra of P*o*PD, P*m*PD and P*p*PD obtained in $K_2Cr_2O_7$ and $(NH_4)_2S_2O_8$ as oxidants.

3.1.2 TGA analysis

The thermogravimetric analysis of PPD-Cr isomers were performed to determine the thermal behaviour under nitrogen atmosphere with the heating rate of 10 °C/min and are given in Figure 2. The significant mass loss at different temperatures were determined from the original curves and the data summarized in Table 1. The foremost degradation between 80-120 °C is related to the removal of moisture entrapped on the polymer. The

distinct weight losses of 5% (at 190 °C, 177 °C and 196 °C) and 10% (at 217 °C, 215 °C and 345 °C) for P*o*PD-Cr, P*m*PD-Cr and P*p*PD-Cr, respectively, is related to the thermal de-doping of polymers and the gradual thermal degradation of the polymer matrix. P*p*PD-Cr exhibited good thermal stability with a char yield of 77% at 800 °C. This could be due to higher symmetry and more intra-chain hydrogen bonding for P*p*PD-Cr (Thenmozhi et al., 2014). The minor asymmetry nature of ortho- and meta-substituted polymers inhibit the close packing of the molecules hence the intra-chain and inter-chain factors are affected leading to imbalance when compared to highly ordered structure of para substitution (Zhou et al., 2011).

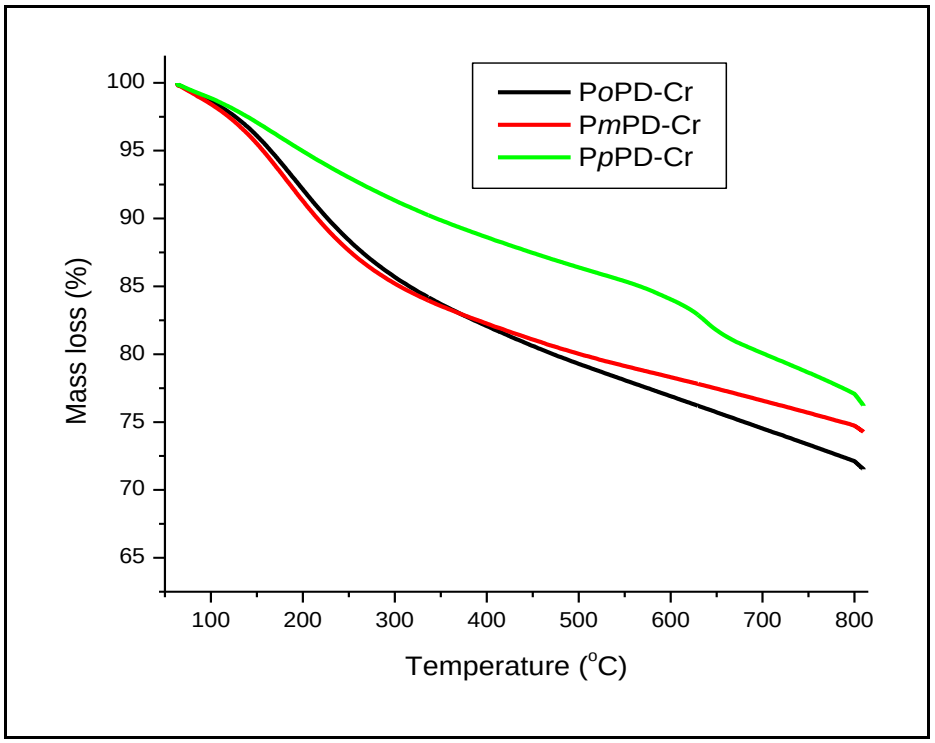

Figure 2. TGA thermograms of P*o*PD-Cr, P*m*PD-Cr and P*p*PD-Cr synthesized using $K_2Cr_2O_7$ as an oxidant.

Table 1: Thermal degradation temperature of poly(phenylenediamine)

Adsorbent	5% mass loss (°C)	10% mass loss (°C)	Char yield at 800 °C (%)
P*o*PD-Cr	189.90	217.38	72.27
P*m*PD-Cr	177.86	215.37	74.76
P*p*PD-Cr	196.33	345.12	77.11

3.1.3 XRD

XRD spectroscopy was used to determine the phase identification of the polymers. Parallel broad peaks (Figure 3) appear for the three PPD-Cr isomers at the region of 25° due to significant amorphous components of the polymers. However, it is evident that P*p*PD-Cr contains a series of sharp lines more than P*o*PD-Cr and P*m*PD-Cr which portrays the semi-crystallinity and long range ordering of the synthesized polymer. This observation is consistent with the TGA analysis where P*p*PD-Cr had a greater thermal stability due to high ordered piles of the polymeric chains. Amorphous polymeric materials are conductive to diffusion and adsorption of ions onto its particles due to the loose and disordered structure of the polymeric chains (Li et al., 2009; Yu et al., 2013). In this instance, P*m*PD-Cr may be more suitable for adsorption applications due to its amorphous structural arrangement.

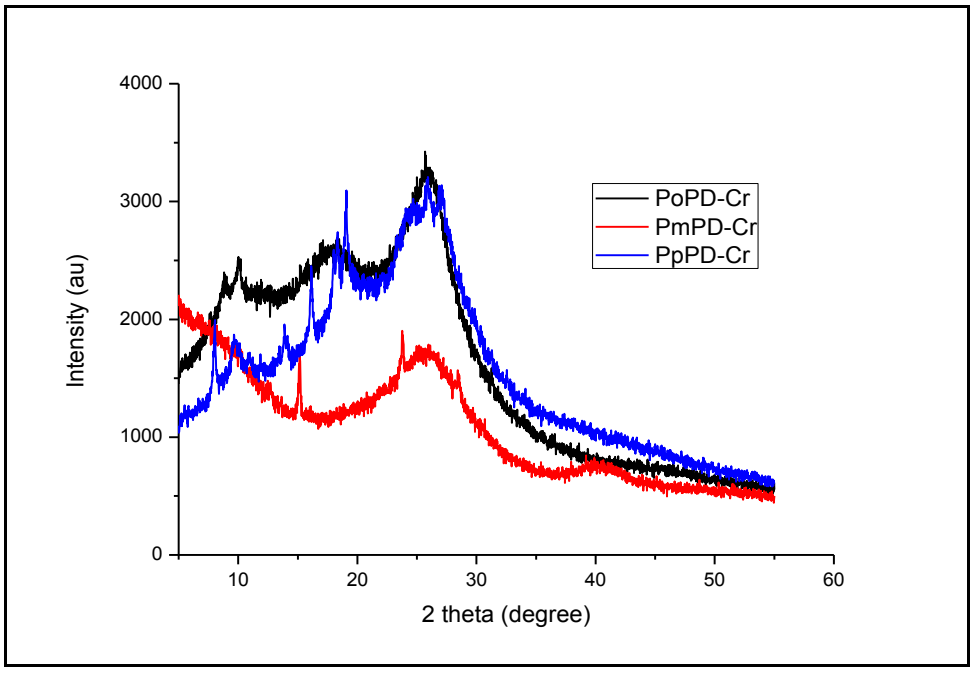

Figure 3. XRD pattern of P*o*PD-Cr, P*m*PD-Cr and P*p*PD-Cr

3.1.4 EDX analysis

Elemental analysis of P*o*PD-Cr, P*m*PD-Cr and P*p*PD-Cr revealed the presence of C, N, O and Cr (Fig. 4). The presence of Cr indicates that it was effectively anchored onto the polymer matrix. Similar elemental ratios were obtained for P*o*PD and P*p*PD while there was an intense N peak for P*m*PD adsorbent. This might be attributed to more amine/imine groups on the P*m*PD chain compared to P*o*PD-Cr and P*p*PD-Cr. Huang et al (2006), reported stronger amine groups on the FT-IR for P*m*PD due to extended in-plane and out-of-plane bending vibrations of C-H bonds on P*m*PD.

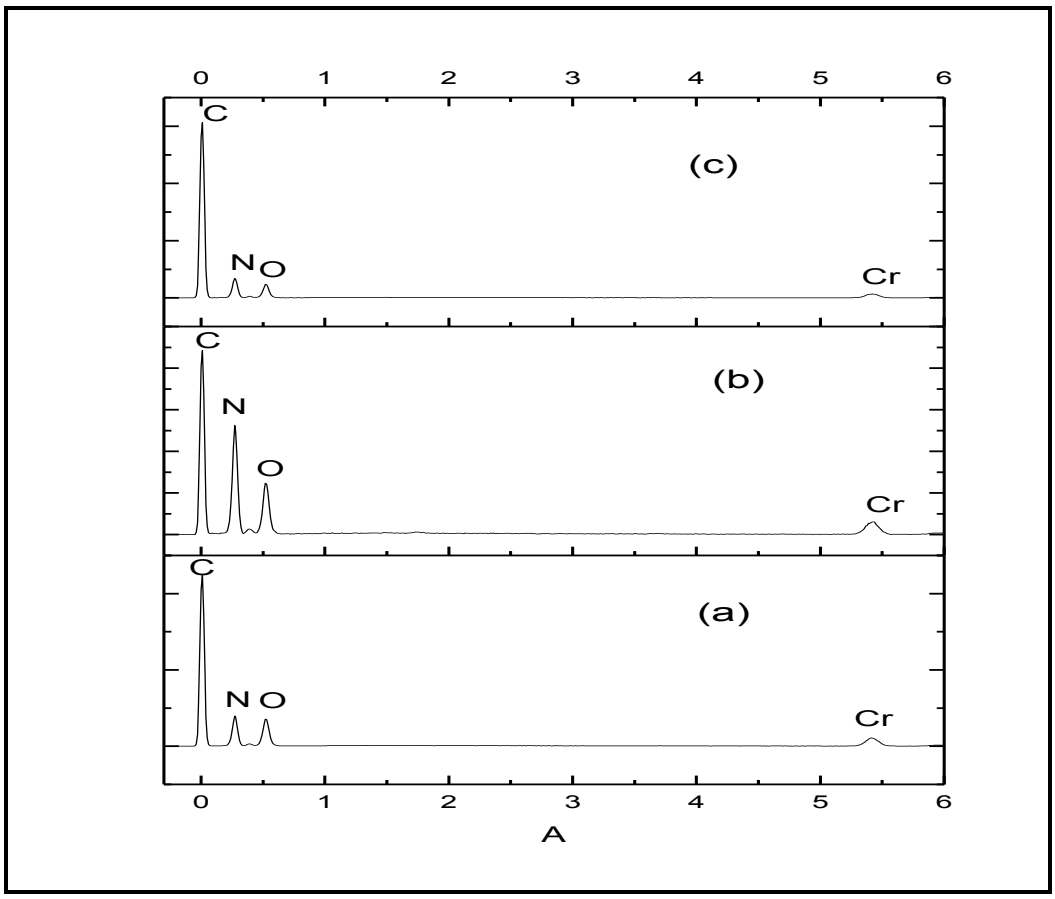

Figure 4. EDX spectra of P*o*PD-Cr, P*m*PD-Cr and P*p*PD-Cr

3.2 Batch adsorption studies

3.2.1 Effect of pH

The effect of pH on the removal of phosphate by the polymers was investigated over a pH range of 2.0-9.0 with a phosphate concentration of 100 mg/L. When $(NH_4)_2S_2O_8$ was used as an oxidant for synthesis a lower phosphate removal by the adsorbent was observed compared to when $K_2Cr_2O_7$ was the oxidant. Additionally a sharp decrease in adsorption

with increasing pH was observed (for P*m*PD). However, when $K_2Cr_2O_7$ was used as an oxidant (Fig 5), the drop in percent removal decreased only gradually with increasing pH from 2-7. For all the polymers there was a significant drop between the pH 7-9. The pH trend is comparable to those previously reported for phosphate on other polymers or metal ions-loaded adsorbents (like ferrihydrite, zirconium binary oxide, zirconium-modified chitosan) and can be associated with the ligand exchange adsorption process (Su et al., 2015; Liu & Zhang, 2015; Acelas et al.,2015). The adsorption process here can be explained on the basis of interaction of phosphate species with adsorbents surface charge. At pH 2 dihydrogen phosphate ($H_2PO_4^-$) is dominant and from pH 3-9 hydrogen phosphate (HPO_4^{2-}) is the main species. $H_2PO_4^-$ has the lower adsorption free energy than HPO_4^{2-} hence more easily adsorbed on the polymer surface (Lu et al., 2013). Additionally, increasing the pH promotes competition between the hydroxyl ions and phosphate species on the polymer active adsorption sites. Although it is evident that adsorption of phosphate by PD polymers reveal a similar pH dependency, $K_2Cr_2O_7$-synthesized polymers displayed superior removal efficiencies and maintained capacity over a wide pH range. This behaviour suggested that the affinity of Cr-loaded polymers is much higher than the $(NH_4)_2S_2O_8$-synthesised polymers for removal of phosphate from water.

$K_2Cr_2O_7$-synthesized polymers were tested for free Cr. No Cr(VI) was detected in the filtrate and less than 0.8 mg/L of total Cr was found in the filtrate solution throughout the pH range of the adsorption study.

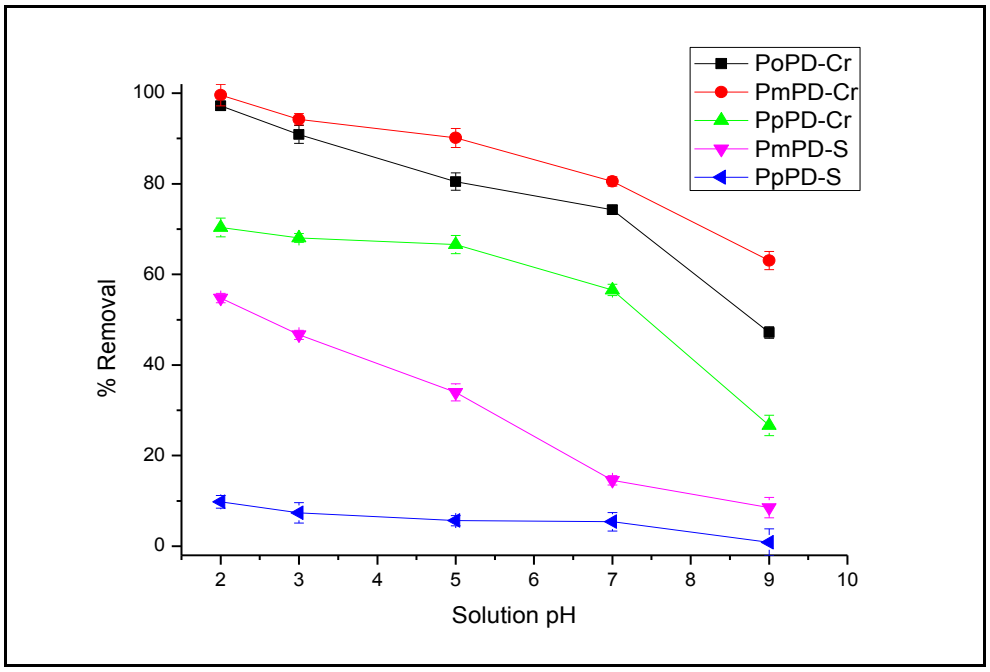

Figure 5. Effect of solution pH on phosphate adsorption onto $K_2Cr_2O_7$ and $(NH_4)_2S_2O_8$ synthesized phenylenediamine polymers. (Temperature= 25 °C, Contact time = 24 h, initial concentration = 100 mg/L, adsorbent dosage = 0.15 g/ 50 mL).

3.2.2 Kinetics study on phosphates adsorption

The adsorption of phosphate on polymers synthesized from $K_2Cr_2O_7$ were investigated as a function of contact time at the initial phosphate concentration of 50 mg/L and 100 mg/L (Fig 6(a)). The adsorption process for all the tests were rapid at the beginning then increased gradually until the plateau of adsorption equilibrium was achieved. Specifically, for 50 mg/L phosphate solution, rapid adsorption occurred within the 90 minutes of contact whereas 120 min was required for 100 mg/L solution. The fast adsorption rate at an early stage is associated to the concentration gradient of ions in solution and the availability of an abundance of active adsorption sites on the surface of the adsorbent (Unuabonah et al., 2007). Adsorption equilibrium and maximum capacity of phosphate were reached at about 200 min and 300 min for 50 mg/L and 100 mg/L solutions, respectively. Additionally, a higher adsorption amount onto the polymers was observed with the increase in initial phosphate concentration while the equilibrium time was also increased.

To understand the adsorption mechanism and potential rate-controlling step, kinetic models such as pseudo-first-order and pseudo-second-order were implemented (eq. 3 and 4). The expression formulas, rate constants and the correlation coefficients (R^2) of these

kinetic models are presented in Table 2. The linear fittings of the experimental data are shown in Fig 6(b). Pseudo-second-order model fitted better with high values of R^2 (> 0.99). The high R^2 values signifies good applicability of the model for phosphate adsorption and that chemical adsorption is mainly involved in the adsorption process (Unuabonah et al., 2007). This means that the adsorption process involved valence forces, possibly through sharing or exchange of electrons between phenylenediamine polymers and phosphate ions (Jeppu & Clement, 2012).

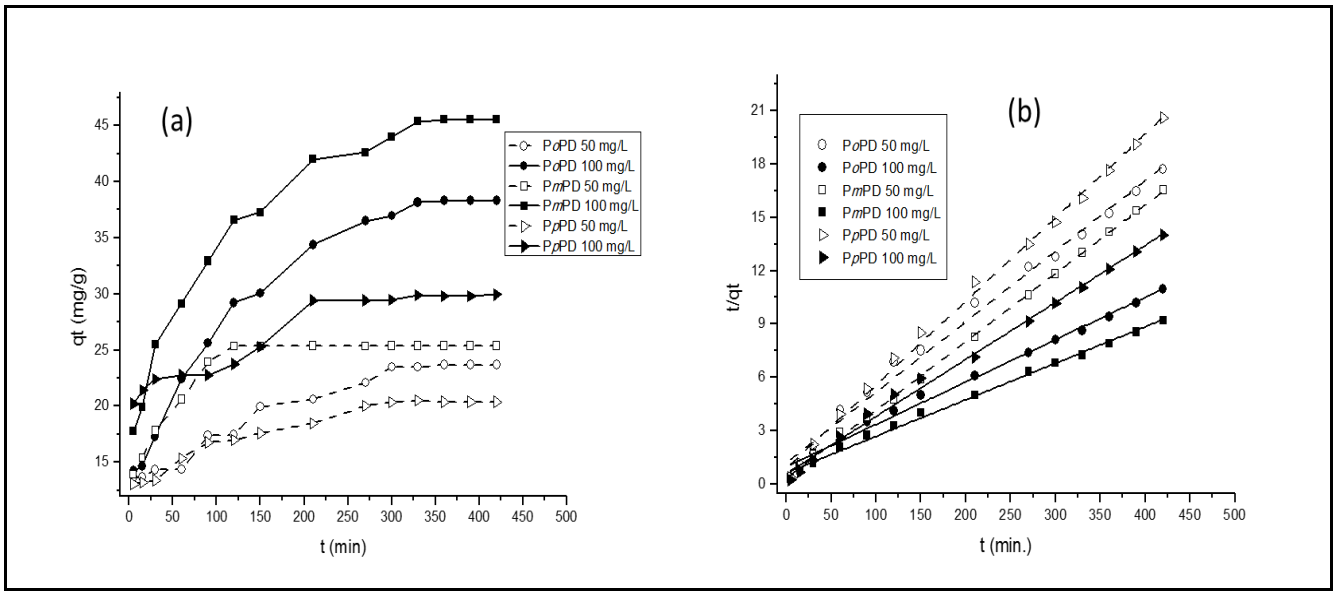

Figure 6. Adsorption kinetics (a) and the pseudo-second order (b) for phosphate adsorption. (Temperature = 25 °C, pH = 2.0, adsorbent dosage = 0.15 g/ 50 mL, initial concentration 100 mg/L).

Table 2: Adsorption kinetic models parameters for phosphates adsorption

		Pseudo-first order model			**Pseudo-second order model**		
Adsorbent	**Co (mg/L)**	**q_e (mg/g)**	**R^2**	**k_1 (1/min)**	**q_e (mg/g)**	**R^2**	**k_2 (g/mg/min)**
P*o*PD	50	14.00	0.630	0.0045	25.19	0.991	0.0013
P*o*PD	50	17.17	0.640	0.0022	26.04	0.999	0.0045
P*m*PD	50	6.64	0.483	0.0031	21.28	0.997	0.0025

P*m*PD	100	27.18	0.821	0.0043	42.02	0.993	0.00058
P*p*PD	100	41.30	0.770	0.0062	48.78	0.995	0.00067
P*p*PD	100	11.79	0.784	0.0046	31.15	0.995	0.0018

3.2.3 Equilibrium adsorption isotherm study on phosphate adsorption

The adsorption capacity of PPD isomers for removal of phosphates was examined by the equilibrium adsorption isotherm experiment as shown in Figure 7. Langmuir and Freundlich isotherm models, as given in eq. 5-7, were used to fit the experimental data and to evaluate the isotherm performance on phosphate removal. These isotherms reveal the specific relation between analyte concentration and its degree of accumulation onto the solid adsorbent surface (Jeppu & Clement, 2012). The Langmuir equation is used to quantify homogeneous adsorption process as a result of monolayer binding whereas Freundlich is regularly used for heterogeneous surface energy systems (Setshedi et al., 2013). The parameters obtained from fitting the experimental data for both models are summarized in Table 3. It was discovered that phosphate adsorption data is best described by the Langmuir adsorption isotherm with the R^2 values > 0.9 and Freundlich produced lower values. The calculated values using the Langmuir function were quite close to the experimentally measured values. Based on the influence of the equilibrium parameter (R_L) (eq. 6), the obtained values were in the range of $0 < R_L < 1$ which indicated that adsorbents were favourable for phosphate removal.

The Langmuir maximum adsorption capacities were 69 mg/g, 143 mg/g and 217 mg/g (about 55.5%, 74.75% and 41.7% adsorption efficiency) for P*p*PD-Cr, P*o*PD-Cr and P*m*PD-Cr, respectively. Phosphate adsorption capacity of P*m*PD-Cr was the highest as indicated by the low equilibrium concentration of phosphate and quite high adsorption capacity as shown in Table 3. The obtained high adsorption capacity for P*m*PD-Cr is in agreement with the TGA and XRD results where amorphous structural arrangement favours adsorption. To demonstrate the prospective of using metal loaded materials as

phosphate adsorbents, a comparative valuation of adsorption capacities and solution pH of various adsorbents were provided in Table 4. The chosen adsorption experiments were also carried out at room temperature using synthetic solutions of phosphate. Comparatively, P*p*PD-Cr, P*o*PD-Cr and P*m*PD-Cr are potential adsorbents for phosphate removal in water.

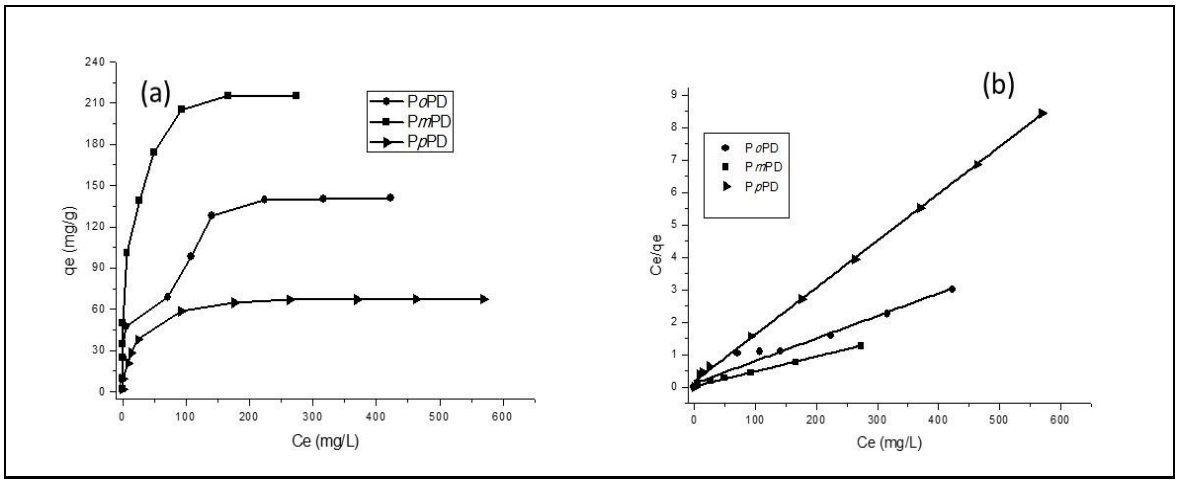

Figure 7. Effect of initial concentration (a) and linearized Langmuir isotherm (b) for phosphate adsorption by P*o*PD-Cr, P*m*PD-Cr and P*p*PD-Cr. (Temperature = 25 °C, contact time = 300 min., adsorbent dosage = 0.15 g/50 ml).

Table 3: Langmuir and Freundlich isotherm parameters for phosphates adsorption

	Langmuir Isotherm				**Freundlich Isotherm**		
Adsorbent	q_e **(mg/g)**	b **(L/mg)**	R_L	R^2	K_F **(mg/g)**	$1/n$	R^2
P*o*PD-Cr	142.9	0.0620	0.184	0.972	94.40	0.235	0.740
P*m*PD-Cr	217.4	0.246	0.077	0.997	188.4	0.217	0.455
P*p*PD-Cr	68.96	0.0818	0.157	0.999	56.51	0.319	0.940

3.2.4 Effect of coexisting anions

In water sources, the phosphates often coexist with nitrates and sulphates and these may likely compete with the phosphate ions for adsorption sites on the adsorbent (Awual eta l., 2014). To assess the effect of these anions on phosphate adsorption, different

concentrations (20 mg/L, 50 mg/L and 100 mg/L) of the coexisting anions were prepared in solution with 50 mg/L of phosphate. All other conditions remained the same as in the preceding experiments with the solution pH at 2. This study was only tested using P*m*PD-Cr and an adsorbent since it outperformed both P*o*PD-Cr and P*p*PD-Cr adsorbents. The presence of nitrates and sulphates, even at higher concentrations, caused insignificant change in the phosphate adsorption capacity (Figure 8).

Phosphate ions are strong bidentate ligands that form inner-sphere complex when interacting with hard Lewis acids like transition metals (Zhao & Sengupta, 1998; Awual et al., 2014). The presence of polyvalent Cr^{3+} metal on the polymer inhibit competing anions on the binding sites since the selective ion pair in the inner sphere complex is for phosphate. Nitrates and sulphates form outer-sphere complexes due to electrostatic interaction and ion exchange with sulphate generally more preferred due to electroselectivity (Acelas et al., 2015).). A proposed adsorption mechanism for phosphate adsorption is shown in Figure 9.

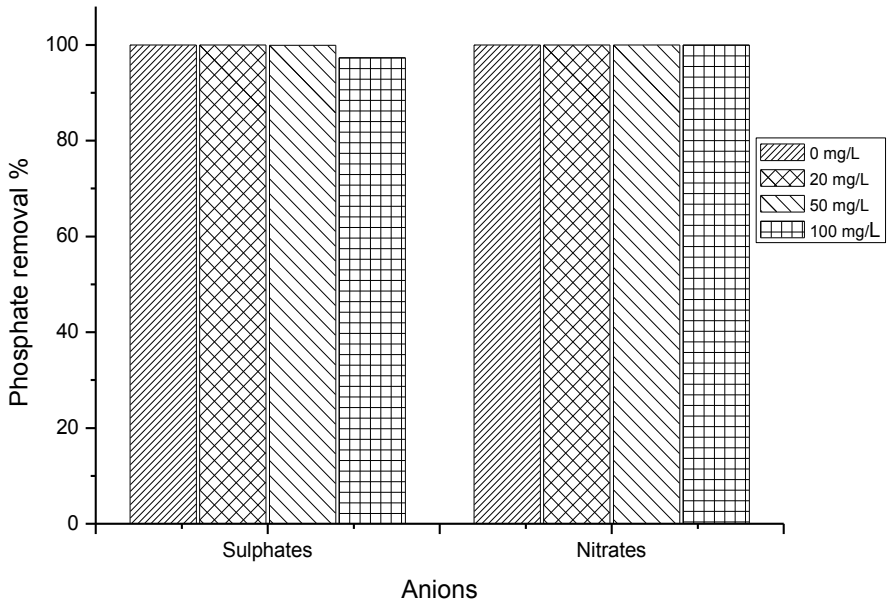

Figure 8. Effect of coexisting anions

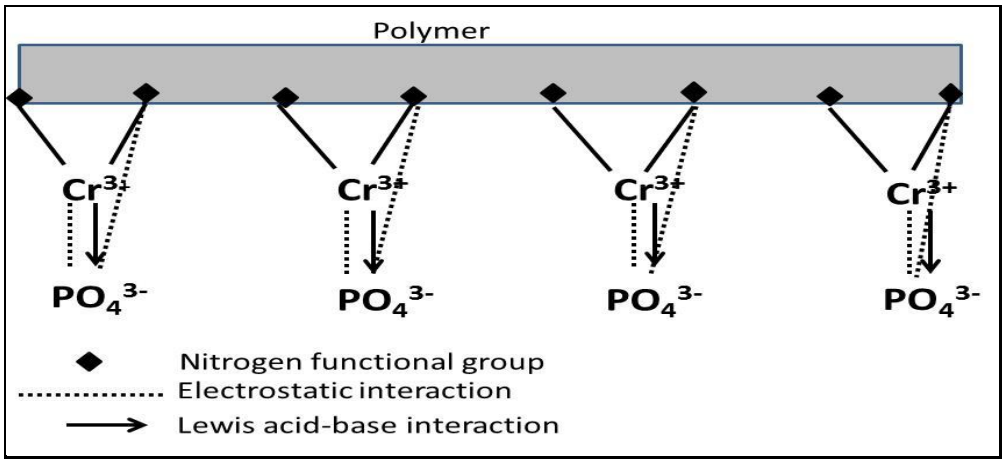

Figure 9. A schematic illustration of phosphates uptake on poly(phenylenediamine) synthesised by $K_2Cr_2O_7$ as an oxidant.

3.2.5 Regeneration experiments

When adsorbents were ladened with 100 mg/L of phosphate species, desorption experiments were carried out to determine its regeneration and ability to be re-used. During the desorption and re-adsorption trials, 0.05 M NaOH solution was found effective to desorb phosphates with over 90% recovery of ions in three hours. The adsorption/desorption cycles were performed for up to five cycles at the same experimental conditions. The adsorption efficiency retained were 89.87%, 94.70% and 98.35% for P*p*PD, P*o*PD and P*m*PD, respectively, at the 5^{th} adsorption cycle. Adsorbents were successfully regenerated for several cycles without deterioration in its performance which make a great potential for practical application.

Table 4: Comparison of adsorption capacity of P*o*PD, P*m*PD and P*p*PD with metal loaded inorganic and polymeric adsorbents for phosphates removal

Adsorbents	Adsorption capacity (mg/g)	pH	Reference
Hydrated ferric oxide-anion exchange resin (IRA-400)	111	-	(Acelas et al., 2015)
Zirconium (IV) loaded bifunctional fibrous	10.7	2.03	(Awual et al., 2014)
Zirconium chitosan beads	60.6	4.0	(Liu & Zhang, 2015)
Cerium-zirconium binary oxide	112	6.2	(Su et al., 2015)
Fe-Al-Mn trimetal oxide	48.3	6.8	(Lǔ et al., 2013)
Tetraethylenepentamine nano magnetic Fe_3O_4	48.3	3.0	(Shen et al., 2015)
P*o*PD	143	2.0	Present work
P*m*PD	217	2.0	Present work
P*p*PD	69.0	2.0	Present work

4. Conclusion

Polyphenylenediamine isomers incorporated with chromium were synthesized and successfully removed phosphate ions from water. The P*m*PD adsorbent demonstrated high adsorption capacity followed by P*o*PD. Adsorption reached equilibrium at about 300 min at an optimum pH of 2.0 and was highly dependent of the adsorbate concentration. The maximum adsorption capacity was attained using at a pH of 2, after 300 min, and adsorbent dose of 0.15 g as optimum adsorption conditions. Moreover, the kinetic and equilibrium data were well fitted by pseudo-second order and Langmuir adsorption models implying the assumption that adsorption was controlled chemisorption and adsorbent surface was homogeneous with only one type of binding site. Most notably, the phosphates uptake by P*m*PD was not noticeably influenced by high concentrations of competing

anions (nitrates and sulphates) and it can be recovered for phosphates re-adsorption for several cycles.

References

Acelas, N.Y., Martin, B. D., López, D., & Jefferson, B., 2015. Selective removal of phosphate from wastewater using hydrated metal oxides dispersed within anionic exchange media. *Chemosphere*, 119, pp.1353–1360.

Awual, M.R., Shenashen, M. A., Jyo, A., Shiwaku, H., & Yaita, T., 2014. Preparing of novel fibrous ligand exchange adsorbent for rapid column-mode trace phosphate removal from water. *Journal of Industrial and Engineering Chemistry*, 20(5), pp.2840–2847.

Huang, M, Peng, Q., Li, X., 2006. Rapid and effective adsorption of lead ions on fine poly(phenylenediamine) microparticles. *Chemistry A European Journal*, 12, pp 4341-4350.

Jeppu, G.P. & Clement, T.P., 2012. A modified Langmuir-Freundlich isotherm model for simulating pH-dependent adsorption effects. *Journal of contaminant hydrology*, 129–130, pp.46–53.

Li, X.G., Huang, M. R., Duan, W., & Yang, Y. L., 2002. Novel multifunctional polymers from aromatic diamines by oxidative polymerizations. *Chemical Reviews*, 102(9), pp.2925–3030.

Li, X.G., Ma, X. L., Sun, J., & Huang, M. R., 2009. Powerful Reactive Sorption of Silver (I) and Mercury (II) onto Poly (o-phenylenediamine) Microparticles. *Langmuir*, 25(3), pp.1675–1684.

Liu, X. & Zhang, L., 2015. Removal of phosphate anions using the modified chitosan beads: Adsorption kinetic, isotherm and mechanism studies. *Powder Technology*, 277, pp.112–119.

Loganathan, P., Vigneswaran, S., Kandasamy, J., & Bolan, N. S., 2014. Removal and Recovery of Phosphate From Water Using Sorption. *Critical Reviews in Environmental Science and Technology*, pp.847–907.

Lǔ, J., Liu, H., Liu, R., Zhao, X., Sun, L., & Qu, J., 2013. Adsorptive removal of phosphate by a nanostructured Fe-Al-Mn trimetal oxide adsorbent. *Powder Technology*, 233, pp.146–154.

Mdlalose, L., Balogun, M., Setshedi, K., Tukulula, M., Chimuka, L., & Chetty, A., 2017. Synthesis, characterization and optimization of poly(p-phenylenediamine)-based organoclay composite for Cr(VI) remediation. *Applied Clay Science*, 139, pp.72–80.

Sestrem, R.H., Ferreira, D. C., Landers, R., Temperini, M. L. a., & do Nascimento, G. M., 2009. Structure of chemically prepared poly-(para-phenylenediamine) investigated by spectroscopic techniques. *Polymer*, 50(25), pp.6043–6048.

Sestrem, R.H., Ferreira, D. C., Landers, R., Temperini, M. L. A., & do Nascimento, G. M., 2010. Synthesis and spectroscopic characterization of polymer and oligomers of ortho-phenylenediamine. *European Polymer Journal*, 46(3), pp.484–493.

Setshedi, K.Z., Bhaumik, M., Songwane, S., Onyango, M. S., & Maity, A., 2013. Exfoliated polypyrrole-organically modified montmorillonite clay nanocomposite as a potential adsorbent for Cr(VI) removal. *Chemical Engineering Journal*, 222, pp.186–197.

Shen, H., Wang, Z., Zhou, A., Chen, J., Hu, M., Dong, X., & Xia, Q., 2015. Adsorption of phosphate onto amine functionalized nano-sized magnetic polymer adsorbents: mechanism and magnetic effects. *RSC Adv.*, 5(28), pp.22080–22090.

Sowmya, A. & Meenakshi, S., 2013. An efficient and regenerable quaternary amine modified chitosan beads for the removal of nitrate and phosphate anions. *Journal of Environmental Chemical Engineering*, 1(4), pp.906–915.

Stejskal, J., 2015. Polymers of phenylenediamines. *Progress in Polymer Science*, 41, pp.1–31.

Su, Y., Yang, W., Sun, W., Li, Q., & Shang, J. K., 2015. Synthesis of mesoporous cerium-zirconium binary oxide nanoadsorbents by a solvothermal process and their effective adsorption of phosphate from water. *Chemical Engineering Journal*, 268, pp.270–279.

Thenmozhi, G., Arockiasamy, P. & Santhi, R.J., 2014. Isomers of Poly Aminophenol: Chemical Synthesis, Characterization, and Its Corrosion Protection Aspect on Mild Steel in 1 M HCl. *International Journal of Electrochemistry*, 2014, pp.1–11.

Tseng, R.-L., Wu, P.-H., Wu, F.-C., & Juang, R.-S., 2014. A convenient method to determine kinetic parameters of adsorption processes by nonlinear regression of pseudo-nth-order equation. *Chemical Engineering Journal*, 237, pp.153–161.

Unuabonah, E.I., Adebowale, K.O. & Olu-Owolabi, B.I., 2007. Kinetic and thermodynamic studies of the adsorption of lead (II) ions onto phosphate-modified kaolinite clay. *Journal of Hazardous Materials*, 144(1–2), pp.386–395.

Wu, R.S.S., Lam, K. H., Lee, J. M. N., & Lau, T. C., 2007. Removal of phosphate from water by a highly selective La(III)-chelex resin. *Chemosphere*, 69(2), pp.289–294.

Yan, L.G., Xu, Y. Y., Yu, H. Q., Xin, X. D., Wei, Q., & Du, B., 2010. Adsorption of phosphate from aqueous solution by hydroxy-aluminum, hydroxy-iron and hydroxy-iron-aluminum pillared bentonites. *Journal of Hazardous Materials*, 179(1–3), pp.244–250.

Yu, W., Zhang, L., Wang, H., & Chai, L., 2013. Adsorption of Cr(VI) using synthetic poly(m-phenylenediamine). *Journal of hazardous materials*, 260, pp.789–95.

Yu, W.T., Chai, L. Y., Zhang, L. Y., & Wang, H. Y., 2013. Synthesis of poly (m-phenylenediamine) with improved properties and superior prospect for Cr(VI) removal. *Transactions of Nonferrous Metals Society of China (English Edition)*, 23(11), pp.3490–3498.

Zhao, D. & Sengupta, A.K., 1998. Ultimate removal of phosphate from wastewater using a new class of polymeric ion exchangers. *Water Research*, 32(5), pp.1613–1625.

Zhou, H., Badashah, A., Luo, Z., Liu, F., & Zhao, T., 2011. Preparation and property comparison of ortho, meta, and para autocatalytic phthalonitrile compounds with amino group. *Polymers for Advanced Technologies*, 22(10), pp.1459–1465.

PAPER V

PHOSPHATES ADSORPTION USING INORGANICALLY MODIFIED BENTONITE CLAY

Adsorption of phosphates using inorganically-modified bentonite clay

Lindani Mdlalose[a,b*], Mohammed Balogun[a], Katlego Setshedi[a], Luke Chimuka[b], Avashnee Chetty[a]

[a]Polymers and Composites, Materials Science and Manufacturing , Council for Scientific and Industrial Research, Pretoria, South Africa, P.O Box 395, Pretoria, 0001

[b]Molecular Sciences Institute, School of Chemistry, University of the Witwatersrand, Johannesburg, South Africa P/Bag 3, WITS, 2050

Corresponding author: Tel.: +27 128412645

E-mail address: lmdlalose1@csir.co.za

Abstract

Phosphorus is a micronutrient which is vital for the existence of all lifeforms; but when it exists in abundance, it can have detrimental environmental and health impacts. Strict environmental limits are set to curb pollution from sewage, household washings and fertilizers. Various technologies have been researched and developed to remove excess phosphates from water. Adsorption technology is a potentially cheap technology which is effective even at low pollutant concentrations. In this work we synthesized and evaluated the performance of bentonite clay modified with Fe, Co and Ni salts for the adsorption and removal of phosphate ions from aqueous solutions. FT-IR spectroscopy and XRD techniques were used to investigate the surface properties of the adsorbents. The results

revealed lower crystallinity in metal-modified bentonite compared to the native bentonite. Phosphate ion uptake improved on modified bentonites by 57%-74% as compared to the native bentonite for phosphate concentration of 100 mg/L. Additionally, adsorption capacity of all studied adsorbents increased with increasing time and initial phosphate concentration at an optimum pH of 3. The maximum phosphate immobilization capacity was attained from Langmuir isotherm model. Adsorption rate parameters were in agreement with pseudo-second order kinetic model for all adsorbents.

Keywords: Modified bentonite; phosphate; hydrated metal oxide, adsorption mechanism

Acknowledgements

This work was supported by the South African Council for Scientific and Industrial Research (Project grant: 88568), National Research Foundation- Professional Development Programme and Erasmus Mundus (Aesop project). The authors acknowledge the University of the Witwatersrand and the University of Latvia for contributions to this project.

1. Introduction

Phosphorus is an extremely vital element for the existence of all life forms and their propagation. Its oxo-acidic form, phosphoric acid, is ubiquitous in the Earth's biosphere mainly as the anion. It makes up the acidic backbone of the nucleic acids DNA and RNA —the putative molecules of life (Cafferty & Hud, 2014). The repeating units of these molecules are covalently linked through di-esters of phosphate and sugar units. It is also found in the hydrophilic head of cell membranes' phospholipids (Cafferty & Hud, 2014).

Enzymatic hydrolysis of anhydride linkages between phosphate units is the source of energy for the biological energy molecule adenosine triphosphate (ATP) (Hofer et al., 2016). ATP is the main energy currency by which life processes are powered. Because of its vital role in these life molecules phosphate is not readily degraded or excreted. It is re-used in a tightly regulated and restricted metabolic process. As such, de novo phosphate is only required during cellular replication processes for repair or growth of new genetic materials and for the metabolic energy to fuel the processes. To avoid toxicity the environmental levels of phosphates must be tightly monitored.

Many anthropological processes increase the levels of phosphates in environmental bodies like water. Fertilizers contain phosphorus as a key nutrient for plant growth. Untreated human and animal wastes contribute significantly to phosphate pollution when sewage is unrestrictedly dumped into aquatic systems. Household materials like detergents, which are released to water bodies through municipal discharge systems, also play a key role in the eutrophication of these aquatic systems. The immediate detrimental environmental impact is the proliferation of some organisms such that the delicate balance of these aquatic ecosystems is destabilized. This is transmitted in a domino effect along the whole ecological chain. A water body with a phosphorus concentration exceeding 0.025 mg/L is considered as polluted (Warwick et al., 2013).

Generally, in wastewater phosphates exist in numerous forms, depending on the origin, but which are grouped into three classes: ortho-phosphates, condensed phosphates and organic phosphorus (Loganathan et al., 2014). The predominant form is ortho-phosphate which ranges between 50% - 70% of phosphorus in wastewater. It exists as in the form of phosphoric acid, dihydrogen phosphate, hydrogen phosphate and phosphate ions, which

are different pH-dependent hydrogenated forms (Tu et al., 2014). Further, these phosphate forms may be bound to an organic compound or exist as the free inorganic molecule. The inorganic form is the more abundant form in aquatic systems since the organic phosphorus present eventually get converted to soluble orthophosphate by hydrolysis. (Warwick et al., 2013). A limit of 1.0 mg/L is set for ortho phosphates in water systems.

The most commonly applied traditional methods for phosphates removal from water are biological processes and chemical precipitation (D. Zhao & Sengupta, 1998); (H. L. Zhang et al., 2015). A process known as enhanced biological phosphorus removal (EBPR) is often implemented for removal of the element (Oehmen et al., 2007). The phosphorus uptake occurs using a bacterial strain called phosphorus-accumulating organism (PAO) which actively stores excess phosphorus against a concentration gradient. Chemical precipitation is considered a flexible approach which depends on the solution pH. In essence, a divalent or trivalent metal salt is added into wastewater to form an insoluble metal phosphate which is separated by sedimentation. The most frequently used salts are of iron and aluminium but lime may also be used to form insoluble calcium phosphate (Boujelben et al., 2008). This procedure produces a metal-bound phosphorus sludge which needs additional treatment steps before recycling for agricultural purposes (Tu et al., 2014).

The major drawbacks with the current methods particularly biological processes are related to high design costs which make them economically unattractive. As alternatives, the development of low cost adsorbent materials is being investigated. Lately, adsorption technique is widely investigated because there are several potential materials that can function as adsorbents for organic and inorganic phosphates (Sowmya & Meenakshi, 2013). This technique is comparatively more economical and highly effective for high and

low phosphate concentrations (Tu et al., 2014). Several low-cost clays and waste by-products such as zeolites, montmorillonite, palygorskite, blast furnace sludge, iron oxide tailings, and fly ash have been used for anion adsorption (Onyango et al. 2010; Chen et al. 2013; Ye et al. 2006; Pengthamkeerati et al., 2008). Engineered activated aluminium oxide, ferric oxide and layered double hydroxides have also been studied extensively for the removal of phosphates in aqueous systems (Huang et al., 2013; Halajnia et al., 2013).

Bentonite is a low cost, environmentally friendly and easily obtained clay made up of negatively charged alumino-silicate usually balanced with alkaline and alkali earth metal cations (typically Na^{+} and Ca^{2+}) (Alkaram et al., 2009). Replacing these cations with inorganic hydroxyl-metal enhances the interlayer spacing of bentonite (Manohar et al., 2006). Different hydroxyl-metals including iron, aluminium, chromium and manganese have been used in the past to remove heavy metals, dyes and other environmental pollutants with hydroxyl-aluminium being well studied and defined (Yan et al., 2010). However, the preparation of bentonite with hydroxyl metal poly-cations of cobalt and nickel is limited. We report here the feasibility of bentonite pillared with iron, cobalt and nickel hydroxyl poly-cations, respectively for adsorption of phosphate ions in aqueous solution.

2. Experimental

2.1 Chemicals

Bentonite and potassium dihydrogen phosphate (KH_2PO_4) were purchased from Sigma Aldrich (South Africa). Analytical grade metal salts of nickel(II) chloride hexahydrate ($NiCl_2.6\ H_2O$), iron(II) chloride tetrahydrate ($FeCl_2.4H_2O$) and cobalt(II) nitrate

hexahydrate ($Co(NO_3)_2$. $6H_2O$) were obtained from Sigma Aldrich. Hydrochloric acid (HCl) and sodium hydroxide (NaOH) were purchased from Merck (South Africa). All solutions were prepared in de-ionized water.

2.2 Adsorbents preparation

The metal bentonite adsorbents were prepared by suspending bentonite clay with metal salts (0.5 M) ($NiCl_2.6H_2O$, $FeCl_2.4H_2O$, $Co(NO_3)_2.6H_2O$) in HCl (0.2 M) at ambient temperature and vigorously shaking for 1 h. Thereafter, NaOH (0.5 M) solution was slowly added into the suspension with continuous shaking for 24 h. The resulting solid was filtered, washed *ad lib* with ethanol and deionized water and later dried in the oven at 60 °C overnight.

2.3 Characterization

The functional groups of the adsorbents were determined using KBr and determined by FT-IR spectroscopy on Spectrum One Apparatus, PerkinElmer. X-ray diffraction (XRD) patterns were acquired with a Bruker AXS D8 Advance with Cu-Kα as the radiation source.

2.4 Adsorption of phosphates

A stock solution of KH_2PO_4 (1000 mg/L) was prepared by dissolving the salt in de-ionized water and aliquots were diluted accordingly for subsequent experiments. The effect of pH on adsorption was investigated by adjusting the solution pH from 2 to 9 using either dilute NaOH or HCl for 100 mg/L phosphate solution. To test for phosphate removal, 0.3 g of the adsorbents were suspended in 50 mL of phosphate solutions and agitated at 120 rpm for 24 h to ensure equilibrium. The suspensions were filtered through syringe filters (RC

membrane, 0.45 μm) and the filtrates' phosphate concentrations were measured by the molybdenum blue colourimetric method in which the absorbance was measured at a wavelength of 880 nm on a Hach Lange DR 2800 spectrometer. The effect of adsorbent dose was assessed by varying the masses from 0.35- 0.7 g in 50 mL phosphate solution at pH 3. The removal percentages and adsorption capacities were determined by using the following Eq. (1) and (2):

$$\% \text{ Removal} = \frac{(C_o - C_e)}{C_0} \times 100 \quad (1)$$

where C_o and C_e are the initial and the equilibrium concentrations (mg/L) of PO_4^{3-}, respectively.

The equilibrium adsorption capacity (q_e) was determined using the following Eq. (2):

$$q_e = \frac{(C_o - C_e)V}{m} \quad (2)$$

where q_e is the equilibrium amount of PO_4^{3-} adsorbed per unit mass (m) of adsorbent (mg/g) and V is the sample volume (L).

The kinetic data from contact time effect was fitted using pseudo-first and second order model. The kinetic rate equations are shown in Eqs (3) and (4), respectively. The study was conducted on 100 mg/L phosphate solution using the optimum dose for each adsorbent. About 10 mL of aliquots were taken from the suspensions at different time intervals.

$$ln(q_e - q_t) = lnq_e - kt \quad (3)$$

$$\frac{t}{q_t} = \frac{1}{k_2 q_e^2} + \frac{t}{q_e} \quad (4)$$

where k_1 (1/min) and k_2 (g/mg/min) are the pseudo-first order and pseudo-second order rate constants, respectively, q_t is the amount of PO_4^{3-} adsorbed at any time (mg/g) and q_e is equilibrium adsorption capacity (mg/g).

Adsorption isotherm at the initial pH of 3 was investigated by varying the initial phosphate concentration from 100-1000 mg/L at ambient temperature. Langmuir and Freundlich isotherms were used to fit the experimental data. The equations are described in Eqs (5) and (6) as follows:

$$\frac{C_e}{q_e} = \frac{C_e}{q_o} + \frac{1}{q_o b} \quad (5)$$

where q_o (mg/g) is the maximum amount of PO_4^{3-} ions per unit mass of adsorbent to form a complete monolayer on the adsorbent surface and b (L/mg) is the binding energy constant. An essential characteristic of the Langmuir isotherm used to define the favourability of an adsorption process, the dimensionless separation factor (R_L) is given by Eq. (6):

$$R_L = \frac{1}{(1 + bC_o)} \quad (6)$$

The values of R_L range between 0 and 1 to confirm a favourable adsorption process. The Freundlich isotherm, which predicts adsorption onto heterogeneous surfaces, is expressed by Eq. (6):

$$\ln q_e = \ln K_F + \frac{1}{n} \ln C_e \quad (7)$$

where K_F (mg/g) and $1/n$ constants are related to the adsorption capacity and affinity of adsorption, respectively.

3 Results and Discussion

3.1 Characterization

The FT-IR spectra of bentonite and inorganically modified bentonite showed bands at 3636 and 1636 cm^{-1} which are assigned to H-O-H stretching dipoles (Fig. 1). This is associated with hydroxyl groups bonded to two octahedrally coordinating cations like Al and Mg (Gates & Bouazza, 2010). The strong band centred at 1033 cm^{-1} is attributed to the asymmetric stretching mode of O-Si-O. The spectrum of the modified bentonites presented the same bands as the native bentonite but the 1033 cm^{-1} band broadened for Co and Fe modified bentonite. The minor change in wavenumber values is indicative of Fe/ Co- Si-O compound stretching (Lu et al., 2013).

The XRD measurements have shown that bentonite and modified bentonite are mainly composed of montmorillonite and quartz minerals (Fig. 2). Modification of bentonite with metallic salts revealed insignificant changes in the crystal structure of native bentonite minerals. The intensity basal spacing peak at 5.55° (2 theta) which corresponds to 15.92 Å for modified bentonites is weaker than that of the bentonite. The decrease in peak intensity could be a result of poor crystallinity compared to parent bentonite due to the presence of irregular stacking of the metals and thus the structure slightly becomes amorphous (Eren and Afsin, 2008).

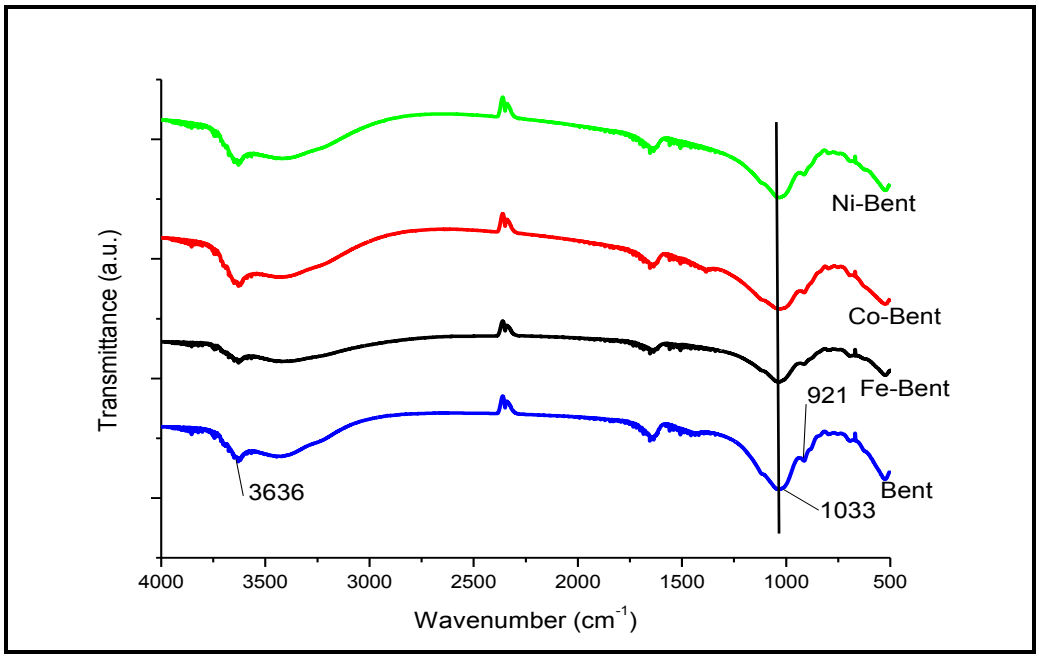

Fig. 1: The FTIR spectra of Bent, Fe-Bent, Co-Bent and Ni-Ben

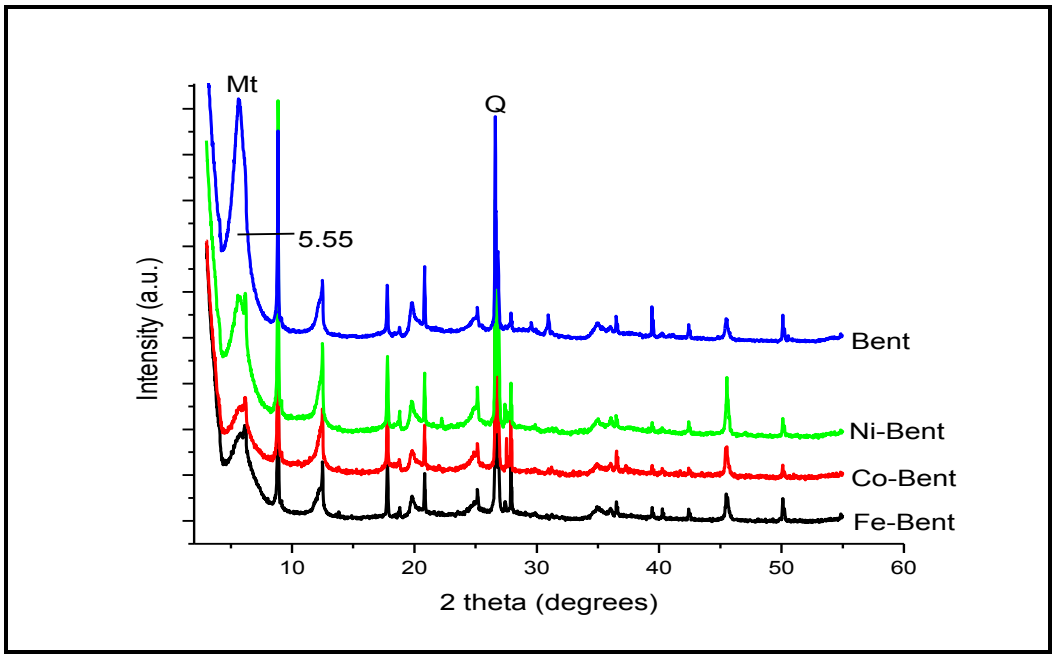

Fig. 2: XRD diffractograms of Bent, Fe-Bent, Co-Bent and Ni-Bent. Mineral denotations: Mt-montmorillonite and Q-quartz.

3.1 Effect of pH

Adsorption of phosphate as a function of pH is demonstrated in Fig. 3. The batch experiments were carried out at a pH range of 2 – 9 and adsorbent content was 0.3 g for

100 mg/L phosphate solution. It was found that the removal percentage of phosphate ions strongly depended on solution pH. Adsorption capacities of the modified bentonites were higher than the native bentonite. This was attributed to the introduction of positively charged metals which increased the electrostatic interaction between phosphate molecules and the modified bentonite surfaces. The optimum pH for phosphates adsorption was obtained at pH 3 and slightly decreased between pH 3 to 7. These conditions were favourable because at this states phosphate is dominant in a form of monovalent $H_2PO_4^-$ (Yan et al., 2010). The poor removal efficiency below pH 3 is attributed to the dominant H_3PO_4 species which is non-ionic. Above pH 7 divalent HPO_4^{2-} species with higher adsorption free energy than monovalent HPO_4^- dominates, hence poor removal as it cannot easily adsorb on the surface.

Additionally, increasing increasing the pH promotes competition between hydroxyl ions (OH^-) and phosphates species on the adsorbent active sites, which then reduce phosphate adsorption (Manohar et al., 2006). Phosphate ions removal were very weak on native bentonite adsorbent. The maximum phosphates adsorption was 84.6%, 80.0%, 68.3% and 11.1% for Fe-Bent, Co-Bent, Ni-Bent and Bent, respectively.

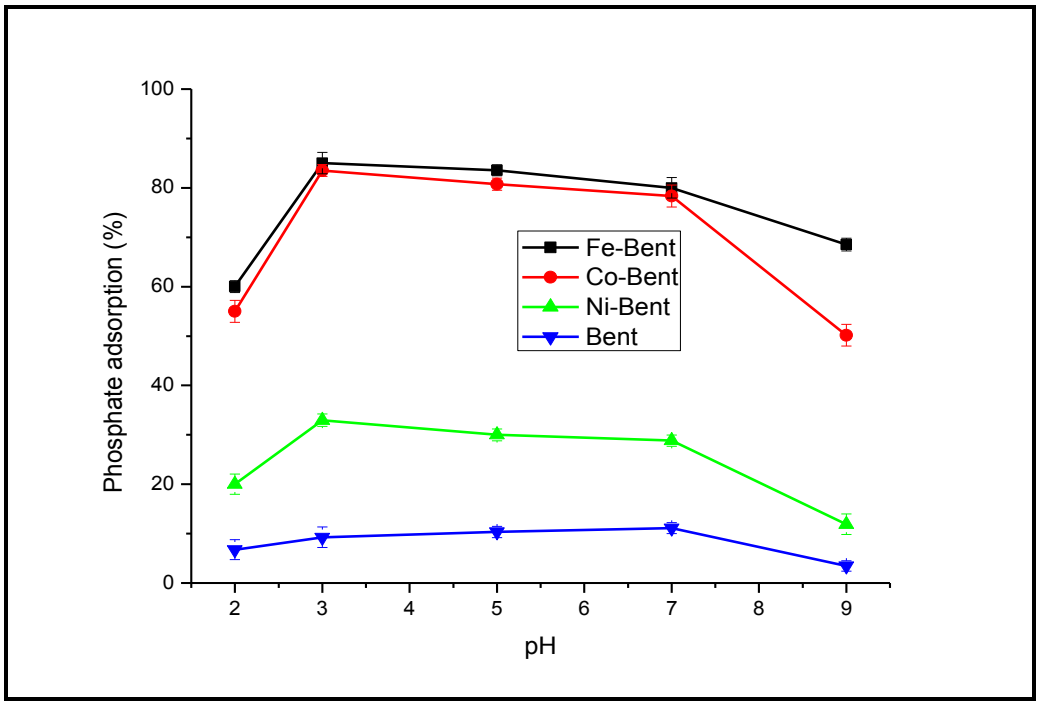

Fig. 3: Effect of initial solution pH for phosphate adsorption on Fe-Bent, Co-Bent, Ni-Bent, and Bent adsorbents. (Temperature = 25 °C, time = 24 h, adsorbent dose = 0.3 g/50 mL, initial concentration = 100 mg/L).

3.1 Effect of adsorbent dose

The dosage effect is an essential parameter to determine the capacity of the adsorbent at a given concentration. The variation was carried out using adsorbent mass of 0.25 g to 0.7 g. It was observed that the uptake per unit mass of the adsorbent was higher for Fe-Bent followed by Co-Bent with Bent been the least. About 0.5 g of Fe- and Co-modified bentonite was required to reach equilibrium but a linear increase was observed with Ni-Bent and Bent adsorption above 0.5 g of the adsorbent. Nominal adsorption performance for Ni-Bent and Bent could be a result of its weaker available adsorption sites which get saturated with 100 mg/L phosphate ions compared to the Fe-Bent and Co-Bent.

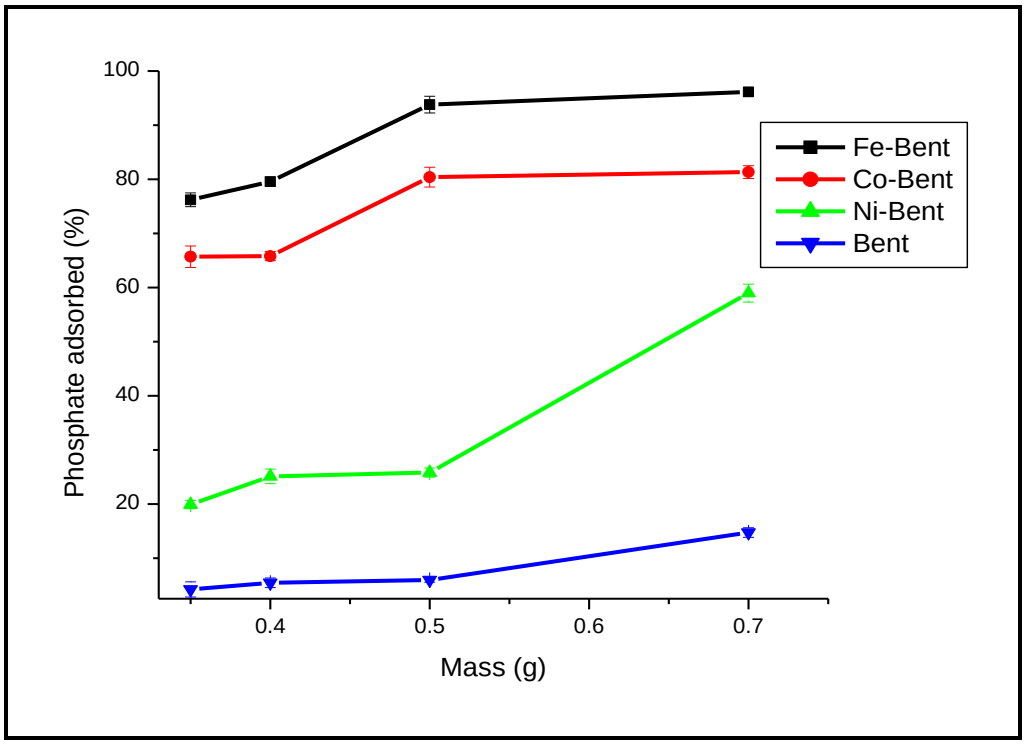

Fig. 4: Effect of adsorbent dosage for phosphates adsorption on Fe-Bent, Co-Bent, Ni-Bent and Bent adsorbents. (Temperature = 25 °C, time = 24 h, pH = 3.0, initial concentration = 100 mg/L).

3.1 Effect of contact time and adsorption kinetics

Adsorption measurements for phosphate ions uptake versus contact time at the initial concentration of 100 mg/L are presented in Fig. 5. Contact time effect is one of the significant factors in evaluating the competence of a material for adsorption. From the obtained experimental results, phosphates removal increased rapidly by 16-84% for the adsorbents with the increase in contact time from 2-70 min. Equilibrium was reached at about 120 min. The initial rapid uptake is associated with electrostatic attraction on the adsorbent surface while the tapering observed towards the end is the result of inner diffusion processes on the adsorbent bulk (Manohar et al., 2006).

The kinetic data of phosphates were determined by using pseudo-first and pseudo-second order kinetic models. The parameters obtained by linear regressions are shown in Table 1. Considering the calculated and the experimental adsorption results with the correlation coefficient (R^2), the kinetic data for bentonite-based adsorbents fitted better by the pseudo-second-order adsorption kinetic rate model as shown in Fig. 6. The agreement with pseudo-second-order kinetic model suggested that chemisorption process is the rate limiting step for the adsorbents active sites and phosphate ions. A similar result of kinetic model was reported for phosphates removal on clay based materials (Yan et al., 2010; Manohar et al., 2006).

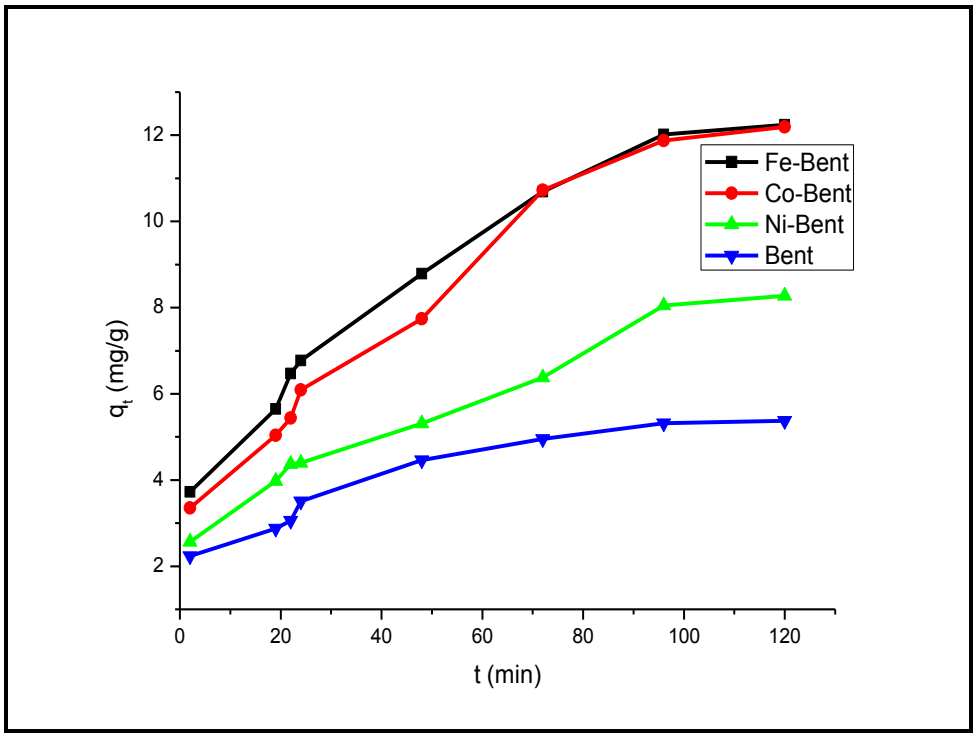

Fig. 5: Effect of contact time for phosphates adsorption on Fe-Bent, Co-Bent, Ni-Bent and Bent adsorbents. (Temperature = 25 °C, pH = 3.0, adsorbent dose = 2 g, Initial solution volume = 200 mL, initial concentration = 100 mg/L).

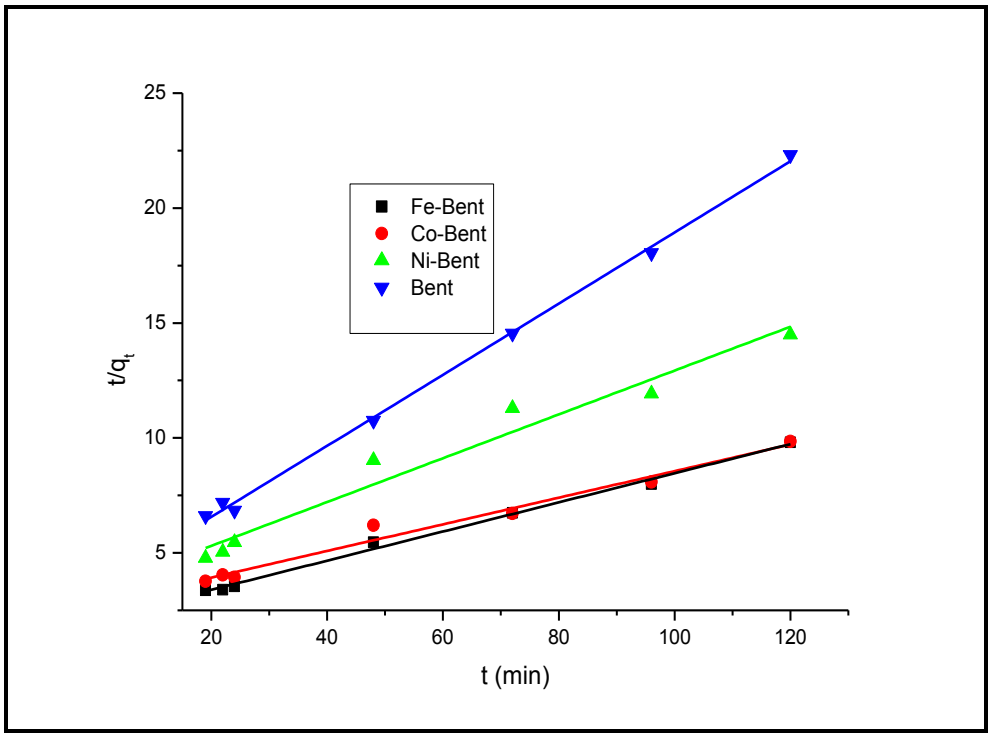

Fig. 6: Pseudo-second order kinetic plots for phosphate adsorption on Fe-Bent, Co-Bent, Ni-Bent and Bent.

Table 1: Adsorption kinetic models parameters for phosphates adsorption

		Pseudo-first order model			**Pseudo-second order model**	
Adsorbent	**q_e (mg/g)**	**R^2**	**k_1 (1/min)**	**q_e (mg/g)**	**R^2**	**k_2 (g/mg/min)**
Fe-Bent	9.563	0.956	0.0090	15.77	0.996	0.0040
Co-Bent	11.31	0.928	0.0020	17.27	0.981	0.0034
Ni-Bent	6.323	0.963	0.0070	10.49	0.965	0.0091
Bent	4.023	0.927	0.0023	6.464	0.998	0.024

3.1 Effect of initial concentration and adsorption isotherms

The effect of initial phosphate concentration was investigated at ambient temperatures with an initial concentration of 100-1000 mg/L. Adsorption capacity gradually increased for native bentonite but more significantly for the modified bentonite adsorbents until equilibrium (Fig. 7). In particular, Co-Bent and Ni-Bent traced linear hypotenuse slopes before reaching equilibrium which suggest favourable adsorptions of high concentrations of phosphate ions. Fe-Bent however traced a steady slope to the maximum adsorption capacity of 20 mg/g, three times more than Bent.

The empirical data values were evaluated according to the Langmuir and Freundlich adsorption isotherms to further investigate the adsorption process. The calculated adsorption parameters and R^2 values (summarized in Table 2) fitted Langmuir isotherm very well. It is known that Langmuir isotherm model caters for homogeneous adsorbent surface while Freundlich model favours heterogeneous surface (Lu et al., 2013). The dimensionless separation factors RL calculated from Langmuir isotherm are between 0-1 which also indicate the high favourability for phosphates on Bent-based adsorbents.

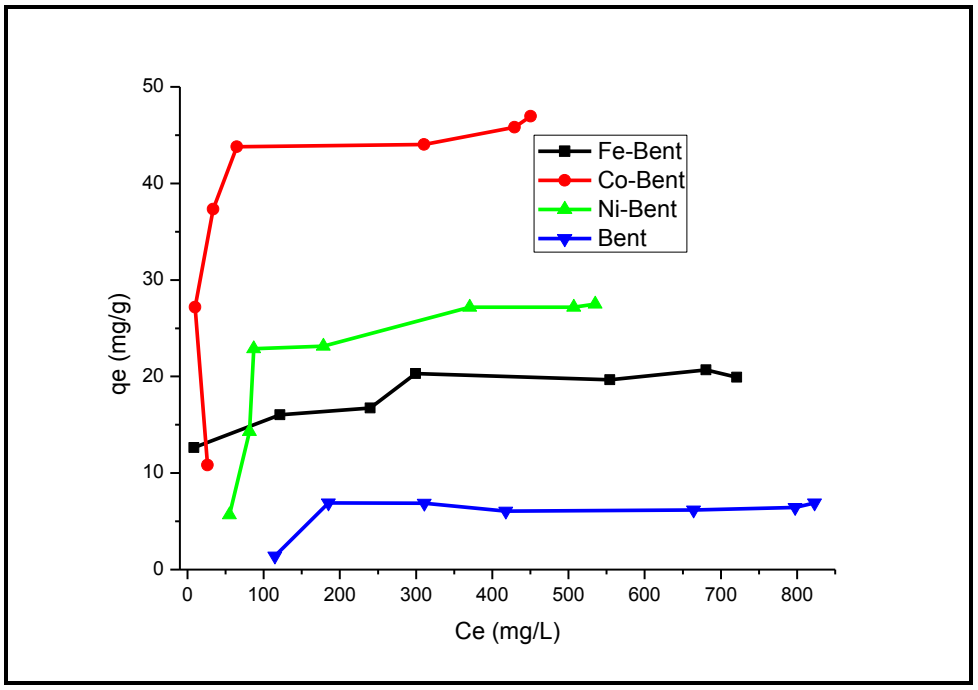

Fig. 7: Effect of initial concentration for phosphates adsorption on Fe-Bent, Co-Bent, Ni-Bent and Bent. (Temperature = 25 °C, time = 180 min., adsorbent dose = 0.3 g/50 mL).

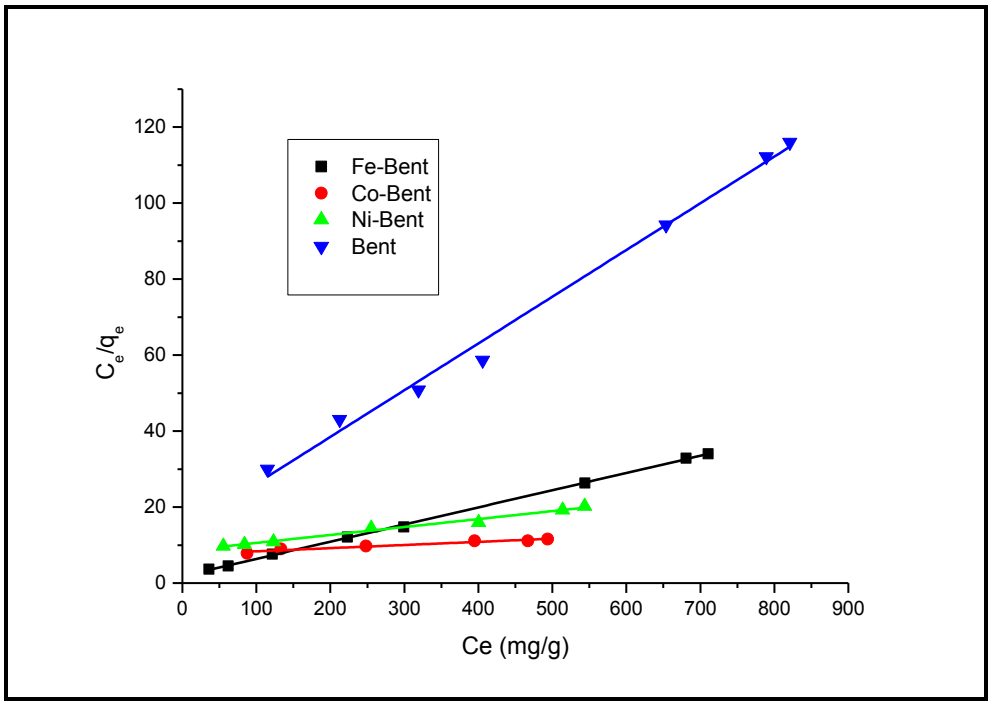

Fig. 8: Model plots of Langmuir isotherm for phosphates adsorption on Fe-Bent, Co-Bent, Ni-Bent and Bent.

Table 2: Langmuir and Freundlich isotherm parameters for phosphates adsorption

		Langmuir Isotherm			Freundlich Isotherm		
Adsorbent	q_e **(mg/g)**	b **(L/mg)**	R_L	R^2	K_F **(mg/g)**	$1/n$	R^2
Fe-Bent	20.88	0.0380	0.111	0.995	9.859	0.110	0.910
Co-Bent	46.95	0.1209	0.648	0.999	23.030	0.120	0.814
Ni-Bent	29.07	0.0311	0.496	0.998	13.442	0.114	0.896
Bent	6.57	0.2113	0.281	0.986	2.435	0.149	0.620

3.2 Phosphates adsorption mechanism

Generally, anions like phosphates, nitrates, arsenates, etc. get adsorbed onto clay or clay-derived materials through electrostatic attraction and ligand exchange mechanisms (Zhao and Sengupta, 1998). In this study, the presence of Fe-OH, Co-OH and Ni-OH functional groups contributed to phosphate adsorption. At acidic pH values, the hydroxyl group gets protonated to an oxonium cation which is a more favourable leaving group. This facilitates a ligand exchange process through the displacement of $–OH_2^+$ from the binding sites.

FT-IR measurements were used to examine adsorbents change before and after phosphate ions adsorption (Fig 9). From FT-IR measurements of the adsorbents before and after phosphate ions adsorption a notable shifting of wavenumbers at around 1033 cm^{-1} to lower wavenumbers was observed for all adsorbents ladened with the anions (Fig 9). This could possibly be due to the formation of metal/oxide/phosphate complex. A similar mechanism was proposed for phosphates adsorption on hydrated metal oxides where the metal-OH band before adsorption at 1123 cm^{-1} shifted to 1070 cm^{-1} after adsorption (Yan et al.,

2010). This indicates the formation of monodentate or bidentate inner-sphere complex between phosphate and hydroxyl groups on metal oxides/hydroxides.

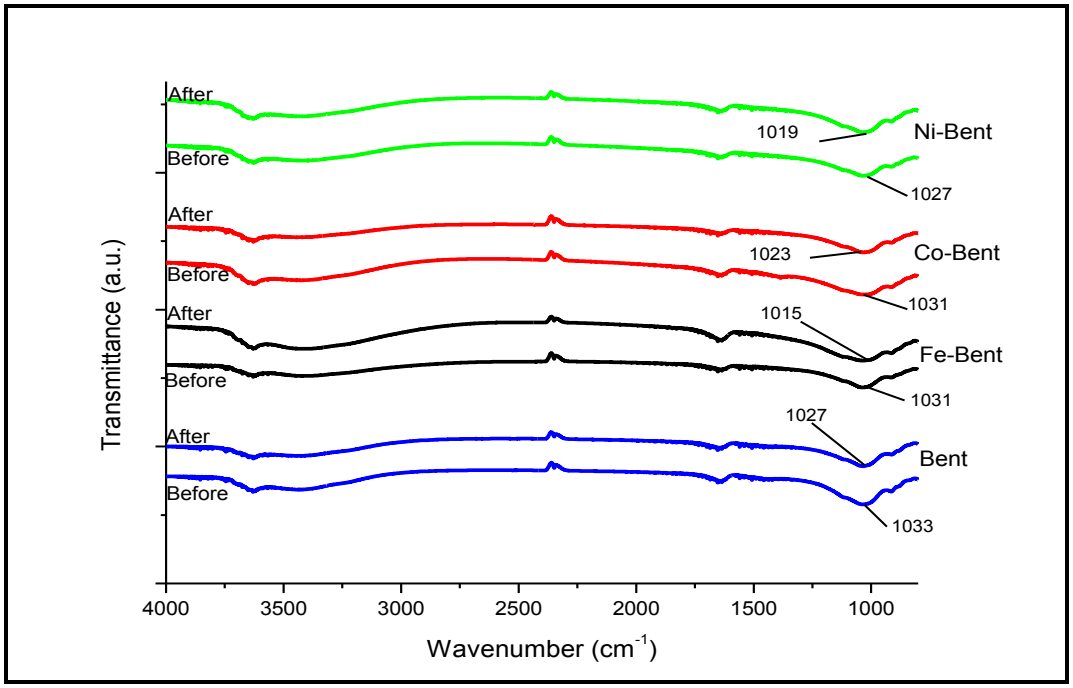

Fig. 9: The FTIR spectra of Bent, Fe-Bent, Co-Bent and Ni-Bent before and after phosphate ions adsorption.

4. Conclusion

Clay is an abundant natural resource which appears to be chemically inert but has been beneficiated in numerous ways. In this work we have shown that modification of bentonite clay with common metals Fe, Co and Ni is a simple way of improving the adsorption properties of clay particles. Hydroxyl-metal polycation-modified bentonites possessed a semi amorphous structure compared to the native bentonite. The phosphate adsorption on the adsorbents was fitted by the Langmuir model at pH 3. Kinetic data was described better by pseudo-second-order kinetic model and the optimum adsorption time was attained at 180 min. The maximum adsorption capacities of 20.88 mg/g, 46.95 mg/g and 29.07 mg/l

and 6.57 mg/g were obtained for Fe-Bent, Co-Bent, Ni-Bent and and Bent adsorbents, respectively. Overall, the modified clay adsorbents displayed enhanced phosphates adsorption as compared to native clay. Adsorption capacities could still be improved by optimizing the concentration of metal salts during the synthesis step.

References

Alkaram, U.F., Mukhlis, A.A. and Al-Dujaili, A.H., 2009. The removal of phenol from aqueous solutions by adsorption using surfactant-modified bentonite and kaolinite. *Journal of Hazardous Materials*, 169(1–3), pp.324–332.

Boujelben, N., Bouzid, J., Elouear, Z., Feki, M., Jamoussi, F., Montiel, A., 2008. Phosphorus removal from aqueous solution using iron coated natural and engineered sorbents. *Journal of Hazardous Materials*, 151(1), pp.103–110.

Chen, D. Li, W., Wu, Y., Zhu, Q., Lu, Z., & Du, G., 2013. Preparation and characterization of chitosan/montmorillonite magnetic microspheres and its application for the removal of Cr (VI). *Chemical Engineering Journal*, 221, pp.8–15.

Eren, E. and Afsin, B., 2008. An investigation of Cu(II) adsorption by raw and acid-activated bentonite: A combined potentiometric, thermodynamic, XRD, IR, DTA study. *Journal of Hazardous Materials*, 151(2–3), pp.682–691.

Gates, W.P. and Bouazza, A., 2010. Bentonite transformations in strongly alkaline solutions. *Geotextiles and Geomembranes*, 28(2), pp.219–225.

Halajnia, A. Oustan, S., Najafi, N., Khataee, A. R., Lakzian, A., 2013. Adsorption-desorption characteristics of nitrate, phosphate and sulfate on Mg-Al layered double hydroxide. *Applied Clay Science*, 80–81, pp.305–312.

Huang, W., Zhu, R., He, F., Li, D., Zhu, Y., Zhang, Y., 2013. Enhanced phosphate removal from aqueous solution by ferric-modified laterites : Equilibrium , kinetics and thermodynamic studies. *Chemical Engineering Journal*, 228, pp.679–687.

Lu, J., Liu, H., Liu, R., Zhao, X., Sun, L., Qu, J., 2013. Adsorptive removal of phosphate by a nanostructured Fe-Al-Mn trimetal oxide adsorbent. *Powder Technology*, 233, pp.146–154.

Manohar, D.M., Noeline, B.F. and Anirudhan, T.S., 2006. Adsorption performance of Al-pillared bentonite clay for the removal of cobalt(II) from aqueous phase. *Applied Clay Science*, 31(3–4), pp.194–206.

Oehmen, A., Lemos, P. C., Carvalho, G., Yuan, Z., Keller, J., Blackall, L. L., Reis, M. A. M., 2007. Advances in enhanced biological phosphorus removal: From micro to macro scale. *Water Research*, 41(11), pp.2271–2300.

Onyango, M.S., Masukume, M., Ochieng, A., Otieno, F., 2010. Functionalised natural zeolite and its potential for treating drinking water ontaining excess amount of nitrate. *Water SA*, 36(5), pp.655–662.

Pengthamkeerati, P., Satapanajaru, T. and Chularuengoaksorn, P., 2008. Chemical modification of coal fly ash for the removal of phosphate from aqueous solution. *Fuel*, 87(12), pp.2469–2476.

Sowmya, A. & Meenakshi, S., 2013. An efficient and regenerable quaternary amine modified chitosan beads for the removal of nitrate and phosphate anions. *Journal of Environmental Chemical Engineering*, 1(4), pp.906–915.

Tu, Y., e You, C., Chang, C., Chen, M., 2014. Journal of the Taiwan Institute of Chemical Engineers Application of magnetic nano-particles for phosphorus removal / recovery in aqueous solution. *Journal of the Taiwan Institute of Chemical Engineers*, pp.3–9.

Yan, L.G., Xu, Y. Y., Yu, H. Q., Xin, X. D., Wei, Q., Du, B., 2010. Adsorption of phosphate from aqueous solution by hydroxy-aluminum, hydroxy-iron and hydroxy-iron-aluminum pillared bentonites. *Journal of Hazardous Materials*, 179(1–3), pp.244–250.

Ye, H., Chen, F., Sheng, Y., Sheng, G., Fu, J., 2006. Adsorption of phosphate from aqueous solution onto modified palygorskites. *Separation and Purification Technology*, 50(3), pp.283–290.

Zhang, H.L., Sheng, G. P., Fang, W., Wang, Y. P., Fang, C. Y., Shao, L. M., Yu, H. Q., 2015. Calcium effect on the metabolic pathway of phosphorus accumulating organisms in enhanced biological phosphorus removal systems. *Water Research*, 84, pp.171–180.

Zhao, D. and Sengupta, A.K., 1998. Ultimate removal of phosphate from wastewater using a new class of polymeric ion exchangers. *Water Research*, 32(5), pp.1613–1625.

CHAPTER 5

CONCLUSIONS AND RECOMMENDATIONS FOR FUTURE WORK

5.1 Conclusion

Pollution of water has diverse adverse effects in the environment and for human health. The presence of these pollutants is of concern and their elimination is essential. In view of remediating polluted water, synthetic polymers were developed through oxidation polymerization (using $(NH_4)_2S_2O_8$ and $FeCl_3$ oxidants) and it yielded adsorbents that are redox active. In situ polymerization of phenylenediamine and pyrrole monomers into galleries of the montmorillonite clay was demonstrated. The synthesis of bulk quantities was simple. According to spectroscopic data, the polymers intercalated onto the clay backbone indicating successful polymerization in clay confined environment. These polymer-based adsorbents proved to be efficient in Cr(VI) uptake. Thorough investigations were done to explicate the behaviour of poly(para-phenylenediamine) before and after Cr(VI) adsorption. The adsorption process mainly involved rapid reduction of Cr(VI) to Cr(III) and chelation between Cr(III) and imine groups on the adsorbent surface. Equilibrium studies revealed that operational condition including solution pH, contact time, adsorbent dose, initial concentration and presence of competing ions were able to affect the adsorption capacity and the efficiency of the adsorbents. Adsorbents performance was optimum at a pH value of 2 which is ideal for to Cr(VI) reduction. Monolayer adsorption described by Lungmuir model for Cr(VI) was obtained and adsorbents were regenerated and re-used .

Potassium dichromate and ammonium peroxydisulphate initiated polymerization of PPD isomers were carried out to remove phosphate ions aqueous solution. The idea of using $K_2Cr_2O_7$ as an oxidant was to introduce Cr(III) which result from Cr(VI) reduction during the synthesis process in acidic medium. Polymers synthesized from $K_2Cr_2O_7$ gave the high adsorption capacity due to the presence of Cr content and the meta polymer had the highest capacity. The phosphate adsorption on the adsorbents was fitted by Langmuir model at pH 2 and the kinetic data were described better by the pseudo-second-order kinetic rate model.

Modification of bentonite clay with Fe, Co and Ni metal salts influenced the changes in property of bentonite. XRD analysis indicated that metal modified bentonite had improved amorphosity compared to natural bentonite. The pseudo-second-order model described the adsorption kinetics well for all the prepared adsorbents and the experimental data agreed with both the Langmuir and Freundlich adsorption isotherms models.

5.2 Recommendations

The background and implementation of polymeric-based and clay adsorbents were explored for wastewater treatment in a batch scale. Further strategies can be explored to improve the treatment process for a wider application. The following are activities that could be undertaken for future investigations:

- Optimization of polymer synthesis method by controlling its oxidation state in different concentrations of acidic or alkaline medium.

- Investigate the effect of the selected transition metals doping on clay followed by polymerization to improve the composite performance, specifically for phosphate ions adsorption.

- Perform more studies on real wastewater samples to test the effect of sample matrix on the chosen analytes.

- Undertake a study of synthesizing polymer-clay composite beads with good strength which can be used effectively in batch and in continuous adsorption on fixed-bed column.

- Lastly, studies regarding the standard techniques for the overall process that can assist on the scalability for industrial applications.